

## **ABSTRACT**

Title: MONITORING LAND DEGRADATION IN  
SOUTHERN AFRICA BY ASSESSING  
CHANGES IN PRIMARY PRODUCTIVITY.

Konrad J. Wessels, Doctor of Philosophy, 2005

Directed By: Professor Stephen D. Prince  
Department of Geography

Land degradation is one of the most serious environmental problems of our time. Land degradation describes circumstances of reduced biological productivity. The fundamental goal of this thesis was to develop land degradation monitoring approaches based on remotely sensed estimates of vegetation production, which are capable of distinguishing human impacts from the effects of natural climatic and spatial variability. Communal homelands in South Africa (SA) are widely regarded to be severely degraded and the existence adjacent, non-degraded areas with the same soils and climate, provides a unique opportunity to test regional land degradation monitoring methods.

The relationship between 1km<sup>2</sup> AVHRR, growth season  $\Sigma$ NDVI and herbaceous biomass measurements (1989-2003) was firstly tested in Kruger National Park, SA. The relationship was moderately strong, but weaker than expected. This was attributed to the fact that the small areas sampled at field sites were not representative of the spatial variability within 1km<sup>2</sup>. The  $\Sigma$ NDVI adequately

estimated inter-annual changes in vegetation production and should therefore be useful for monitoring land degradation.

Degraded areas mapped by the National-Land-Cover in north-eastern SA were compared to non-degraded areas in the same land capability units. The  $\Sigma$ NDVI of the degraded areas was consistently lower, regardless of large variations in rainfall. However, the ecological stability and resilience of the degraded areas, as measured by the annual deviations from each pixel's mean  $\Sigma$ NDVI, were no different to those of non-degraded areas. This suggests that the degraded areas may be in an alternative, but stable ecological state.

To monitor human-induced land degradation it is essential to control for the effects of rainfall on vegetation production. Two methods were tested (i) Rain-Use Efficiency ( $RUE = NPP / \text{Rainfall}$ ) and (ii) negative trends in the differences between the observed  $\Sigma$ NDVI and the  $\Sigma$ NDVI predicted by the rainfall using regressions calculated for each pixel (RESTREND). RUE had a strong negative correlation with rainfall and did not provide a reliable index of degradation. The RESTREND method identified areas in and around the degraded communal lands that exhibit negative trends in production per unit rainfall. This research made a significant contribution to the development of remote sensing based land degradation monitoring methods.

MONITORING LAND DEGRADATION IN SOUTHERN AFRICA BY  
ASSESSING CHANGES IN PRIMARY PRODUCTIVITY.

By

Konrad J. Wessels

Dissertation submitted to the Faculty of the Graduate School of the  
University of Maryland, College Park, in partial fulfillment  
of the requirements for the degree of  
Doctor of Philosophy  
2005

Advisory Committee:  
Professor Stephen D. Prince, Chair  
Professor Ruth DeFries  
Professor Ralph Dubayah  
Professor John R.G. Townshend

© Copyright by  
Konrad J. Wessels  
2005

*To my wife,*

*Lucia....*

## **Acknowledgements**

I am grateful to Philip Frost and Dawie VanZyl (ARC- Institute for Soil, Climate and Water, ARC-ISCW) for processing the AVHRR data and to Johan Malherbe (ARC-ISCW) for developing the spatial rainfall data. Terry Newby facilitated the collaboration between University of Maryland and ARC-ISCW. I thank the South Africa National Parks for allowing access to the vegetation data of Kruger National Park and appreciate the contributions of Sandra MacFadyen and Nick Zambatis.

I would like to thank Dirk Pretorius of the National Department of Agriculture (Directorate: Land Use and Soil Management), for supporting and partially funding this research. Additional funding was provided by NASA, Earth Systems Sciences Fellowship O2-0000-0130 and SA Department of Science and Technology (LEAD project funding). I also thank the other members of my committee, Dr. Ruth DeFries, Dr. John Townshend, and Dr. Ralph Dubayah, for their enthusiastic guidance.

I am particularly grateful to my advisor, Prof. Stephen Prince, for his mentorship and support during the course of my PhD studies. His knowledge, enthusiasm and dedication provided an unmatched learning experience.

## Table of Contents

|  |     |
|--|-----|
| ACKNOWLEDGEMENTS.....  | III |
| TABLE OF CONTENTS.....   | IV  |
| LIST OF TABLES.....  | VI  |
| LIST OF FIGURES.....   | VII |
| CHAPTER 1. INTRODUCTION.....   | 1   |
| 1.1 Background.....  | 1   |
| 1.2 Land degradation in South Africa.....  | 2   |
| 1.3 Estimating vegetation production with remotely sensed data.....  | 5   |
| 1.4 Research Objectives.....   | 6   |
| 1.5 Outline of Dissertation.....   | 7   |
| CHAPTER 2. RELATIONSHIP BETWEEN HERBACEOUS BIOMASS AND<br>1KM <sup>2</sup> ADVANCED VERY HIGH RESOLUTION RADIOMETER (AVHRR)<br>NDVI IN KRUGER NATIONAL PARK.....     | 9   |
| 2.1 Introduction.....  | 9   |
| 2.2 Methods.....   | 12  |
| 2.2.1 Study area: Kruger National Park.....  | 12  |
| 2.2.2 Landscape groups.....  | 12  |
| 2.2.3 1km <sup>2</sup> AVHRR data processing.....  | 15  |
| 2.2.4 Herbaceous biomass data.....   | 16  |
| 2.2.5 Removing highly heterogeneous field sites.....   | 18  |
| 2.2.6 Rainfall data.....   | 19  |
| 2.2.7 Overview of data analyses.....   | 19  |
| 2.2.8 $\Sigma$ NDVI-biomass relationship.....  | 19  |
| 2.2.9 Estimating biomass from $\Sigma$ NDVI.....   | 21  |
| 2.3 Results and Discussion.....  | 23  |
| 2.3.1 Correlation between growth season mean biomass, mean $\Sigma$ NDVI and<br>rainfall.....  | 23  |
| 2.3.2 $\Sigma$ NDVI-biomass relationship.....  | 28  |
| 2.3.3 Estimating biomass from $\Sigma$ NDVI.....   | 34  |
| 2.4 Conclusions.....   | 40  |
| CHAPTER 3. ASSESSMENT OF THE EFFECTS OF HUMAN-INDUCED LAND<br>DEGRADATION IN THE FORMER HOMELANDS OF NORTHERN SOUTH<br>AFRICA WITH A 1KM AVHRR NDVI TIME-SERIES..... | 44  |
| 3.1 Introduction.....  | 44  |
| 3.2 Land degradation in the communal lands of South Africa.....  | 45  |
| 3.3 Materials and Methods.....   | 47  |
| 3.3.1 Study Area.....  | 47  |
| 3.3.2 1km <sup>2</sup> AVHRR NDVI data.....  | 48  |
| 3.3.3 Comparison of degraded and non-degraded rangelands.....  | 50  |
| 3.3.4 Land capability units (LCUs) and climate data.....   | 51  |
| 3.3.5 Testing for differences in $\Sigma$ NDVI of non-degraded and degraded areas<br>52  |     |

|  |  |     |
|--|--|-----|
| 3.3.6  | Relative degradation impact .....  | 53  |
| 3.3.7  | $\Sigma$ NDVI - rainfall relationship .....  | 53  |
| 3.3.8  | RDI – rainfall relationship .....  | 54  |
| 3.3.9  | Ecological Stability .....   | 54  |
| 3.4  | Results .....  | 56  |
| 3.4.1  | Differences between non-degraded and degraded areas .....  | 56  |
| 3.4.2  | Relative degradation impact (RDI) .....  | 64  |
| 3.4.3  | $\Sigma$ NDVI - rainfall relationship .....  | 64  |
| 3.4.4  | RDI – rainfall relationship .....  | 68  |
| 3.4.5  | Ecological Stability .....   | 68  |
| 3.5  | Discussion .....   | 69  |
| <b>CHAPTER 4. CAN THE IMPACTS OF HUMAN-INDUCED LAND DEGRADATION BE DISTINGUISHED FROM THE EFFECTS OF RAINFALL VARIABILITY?</b> ..... |  |     |
| 76   |  |     |
| 4.1  | Introduction .....   | 76  |
| 4.1.1  | Remote sensing estimates of vegetation production .....  | 80  |
| 4.2  | Materials and Methods .....  | 81  |
| 4.2.1  | Study area - Summer rainfall region of South Africa .....  | 81  |
| 4.2.2  | NPP – GLO-PEM .....  | 83  |
| 4.2.3  | Rainfall data .....  | 84  |
| 4.2.4  | Relationship of NPP and $\Sigma$ NDVI with rainfall .....  | 84  |
| 4.2.5  | Comparison of $\Sigma$ NDVI-RUE of degraded and non-degraded areas. ..                           | 85  |
| 4.2.6  | Variability of NPP-RUE in time and space. ....   | 87  |
| 4.2.7  | Identifying long-term trends in $\Sigma$ NDVI .....  | 87  |
| 4.2.8  | Detecting negative trends in the $\Sigma$ NDVI-rainfall relationships –<br>RESTREND method ..... | 88  |
| 4.3  | Results and discussion .....   | 88  |
| 4.3.1  | Relationship of NPP and $\Sigma$ NDVI with rainfall .....  | 88  |
| 4.3.2  | Comparison of $\Sigma$ NDVI-RUE of degraded and non-degraded areas. ..                           | 92  |
| 4.3.3  | Variability of NPP-RUE through time and space .....  | 96  |
| 4.3.4  | Identifying long-term trends in $\Sigma$ NDVI .....  | 100 |
| 4.3.5  | Detecting negative trends in the $\Sigma$ NDVI-rainfall relationships –<br>RESTREND .....        | 103 |
| 4.4  | Conclusions .....  | 111 |
| <b>CHAPTER 5. SYNTHESIS, SIGNIFICANCE AND GLOBAL APPLICATIONS</b> 117  |  |     |
| 5.1  | Synthesis of research .....  | 117 |
| 5.2  | Monitoring and Mapping land degradation. ....  | 123 |
| 5.3  | Global maps of land degradation .....  | 125 |
| <b>SUMMARY</b> .....   |  |     |
| 129  |  |     |
| <b>BIBLIOGRAPHY</b> .....  |  |     |
| 134  |  |     |

## **List of Tables**

Table 2.1 Description of landscape groups of Kruger National Park (fig. 2.1b) (after Gertenbach, 1983)

Table 2.2 Correlation coefficients ( $r$ ) for each landscape group's relationships derived from growth season average rainfall,  $\Sigma$ NDVI and biomass data.

Table 2.3 Coefficients of determination ( $R^2$ ) for  $\Sigma$ NDVI-biomass relationships for each landscape group and changes in  $R^2$  after adding tree cover to the regression. Tree cover was measured at a total of 100 sites (tree sites).

Table 2.4 Multiple regression analyses to predict biomass from independent variables  $\Sigma$ NDVI, MODIS tree cover and landscape group.

Table 2.5 Coefficients of determination ( $R^2$ ) for predicting biomass from  $\Sigma$ NDVI using smoothed data.

Table 3.1. Results of analyses of  $\Sigma$ NDVI for non-degraded (n) and degraded areas (d) of land capability units.

Table 4.1 Average slope and intercept for  $\Sigma$ NDVI-Rainfall relationship in degraded and non-degraded areas of each land capability unit (LCU). The number of pixels varied between degraded and non-degraded areas of each LCU.

Table 5.1 Previous maps of global land degradation, methods used in assessments and references.

## List of Figures

- Figure 1.1 Former homelands / current communal lands of South Africa.
- Figure 2.2 Growth season average  $\Sigma$ NDVI, biomass and rainfall for each landscape group. The landscape groups are described in Table 2.1 and mapped in fig. 2.1b. Error bars indicate  $\pm$  one standard deviation.
- Figure 2.3 Growth season sum NDVI of Kruger National Park for selected growth seasons.
- Figure 2.4 Average growth season rainfall of Kruger National Park, 1989-90 to 2002-2003.
- Figure 2.5 Herbaceous biomass and  $\Sigma$ NDVI for a field site near Skukuza where the rainfall was recorded.
- Figure 2.6 Relationship between herbaceous biomass and percentage tree cover measured at selected field sites (N=100) for the 1995-96 growth season.
- Figure 2.7 Trend lines of  $\Sigma$ NDVI vs. herbaceous biomass for field sites grouped according to tree cover ranges.
- Figure 2.8 Smoothed biomass and  $\Sigma$ NDVI data of each growth season and their linear regression. The 95% confidence limits are indicated.
- Figure 3.1 (a) Provinces of South Africa with location of study area and former homelands. (b) Study area indicating severity of rangeland degradation per district according to National Review of Land Degradation (after Hoffman et al. 1999) and degraded areas mapped by the National Land Cover (Fairbanks et al. 2000).
- Figure 3.2 Grayscale  $\Sigma$ NDVI of Southern Africa for 1998-99.

Figure 3.3 Selected land capability units (LCU) and weather stations used to calculate mean growth season rainfall for each LCU.

Figure 3.4 (a)  $\Sigma$ NDVI and rainfall per growth season for each land capability unit (LCU). Error bars indicate standard deviation. (b) Relative degradation impact (RDI) and rainfall per growth season. (c) Departures from long-term mean  $\Sigma$ NDVI and rainfall per growth season.

Figure 3.5 Average non-degraded  $\Sigma$ NDVI of land capability units, for 1995 to 2000. Error bars indicate standard deviation.

Figure 3.6 Mean growth season rainfall for all weather stations (N=151) in study area for 1965 to 2003.

Figure 3.7  $\Sigma$ NDVI of study area for (a) 1991-92 and (b) 1999-2000. (c)  $\Sigma$ NDVI for central parts of study area (1997-98) overlaid with degraded areas mapped by National Land Cover (NLC).

Figure 4.1 (a) Rain seasons and former homelands, (b) biomes and (c) average rainfall of South Africa.

Figure 4.2 Selected land capability units (LCU) containing degraded areas in north-eastern South Africa.

Figure 4.3 Maps of coefficients of determination for (a)  $\Sigma$ NDVI-rainfall and (b) NPP-rainfall regressions for the summer rainfall region of South Africa.

Figure 4.4 Coefficients of variation for precipitation (after Schulze 1997) NPP and  $\Sigma$ NDVI of the summer rainfall region of South Africa.

Figure 4.5 Average  $\Sigma$ NDVI-RUE of degraded and non-degraded rangelands per growth season, in specified land capability units (LCUs) in north-eastern SA.

The locations of the LCUs are shown in Figure 4.2.

Figure 4.6 Average NPP-RUE, 1991-92 NPP-RUE and 1997-98 to 1999-2000 NPP-RUE. Note that the NPP includes both above and below ground production.

Figure 4.7 Average NPP-RUE of 1500 random points plotted against average rainfall for the summer rainfall region of South Africa.

Figure 4.8 Map of slope of the NPP-RUE-time regression indicating positive or negative trends. The locations of two sites are indicated for which NPP, rainfall and RUE values are given in figure 4.9.

Figure 4.9 NPP-RUE profile for two locations with negative trends in figure 4.8.

Figure 4.10 (a) Map of slope of the  $\Sigma$ NDVI-time regression indicating positive or negative trends. (b) Map of slope of the residual-time regression. The residuals were calculated as the difference between the observed  $\Sigma$ NDVI and predicted  $\Sigma$ NDVI using the linear  $\Sigma$ NDVI-rainfall relationships. Pixels without statistically significant slopes were omitted (white).

Figure 4.11 Linear regression of  $\Sigma$ NDVI and rainfall (top panel). Trend of residuals plotted against  $\Sigma$ NDVI and rainfall per growth season for a typical pixel in area 1 of fig. 4.12 (bottom panel).

Figure 4.12 Enlargement of Figure 10a for north-eastern SA with former homelands and areas of interest showing negative trends (circles). Map of slope of the residual-time regression. The residuals were calculated as the difference between

the observed  $\Sigma$ NDVI and predicted  $\Sigma$ NDVI using the linear  $\Sigma$ NDVI-rainfall relationships. Pixels without statistically significant slopes were omitted (white).

Figure 4.13 Linear regression of  $\Sigma$ NDVI and rainfall (top panel). Trend of residuals plotted against  $\Sigma$ NDVI and rainfall per growth season for a typical pixel in area 4 of fig. 4.12 (bottom panel).

Figure 4.14 Linear regression between  $\Sigma$ NDVI and rainfall (top panel). Trend of residuals plotted against  $\Sigma$ NDVI and rainfall per growth season for a typical pixel in area 6 in (Kruger National Park) of fig. 4.12 (bottom panel).

Figure 4.15 Linear regression between  $\Sigma$ NDVI and rainfall (top panel). Trend of residuals plotted against  $\Sigma$ NDVI and rainfall per growth season for a typical pixel in Kruger National Park (fig. 4.12) (bottom panel). Figure 4.16 Linear regression between  $\Sigma$ NDVI and rainfall (top panel). Trend of residuals plotted against  $\Sigma$ NDVI and rainfall per growth season for a typical pixel in large area with negative residual trends around Hopetown in fig. 4.10b (bottom panel).

Figure 4.16 Linear regression between  $\Sigma$ NDVI and rainfall (top panel). Trend of residuals plotted against  $\Sigma$ NDVI and rainfall per growth season for a typical pixel in large area with negative residual trends around Hopetown in fig. 4.10b (bottom panel).

Figure 4.17 Potential effects of degradation on the observed rainfall- $\Sigma$ NDVI relationships (OR) in comparison with the non-degraded rainfall- $\Sigma$ NDVI relationships (NR)(top panel), and trends in the residuals with respect to time (lower two panels). (a-b) Condition 1, degradation causes a fixed reduction in production, independent of rainfall. (c-e) Condition 2, degradation reduces

production more at lower rainfall, showing the effect on trends in the residuals if rainfall decreases (d) or increases (e) during the time-series. (f-h) Condition 3, degradation reduces production more at higher rainfall, showing the effect on trends in the residuals if rainfall increases (g) or decreases (h) during the time-series.

Figure 4.18 Effect of timing of the occurrence of degradation on the slope of temporal trends of residuals. Simulations were based on a fixed 15% reduction in  $\Sigma$ NDVI starting in each of the 16 years in the time-series.

Figure 5.1. Previous maps of land degradation for South Africa: (a) Acocks, 1953, (b) UNCOD, 1977a, (c) Dregne, 1983, (d) UNEP, 1992, (e) Roux, 1990 and (f) Hoffman et al., 1999.

Figure 5.2. Global RESTREND map of the residual-time regression (1981-1999). The residuals were calculated as the difference between the observed annual NPP and NPP predicted using the linear NPP-AET relationships. Pixels without statistically significant slopes were omitted (white).

# Chapter 1. Introduction

## 1.1 Background

Land degradation is believed to be one of the most serious global environmental problems of our time (Dregne, Kassas & Rozanov, 1991; UNCED, 1992; Reynolds & Stafford Smith, 2002b). Over 250 million people are believed to be directly affected by desertification and some one billion people in over one hundred countries are at risk (Adger *et al.*, 2000). The United Nations furthermore estimates that desertification costs \$45 billion (US) per year in lost income. Land degradation affects food security, international aid programs, national economic development and natural resource conservation strategies. Currently 184 nations are signatories to the United Nations Convention to Combat Desertification (UNCCD) (UNEP, 1994).

Desertification is defined as land degradation in arid, semi-arid and dry sub-humid areas resulting from factors, including climatic variations and human activities (UNEP, 1994). Land degradation includes diverse processes from changes in plant species composition to soil erosion, but essentially describes circumstances of reduced biological productivity of the land (Thomas & Middleton, 1994; Reynolds, 2001; UNCCD, 1994; Reynolds & Stafford Smith, 2002b). The terms “desertification” and “land degradation” are often used interchangeably, but “land degradation” is preferred, since it helps to avoid confusion with the effects of drought and focuses primarily on human impacts.

Regional land degradation has proven extremely difficult to quantify and the lack of appropriate data is widely regarded as a major obstacle to progress in this field

(Thomas & Middleton, 1994; Williams & Balling, 1996; Nicholson, Tucker & Ba, 1998). Early efforts to map desertification (UNCOD, 1977b; UNEP, 1987) have been severely criticized (Hellden, 1991; Thomas & Middleton, 1994) and recently described by Stocking (2001) as “sterile, inaccurate and misleading”. There is a pressing need for an objective, repeatable, systematic and spatially explicit measure of degradation. The tragic shortage of data has been evident since the 1977 United Nations Conference on Desertification (UNCOD, 1977b) and continues today (Dregne, 2002). In this dissertation novel methods were developed to use remotely sensed data to detect and monitor human-induced land degradation.

## **1.2 Land degradation in South Africa**

Land degradation poses a serious threat to the natural resources and economic development of South Africa (Beinart, 1996; Hoffman *et al.*, 1999; SADC-ELMS, 1999; Hoffman & Todd, 2000). The SA National Report on Land Degradation (NRLD), recently directed attention to severe land degradation in the former “homelands”, now communal areas (Shackleton, 1993; Hoffman *et al.*, 1999; Hoffman & Todd, 2000; Hoffman & Ashwell, 2001) (fig. 1.1).

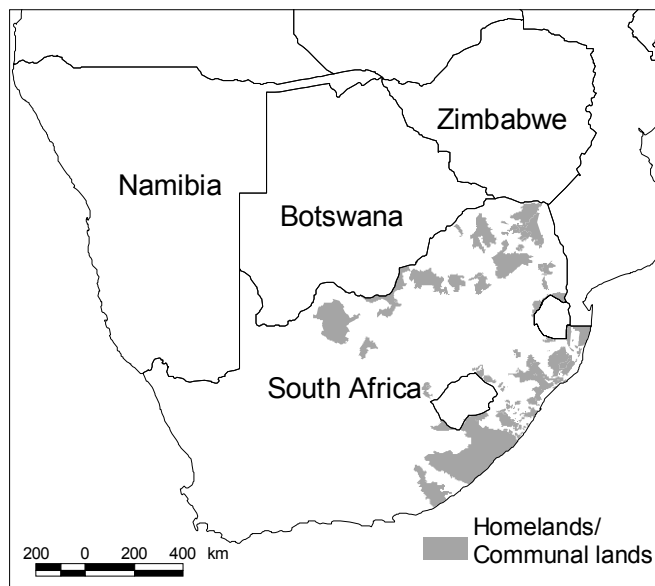


**Figure 1.1** Former homelands / current communal lands of South Africa.

The “homelands” or self-governing territories were established under the Natives Land Acts of 1913 and 1936 and during the apartheid-era, prior to majority rule in 1994, indigenous African people were involuntarily resettled and confined to these areas (Christopher, 1994; Fox & Rowntree, 2001). Stable communities were uprooted and compelled to settle in areas where the unsustainable land use degraded the local resource base upon which their rural livelihoods depended (Fox & Rowntree, 2001; Shackleton, Shackleton & Cousins, 2001; Ross, 1999). Between 1960 and 1985 more than 3.5 million people were forcibly relocated under the Nationalist party’s policy of “apartheid” or separate development (Hoffman *et al.*; 1999). By 1994 80% of South Africa’s total population had access to only 13% of the land (Kerr Watson, 2001).

Today communal areas are generally characterized by high human populations, overgrazing, soil erosion, excessive wood harvesting and increases in

unpalatable plant species (Hoffman & Todd, 2000). These areas are predominantly populated by black South Africans, engaged in the production of crops and livestock mainly for own consumption or for sale on local, informal markets. In these communal areas the land is owned by the State. In contrast, commercial areas consist of land that is privately owned by mainly white farmers who market their produce through the formal commercial sector (Hoffman & Todd, 2000). Livestock numbers in communal areas are 2-4 times higher than the recommended stocking rates and twice that of commercial farms (Shackleton, 1993; Meadows & Hoffman, 2002). These communal areas are therefore widely regarded as degraded (Hoffman & Todd, 2000). Current land redistribution programs in SA could potentially expose historically commercial and highly productive lands to the socio-economic driving forces of land degradation (Dean, Hoffman & Wills, 1996; Fox & Rowntree, 2001), as has occurred in Zimbabwe (Prince, 2004). Therefore in SA, as in many arid countries, there is an urgent need for national land degradation monitoring systems.

Although the result of a policy that has caused extensive human suffering, the homelands in SA provides an extraordinarily valuable, if unintended experiment on the effects of long-term, heavy utilization of the land that can be compared to adjacent, non-degraded, commercial areas that are equivalent in all other respects (e.g. soils, local climate and topography). The existence of these comparable degraded and non-degraded areas, together with the country's biophysical diversity and abundance of relevant data, make SA an ideal study area for testing land degradation monitoring methods.

### 1.3 Estimating vegetation production with remotely sensed data

Vegetation production and biomass have been successfully estimated with the Normalized Difference Vegetation Index (NDVI) derived from satellite data (Deering, 1975; Prince & Tucker, 1986; Tucker & Sellers, 1986; Prince, 1991b; Jury, Weeks & Godwe, 1997; Myneni *et al.*, 1997). NDVI has a strong linear relationship with the fraction of photosynthetically active radiation (PAR) absorbed by the plant ( $f_{\text{PAR}}$ ) (Monteith, 1972; Monteith, 1977; Kumar & Monteith, 1982; Asrar *et al.*, 1984; Goward & Dye, 1987; Sellers, 1987; Sellers *et al.*, 1997) and is routinely employed in production efficiency models (Prince, 1991a; Potter *et al.*, 1993; Field, Randerson & Malmstrom, 1995; Prince & Goward, 1995; Ruimy, Dedieu & Saugier, 1996; Gower, Kucharik & Norman, 1999; Running *et al.*, 1999; Behrenfeld *et al.*, 2001) where it sets the upper limit for unstressed net primary productivity (NPP) (Schloss, Kicklighter & Kaduk, 1999). In arid and semi-arid lands seasonal sums of multi-temporal NDVI are strongly correlated with vegetation production (Prince & Tucker, 1986; Prince, 1991b; Nicholson & Farrar, 1994; Nicholson *et al.*, 1998).

Human-induced land degradation can be expected to alter the vegetation cover and function before soil erosion accelerates or local climate change through positive feedbacks (Charney *et al.*, 1977; Xue & Fennessy, 2002). If so, changes in  $f_{\text{PAR}}$  should be among the first factors related to primary production that can alert us to degradation. Therefore, remotely sensed NDVI may provide the basis for an early warning of degradation. NDVI derived from the Advanced Very High Resolution Radiometer (AVHRR) has shown to be capable of systematic, repeatable and spatially extensive monitoring of vegetation productivity to assess desertification

(Prince & Justice, 1991; Tucker, Dregne & Newcomb, 1991a; Tucker *et al.*, 1991b; Nicholson *et al.*, 1998; Prince, Brown de Colstoun & Kravitz, 1998; Diouf & Lambin, 2001). The remaining challenge in developing a monitoring approach is how to interpret the NDVI data so that human impacts can be distinguished from both natural, spatial variation in the landscape and the short-term inter-annual climate variability that is particularly pronounced in SA due to the El Niño-Southern Oscillation (ENSO) phenomenon.

#### **1.4 Research Objectives**

Vegetation production is greatly influenced by variations in the landscape and climate and as a result it is very difficult to detect human impacts on vegetation production against this background variability (Pickup, Bastin & Chewings, 1998; Prince, 2002). The fundamental goal of this dissertation was therefore to develop improved land degradation monitoring approaches based on remotely sensed estimates of vegetation production, which are capable of distinguishing human impacts from the effects of landscape and rainfall variability. The general hypothesis was that negative deviations in remote sensing estimates of vegetation production can be used to detect degraded areas.

The following specific research objectives were addressed:

1. Analyze the underlying relationship between growth season  $\Sigma$ NDVI from 1km<sup>2</sup> AVHRR data and herbaceous biomass in Kruger National Park (KNP), SA. (Chapter 2)

2. Quantify the difference in  $\Sigma$ NDVI and compare the resilience and stability of vegetation production of degraded and non-degraded areas within the same land capability units. (Chapter 3)
3. Characterize the relationship between rainfall and remotely sensed estimates of vegetation production for SA. (Chapter 4)
4. Evaluate the inter-annual variability of the RUE maps to determine if they can be used as a robust indicator of land degradation. (Chapter 4)
5. Apply and evaluate the residual trends method (RESTRENDS) which identifies negative trends in the production-rainfall relationship to facilitate the detection of human-induced land degradation. (Chapter 4)

## **1.5 Outline of Dissertation**

This dissertation consists of five chapters. Chapter 1 introduces the topic of land degradation, specifically in the communal areas of SA and sets the research objectives. In Chapter 2, the relationship between 1km<sup>2</sup> Advanced Very High Resolution Radiometer (AVHRR), growth season-integrated Normalized Difference Vegetation Index ( $\Sigma$ NDVI) and multi-year biomass measurements (1989 to 2003) is tested in Kruger National Park (KNP), SA. This was done to explore the ability of the AVHRR,  $\Sigma$ NDVI to estimate vegetation production for the purpose of monitoring land degradation throughout the region. An application to develop herbaceous biomass maps from the AVHRR NDVI data was also investigated as an aid to fire management decisions in KNP.

Chapter 3 focuses on northern SA which includes several communal lands that have been reported to be severely degraded. The degraded and non-degraded areas within the same biophysical strata (land capability units) were compared in terms of their  $\Sigma$ NDVI (1985 to 2003), as well as their ecological resilience and stability. This chapter also demonstrates the importance of detailed stratification to control for spatial landscape variation.

In Chapter 4, the relationship between rainfall and remotely sensed estimates of vegetation production is characterized on a per-pixel basis, for the entire summer rainfall region of SA. In order to facilitate the detection of human-induced land degradation, two methods were tested to control for the effects of rainfall variability on vegetation production: (i) Rain-use Efficiency ( $RUE = NPP / \text{rainfall}$  or  $\Sigma$ NDVI/rainfall), (ii) negative trends in the differences between the observed  $\Sigma$ NDVI and the  $\Sigma$ NDVI predicted by the rainfall using regressions calculated for each pixel (residual trends method - RESTREND). Finally, Chapter 5 summarizes the findings and explores the potential global application of the degradation monitoring methods.

## **Chapter 2. Relationship between herbaceous biomass and 1km<sup>2</sup> Advanced Very High Resolution Radiometer (AVHRR) NDVI in Kruger National Park.**

### **2.1 Introduction**

The normalized difference vegetation index (NDVI) derived from the Advanced Very High Resolution Radiometer (AVHRR) has been widely used to estimate vegetation production (Prince & Justice, 1991; Tucker *et al.*, 1991a; Tucker *et al.*, 1991b; Myneni *et al.*, 1997; Nicholson *et al.*, 1998; Prince *et al.*, 1998; Diouf & Lambin, 2001). A number of studies have reported a strong linear relationship between seasonal sums of AVHRR, NDVI and field measurements of vegetation production in arid and semi-arid lands (Prince & Tucker, 1986; Nicholson, Davenport & Malo, 1990; Diallo *et al.*, 1991; Prince, 1991b; Wylie *et al.*, 1991; Nicholson & Farrar, 1994; Diouf & Lambin, 2001). These studies revealed that the nature of the relationship (coefficient of determination, slope and y-intercept) between NDVI and field measurements varies considerably between studies and study areas (Du Plessis, 1999). In southern Africa the biomass-AVHRR NDVI relationship has been tested in Namibia (Du Plessis, 1999) and Botswana (Prince & Tucker, 1986), but so far not in South Africa (SA).

Comprehensive field data on NPP are rare since these require measurements of components (e.g. below ground production, decay and herbivory) that are difficult

to make (Reich, Turner & Bolstad, 1999). Above-ground biomass is relatively easy to measure and is therefore frequently used to estimate production (Scurlock *et al.*, 1999; Zheng, Prince & Wright, 2003). In the Kruger National Park (KNP) of SA various vegetation measurements, including end-of-season above-ground herbaceous biomass, have been collected at approximately 533 locations since 1989 (Trollope, 1990; Zambatis, 2002). These vegetation condition assessments (VCA) are used to monitor the effect of management practices on vegetation, e.g. man-made watering points, game culling and burning. Although the KNP VCA data were not initially intended for validating coarse resolution remote sensing data, they constitute the best field data available in SA and are used here to assess the ability of 1km<sup>2</sup> AVHRR  $\Sigma$ NDVI data to monitor vegetation production.

The purpose of this study was twofold, (i) to develop spatial maps of herbaceous biomass from AVHRR NDVI data to aid management decisions in KNP and (ii) to evaluate the ability of AVHRR NDVI data to monitor vegetation production in KNP so that it may be used to monitor land degradation the region.

Firstly, since the extent of fires in KNP is strongly related to the amount of grass fuel accumulated during the preceding growing season, fire management decisions are largely dependent upon spatially explicit estimates of herbaceous fuel load (Trollope & Potgieter, 1986). The adaptive fire management policy of KNP strives to ensure the maintenance of biodiversity through a combination of planned and unplanned fires (Biggs, 2002; Van Wilgen *et al.*, 2004). During the dry season park managers apply planned patch mosaic burns after identifying “burn-targets” based on estimates of standing herbaceous biomass fuel load. Currently these fuel

load estimates are either based on subjective visual estimates by rangers or spatial interpolation of the VCA point measurements. Since the distance between VCA sites is 3-12km, the interpolations do not provide reliable spatial biomass maps. Fire management and other research in KNP could benefit significantly from more reliable spatial biomass data. To date, there have been no attempts to compare the VCA biomass data to the 17 years of 1km<sup>2</sup> AVHRR data.

Second, there is an urgent need for an objective and repeatable measure of land degradation in South Africa (SA), since the former homelands (current communal lands) that abuts KNP, are widely regarded as severely degraded (Palmer, Ainslie & Hoffman, 1999; Hoffman & Todd, 2000; Wessels, van Den Berg & Pretorius, 2000; Hoffman & Ashwell, 2001; Pollard, Shackleton & Curruthers, 2003; Wessels *et al.*, 2004). Establishing the relationship between vegetation production and AVHRR  $\Sigma$ NDVI is essential to developing a reliable land degradation monitoring approach based on these satellite observations (Wessels *et al.*, 2000; Pollard *et al.*, 2003; Wessels *et al.*, 2004).

The objectives of this study were: (1) to analyze the underlying relationship between growth season  $\Sigma$ NDVI from 1km<sup>2</sup> AVHRR data and herbaceous biomass for KNP and (2) to investigate the production herbaceous biomass maps for each growth season from the  $\Sigma$ NDVI.

## 2.2 Methods

### 2.2.1 Study area: Kruger National Park

The Kruger National Park (KNP) is situated on the eastern side of the Limpopo and Mpumalanga provinces of South Africa, between E 30° 53' 18'', S 22° 19' 40'' and E 32° 01' 59'', S 25° 31' 44'' (fig. 2.1a). The KNP extends 360km from north to south and covers an area of almost 2 000 000 ha, making it one of the largest conservation areas in the world (Mabunda, Pienaar & Verhoef, 2003). The KNP falls within the savanna biome with a mean annual rainfall of 537mm, which ranges from 350mm in the north to 950mm in the south-western parts of the park. The inter-annual coefficient of variation of rainfall ranges from 25% in the south to 35% in the north (Venter, Scholes & Eckhardt, 2003). KNP experiences a four to eight month hot, wet season (October to April) and a mild, dry winter (May to August).

KNP is crossed by seven major river systems, all of which originate to the west of the KNP and drain a combined area of about 8 860 000 ha (Mabunda *et al.*, 2003). The tree canopy cover ranges from 5-60% and is dominated by *Acacia* spp., *Combretum* spp. and *Colophospermum mopane* (Venter *et al.*, 2003). At least 2 million people reside within 50km of the western boundary of KNP with the vast majority concentrated in the former homelands which are densely populated and managed as communal rangelands and subsistence agriculture (Pollard *et al.*, 2003).

### 2.2.2 Landscape groups

The diverse landscape of KNP has been classified into significant environmental units for the purpose of practical conservation planning and

management. 35 landscapes have been identified based on geomorphology, climate, soil, vegetation pattern and associated fauna (Gertenbach, 1983). A simplified classification joined the 32 landscapes into 17 landscape groups (LGs, fig. 2.1b) according to the scheme outlined in table 2.1 (Solomon *et al.*, 1999). The dominant topography, geology and vegetation of the LGs are described in table 2.1.

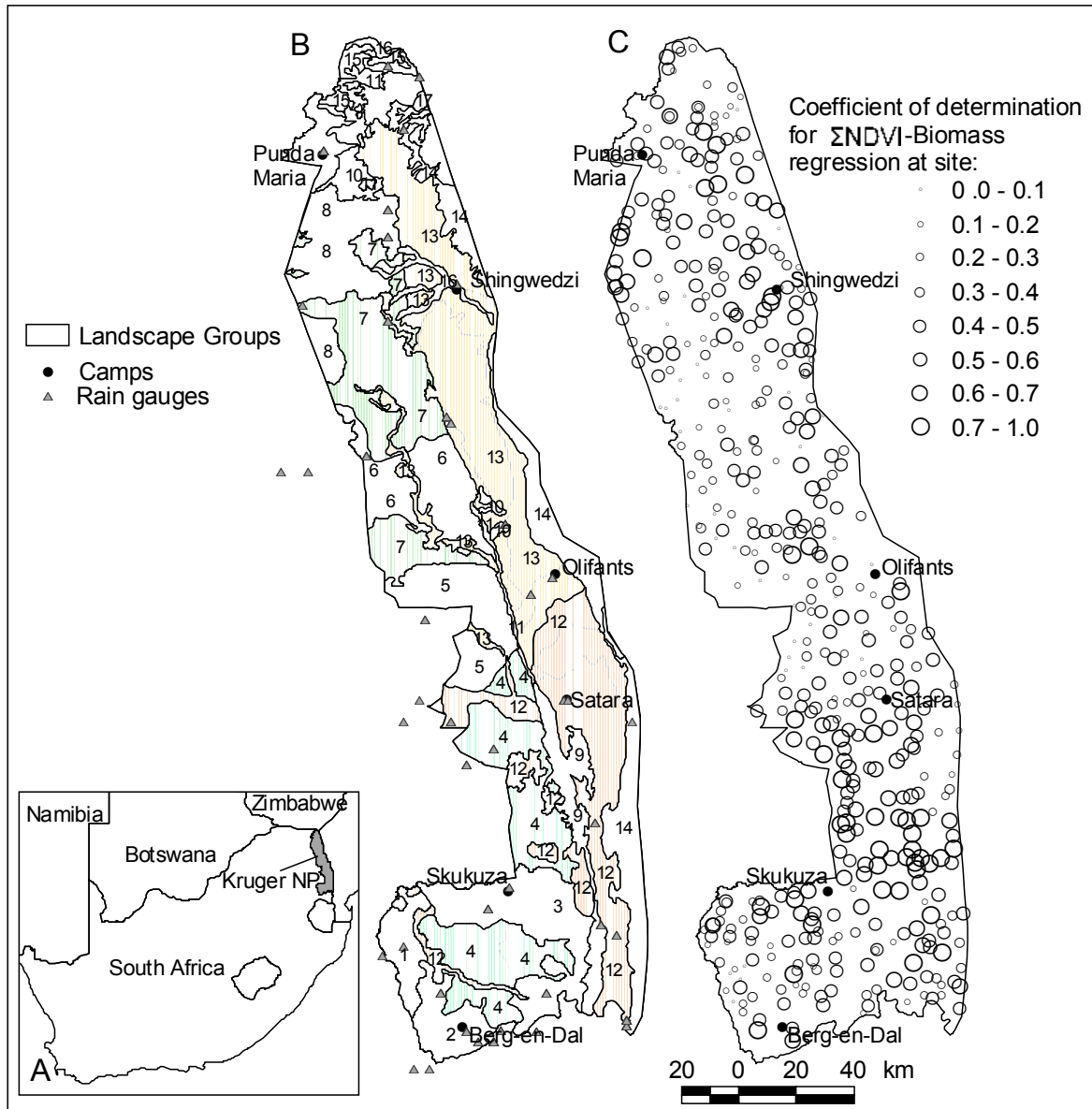


**Figure. 2. 1** (a) Location of Kruger National Park within southern Africa. (b) Landscape groups (see Table 2.1 for descriptions) and location of rain gauges. (c)  $R^2$  for  $\Sigma$ NDVI-Biomass relationship at each field site. The size of the circle at each site indicates the  $R^2$  and not the size of the field site.

**Table 2.1** Description of landscape groups of Kruger National Park (fig. 2.1b) (after Gertenbach, 1983)

| Landscape Group | Gertenbach landscapes | Description  |
|-----------------|-----------------------|--|
| 1               | 1                     | Moderately undulating granitic flats with <i>Terminalia sericea</i> Tree Savanna   |
| 2               | 2                     | Low granitic mountains with <i>Combretum apiculatum</i> Bush Savanna.  |
| 3               | 4                     | Lowlands with <i>Acacia grandicornuta</i> Tree Savanna.  |
| 4               | 3, 5                  | Moderately undulating granitic plains with <i>Combretum. zeyheri</i> , or with <i>Combretum apiculatum</i> Bush Savanna.   |
| 5               | 6, 7                  | Slightly irregular granitic plains with <i>Colophospermum mopane</i> Bush Savanna, or irregular granitic hills with <i>C. mopane</i> Tree Savanna.   |
| 6               | 9, 10                 | Slightly undulating metalava plains with <i>Colophospermum mopane</i> Tree Savanna, or very irregular granitic plains with <i>C. mopane</i> Tree Savanna.  |
| 7               | 8, 11                 | Moderately undulating granitic plains with <i>Colophospermum mopane</i> Bush Savanna, or slightly undulating plains with <i>C. mopane</i> Bush Savanna   |
| 8               | 12, 33                | Metalava plains with <i>Colophospermum mopane</i> Tree Savanna, or andesitic plains with <i>Combretum collinum</i> Shrub Savanna.  |
| 9               | 13, 14                | Karoo sediment plains with <i>Acacia welwitschii</i> Tree Savanna, or with <i>Terminalia sericea</i> Bush Savanna.   |
| 10              | 15                    | Karoo sediment plains with <i>Colophospermum mopane</i> Tree Savanna.  |
| 11              | 16, 34                | Very irregular Clarens sandstone hills with <i>Terminalia sericea</i> Bush Savanna, or low Soutpansberg Group mountains with <i>Burkea africana</i> Tree Savanna.  |
| 12              | 17, 18, 19, 20        | Basaltic plains with <i>Scleorcarya birrea</i> Tree Savanna; or slightly undulating basaltic plains with <i>Acacia nigrescens</i> Shrub Savanna; or moderately undulating basaltic plains with <i>A. nigrescens</i> Bush Savanna; or moderately undulating basaltic plains with <i>A. nigrescens</i> Tree Savanna. |
| 13              | 21, 22, 23, 24        | Irregular basaltic plains with <i>A. nigrescens</i> Bush Savanna; or with <i>Colophospermum mopane</i> Bush Savanna; or basaltic plains with <i>C. mopane</i> Shrub Savanna; or slightly undulating gabbroic plains with <i>C. mopane</i> Shrub Savanna.   |
| 14              | 27, 29, 31            | Slightly undulating basaltic plains; or low rhyolitic mountains with <i>Combretum apiculatum</i> Bush Savanna; or low rhyolitic mountains with <i>Colophospermum mopane</i> Bush Savanna.  |
| 15              | 25, 26                | Moderately undulating gabbroic plains with <i>Colophospermum mopane</i> Shrub Savanna; or irregular calcitic plains with <i>C. mopane</i> Shrub Savanna.   |
| 16              | 28, 35                | Alluvial plains with <i>Faidherbia albida</i> ; or with <i>Salvadora angustifolia</i> Tree Savanna.  |
| 17              | 30, 32                | Recent sand plains with <i>Terminalia sericea</i> Bush Savanna; or with <i>Baphia massaiensis</i> Bush Savanna.  |

### 2.2.3 1km<sup>2</sup> AVHRR data processing.

The AVHRR instruments are carried onboard the National Oceanic and Atmospheric Administration (NOAA) polar-orbiting satellites. Daily AVHRR High Resolution Picture Transmission (HRPT, 1.1 km resolution) data were received by the Satellite Application Centre (SAC) at Hartebeeshoek SA and processed by the Agricultural Research Council, Institute for Soil, Climate and Water (ARC-ISCW). Data from 1985 to 2003 were processed consistently and calibrated to correct for sensor degradation and satellite changes (Rao & Chen, 1995; Rao & Chen, 1996). Due to the failure of NOAA13, data for 1994 were unavailable.

The daily images were geometrically corrected by firstly using the values of orbital parameters and secondly an automated georeferencing system based on 300 ground control image subsets. Images were processed to the Plate Carrée map projection at 1km<sup>2</sup>. Although atmospheric correction of time-series AVHRR data is desirable for inter-annual comparison of NDVI data (Huete & Tucker, 1991; Justice *et al.*, 1991b; El Saleous *et al.*, 2000; Cihlar *et al.*, 2004), no atmospheric correction was performed since atmospheric water vapor and aerosol optical depth data were not available for the entire time-series at sufficiently high resolution - for example, National Center for Environmental Prediction (NCEP) precipitable water vapor data are only available at a 2.5° x 2.5° resolution (Cihlar *et al.*, 1997; Cihlar *et al.*, 2001; DeFelice *et al.*, 2003; Cihlar *et al.*, 2004). A cloud mask was applied based on channel 1, channel 4 and the difference between channels 4 and 5 (Agbu & James, 1994). NDVI was calculated from the red (0.55-0.68 μm) and near infrared (NIR; 0.73-1.1 μm) bands ( $NDVI = (NIR-Red)/(NIR+Red)$  ).

Ten day maximum NDVI composites were calculated to remove residual clouds, reduce atmospheric effects and the influence of varying solar zenith angles (Holben, 1986). Several other procedures have been described that remove noise caused by cloud contamination, atmospheric perturbations or variable solar zenith angles from time-series data (Viovy & Arino, 1992; Yang *et al.*, 1998; Swets *et al.*, 1999). Here a statistical filter was applied to interpolate cloud flagged or atmospherically affected data, identified whenever a relative decrease in the signal of 5% or more was followed within 4 weeks by an equivalent increase (Lo Seen Chong, Mougin & Gastellu-Etchegorry, 1993). The 10-day composites were weighted by the number of days in each composite and summed over the entire growing season, October to April (hereafter referred to as  $\Sigma$ NDVI) (Goward, Tucker & Dye, 1985; Prince, 1991b; Lo Seen Chong *et al.*, 1993; Yang *et al.*, 1998; Diouf & Lambin, 2001). The above-mentioned ten-day compositing, data interpolation and growth season sum procedures all contributed to reducing the atmospheric effects. However, inter-annual comparisons of  $\Sigma$ NDVI may be influenced by the remaining atmospheric effects (Justice *et al.*, 1991b; Cihlar *et al.*, 2004).

#### 2.2.4 *Herbaceous biomass data*

Vegetation condition assessments (VCA) have been conducted at approximately 533 field sites (number varies slightly from year to year) in KNP since 1989 (Trollope, 1990). The number of sites assigned to each landscape (Gertenbach, 1983) was proportional to the area of the Park covered by the specific landscape. The sites were placed evenly throughout each landscape type and in a small number of cases,

following field inspection, their positions were adjusted to avoid local conditions not representative of the landscape as a whole. Fixed sampling areas were then marked at each site.

The VCA surveys are carried out between the end of March and mid-April, commencing whenever the herbaceous vegetation first appears to be drying out. At each site vegetation composition, structure and herbaceous biomass were surveyed (Zambatis, 2002). Within each 50 x 60m site (0.003km<sup>2</sup>), 100 herbaceous biomass estimates were recorded at 2m intervals along four 50m transects using a disc pasture meter. The disc pasture meter was calibrated for wet grass fuel loads (herbaceous biomass - kg/ha) in the seven main landscapes of the KNP by sampling areas that had been lightly, moderately and heavily grazed (Trollope & Potgieter, 1986). Moisture content was estimated using gravimetric methods. A regression equation was derived which accounted for 89.5% of the variation in grass fuel load over these diverse grassland communities (Trollope & Potgieter, 1986):

$$y = -3019 + 2260 \sqrt{x}$$

Where: y = estimated herbaceous biomass – kg/ha

x = mean disc pasture meter height of 100 measurements - cm

$$R^2=0.895$$

The confidence limits ( $P \leq 0.05$ ) of the herbaceous biomass estimates from the disc pasture meter were 286 kg/ha for the mean biomass estimate of 4200 kg/ha and ranged from 328kg/ha for 1500 kg/ha to 526 kg/ha for 9360 kg/ka. This level of precision was considered more than adequate for fire studies in KNP (Trollope & Potgieter, 1986).

The 0.003km<sup>2</sup> sampled at each VCA site in KNP may not be fully representative of the average conditions in the 1km<sup>2</sup> area covered by each AVHRR pixel due to local landscape variations (Reich *et al.*, 1999; Scurlock *et al.*, 1999; Cramer, Olson & Prince, 2001). Field measurements of herbaceous biomass for comparison with 1km<sup>2</sup> AVHRR data typically sampled sites between 4km<sup>2</sup> and 9km<sup>2</sup> (Du Plessis, 1999; Diouf & Lambin, 2001), or multiple transects (or plots) within larger 25km<sup>2</sup> to 100km<sup>2</sup> homogenous sites (Diallo *et al.*, 1991; Wylie *et al.*, 1991). Therefore Landsat ETM+ and TM data were used assess the spatial heterogeneity of the 700m radii around the VCA sites (section 2.2.5).

#### 2.2.5 *Removing highly heterogeneous field sites.*

Landsat 7 ETM+ and Landsat 5 TM NDVI images were used to quantify the heterogeneity of the field sites (Fensholt, Sandholt & Rasmussen, 2004). Two images were selected for each of the two Landsat scenes to coincide with the end of a dry growth season (169-76: 18 March 1998, 168-77: 28 April 2001) and a wet growth season (169-76: 24 April 2000, 168-77: 9 April 2000). The standard deviation (and coefficient of variance) of the Landsat NDVI pixels within a 700m radius centered at each field site were calculated. The standard deviations in the NDVI of sites were slightly higher in the low rainfall growth seasons (1997-98 and 2000-2001), but in all the images the sites with very high standard deviations were generally closer than 600m to rivers and often contained riparian woodland vegetation along drainage channels with seasonal water or bare sand. These sites (N=37) were therefore excluded from further analysis. After this removal there was no relationship between

the Landsat NDVI variation of the sites and their coefficient of determination between biomass and AVHRR  $\Sigma$ NDVI (section 3.2.1). Visual inspection of the Landsat images around each field site, showed that the spatial patterns within the 700m radii were representative of the surrounding landscape pattern. Therefore all remaining sites (N=464) were included in the subsequent analyses.

#### *2.2.6 Rainfall data*

Rainfall measurements were recorded at rain gauges (N=44) in and around KNP (fig. 2.1b). Rain gauges were assigned to one or more LGs during visual interpretation based on distance and topography. The total growth season rainfall (October to April) was calculated for each rain gauge. For each LG the average growth season total rainfall was calculated from all its assigned stations.

#### *2.2.7 Overview of data analyses*

The underlying relationship between  $\Sigma$ NDVI and biomass was first analyzed with  $\Sigma$ NDVI as the dependent variable (section 2.2.8). Thereafter regression analyses were used to predict biomass for each growth season using  $\Sigma$ NDVI as an independent variable to potentially map herbaceous biomass (section 2.2.9).

#### *2.2.8 $\Sigma$ NDVI-biomass relationship*

The underlying relationship between  $\Sigma$ NDVI and biomass was first analyzed with  $\Sigma$ NDVI as the dependent variable.

2.2.8.1 Correlation between growth season mean biomass, mean  $\Sigma$ NDVI and rainfall of landscape groups.

The underlying general relationships between biomass,  $\Sigma$ NDVI and rainfall were investigated by plotting the mean growth season values of all the sites in each LG and calculating the correlation between these means.

2.2.8.2 Regression between  $\Sigma$ NDVI and biomass per site, through time

$\Sigma$ NDVI values were extracted from the single pixels coinciding with the location of each field site. Since both the dependent and independent variables ( $\Sigma$ NDVI and biomass respectively) were subject to error, the geometric mean regression (also known as MODEL II regression) was calculated since ordinary least squares tends to underestimate the true slopes of regression lines (Riggs, Guarnieri & Addelman, 1978). Only field sites with more than nine growth seasons (N=9-13) of biomass data were used and whenever zero biomass was measured at a site, such data were excluded, since these created extreme outliers.

2.2.8.3 Regression between  $\Sigma$ NDVI and biomass, per landscape group, through time.

Data for all the sites and all the years were lumped together for each landscape group to test the strength of the relationship between  $\Sigma$ NDVI and biomass through time. The geometric mean regression was again used because both the  $\Sigma$ NDVI and biomass data were subject to error (Riggs *et al.*, 1978).

#### *2.2.8.4 Influence of tree cover on $\Sigma$ NDVI-biomass relationship.*

In 1996 woody vegetation cover was measured along two 5x50m (500m<sup>2</sup> / 0.0005km<sup>2</sup>) transects at approximately 100 of the VCA sites. The percentage tree cover of each field site was calculated from the crown diameter of all the trees taller than 1.5m. Multiple regression models were created for each landscape group with  $\Sigma$ NDVI as the dependent variable and biomass and tree cover being successively added as independent variables. In this manner it could be tested whether adding tree cover increased the total variance in  $\Sigma$ NDVI accounted for by the linear model.

Fixed point photographs taken in 1984 and in 1996 showed that the density of trees 2-5m in height increased from 10.1% to 12.2% and trees taller than 5m decreased from 4.7% to 2.9%, on soils derived from basalt (LG 12, 13,15) (Eckhardt, Van Wilgen & Biggs, 2000). While on granite soils (LG 1, 2, 4-7) 2-5m tree density increased from 3.5% to 4.5 % and trees taller than 5m decreased from 4.6% to 3.9%. Although these changes were statistically significant and the decrease in the density of large trees (>5m) is a major management concern, these relatively small changes are unlikely to have had a major influence on the signal detected by the AVHRR sensor (Prince, 1987; Fuller, Prince & Astle, 1997). Therefore, it was assumed that tree cover remained unchanged throughout the study period.

#### *2.2.9 Estimating biomass from $\Sigma$ NDVI.*

To investigate the potential for producing biomass maps from the  $\Sigma$ NDVI data (e.g. Diallo *et al.*, 1991), regression analyses were used to predict biomass (dependent variable) for each growth season.

#### 2.2.9.1 Predicting biomass using multiple independent variables.

The landscape group was added as a categorical variable to establish how much of the remaining variance in biomass could be accounted for after using  $\Sigma$ NDVI and the MODIS tree cover estimates as independent variables in multiple regression models. The percentage of the total variance (sums of squares) accounted for by the overall model and each of the independent variables were determined. This percentage is always dependent upon the order in which the independent variables are added to the model, i.e.,  $\Sigma$ NDVI, MODIS tree cover and landscape group. The inclusion of interactions between the variables did not significantly increase the amount of variance explained by the model and therefore interactions were not considered.

#### 2.2.9.2 Estimating biomass using smoothed data.

Since there was considerable variability in the biomass data collected from the small sampling sites, a smoothing procedure was applied to the data to elucidate the predictive ability of  $\Sigma$ NDVI. As described by Du Plessis (1999), ranges of 10 consecutively paired values of biomass and  $\Sigma$ NDVI (ordered according to biomass) were smoothed by calculating the arithmetic means of the pairs. This smoothing method was chosen to demonstrate the underlying relationship between the variables. Other smoothing methods, e.g. moving average smoothing, Gaussian kernel smoothing or spline smoothing, are more appropriate for time series analyses.

## 2.3 Results and Discussion

### 2.3.1 Correlation between growth season mean biomass, mean $\Sigma$ NDVI and rainfall.

There was a positive relationship between the growth season mean biomass and mean  $\Sigma$ NDVI of all the sites in a LG (fig. 2.2). Both mean biomass and mean  $\Sigma$ NDVI were strongly correlated with rainfall and each other (fig. 2.2; table 2.2).

**Table 2.2** Correlation coefficients (r) for each landscape group's relationships derived from growth season average rainfall,  $\Sigma$ NDVI and biomass data.

| Group   | r Biomass- $\Sigma$ NDVI | r Biomass-Rain | r $\Sigma$ NDVI-Rain |
|---------|--------------------------|----------------|----------------------|
| 1       | 0.64                     | 0.88           | 0.63                 |
| 2       | 0.76                     | 0.71           | 0.76                 |
| 3       | 0.86                     | 0.90           | 0.81                 |
| 4       | 0.85                     | 0.85           | 0.82                 |
| 5       | 0.52                     | 0.71           | 0.82                 |
| 6       | 0.67                     | 0.70           | 0.87                 |
| 7       | 0.67                     | 0.75           | 0.88                 |
| 8       | 0.80                     | 0.78           | 0.91                 |
| 9       | 0.92                     | 0.83           | 0.87                 |
| 10      | 0.74                     | 0.55           | 0.88                 |
| 11      | 0.82                     | 0.82           | 0.83                 |
| 12      | 0.89                     | 0.89           | 0.93                 |
| 13      | 0.84                     | 0.85           | 0.94                 |
| 14      | 0.80                     | 0.71           | 0.85                 |
| 15      | 0.75                     | 0.63           | 0.77                 |
| 16      | 0.65                     | 0.72           | 0.92                 |
| 17      | 0.67                     | 0.60           | 0.82                 |
| average | 0.76                     | 0.76           | 0.84                 |

The average of the correlation coefficients of all the LGs for biomass- $\Sigma$ NDVI, biomass-rainfall and  $\Sigma$ NDVI-rainfall were 0.76, 0.76 and 0.84 respectively. However, if the extreme dry (low biomass) growth seasons and the wet (high biomass) growth seasons were excluded (fig. 2.2), the relationship for the remaining average growth seasons would not be as strong.

The biomass measured in each LG, each growth season varied considerably with an average range (maximum – minimum) of 4570 kg/ha. The corresponding average standard deviation was approximately 50% of the mean biomass (fig. 2.2). The influence of herbivory by vertebrates and insects on the end-of-season biomass could not be taken into account because detailed data of the distribution and intensity of herbivory are not available. Differences in the intensity of herbivory at the sampling sites, as well as variations in soils within LGs, may have contributed to the large variation in biomass measurements observed within a LG for a single growth season (fig. 2.2).

The  $\Sigma$ NDVI of KNP was strongly related to rainfall (figs 2.2, 2.3 and 2.4). The effects of the 1991-92, 1997-98 and 2002-3 El Niño's and the 1999-2000 La Niña conditions on the  $\Sigma$ NDVI were clearly visible (figs 2.3 and 2.4)(Anyamba, Tucker & Mahoney, 2002). The geographical pattern of  $\Sigma$ NDVI reflected the general patterns of rainfall and biomass.

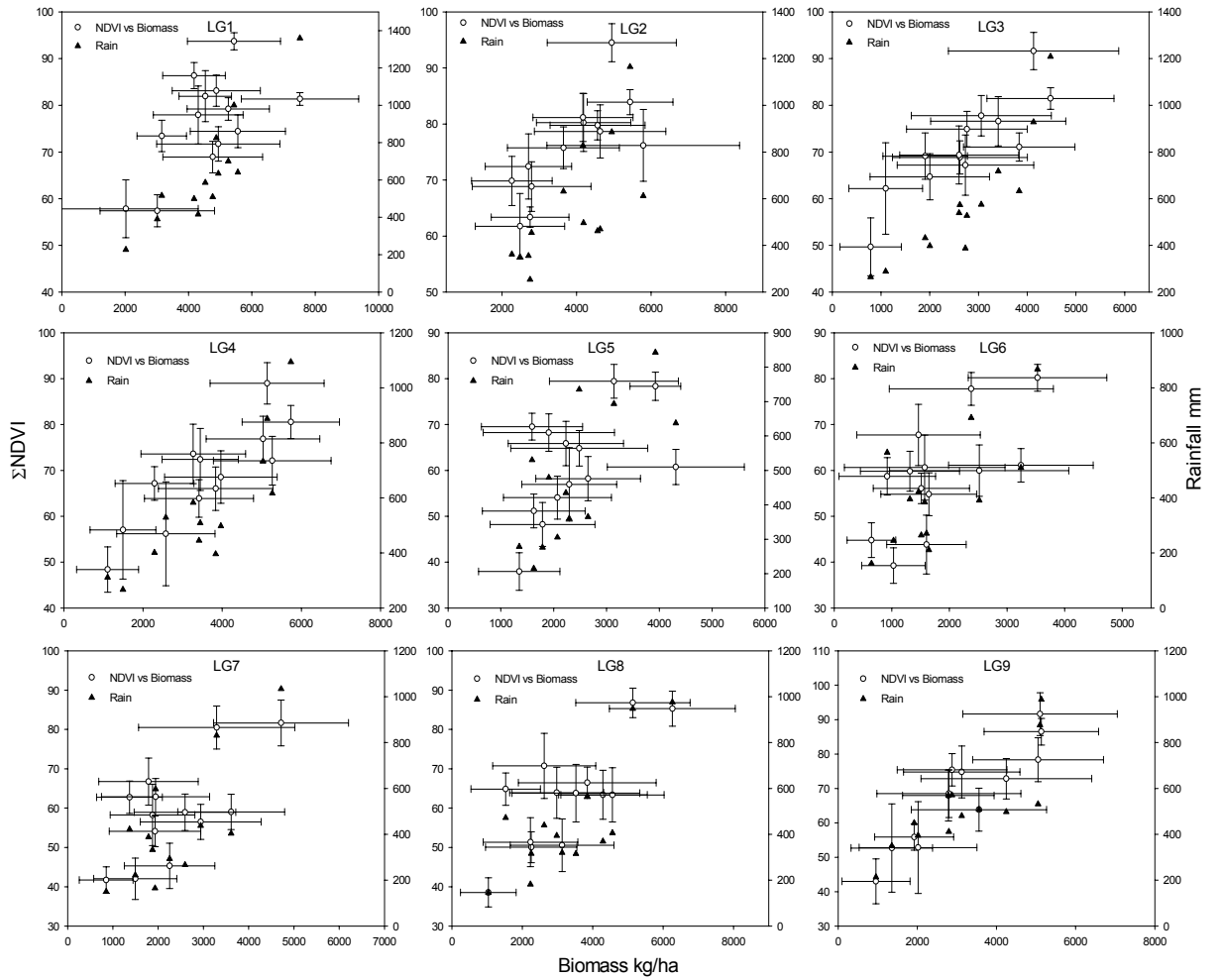


**Figure. 2.2** Growth season average  $\Sigma$ NDVI, biomass and rainfall for each landscape group. The landscape groups are described in Table 2.1 and mapped in fig. 2.1b. Error bars indicate  $\pm$  one standard deviation.

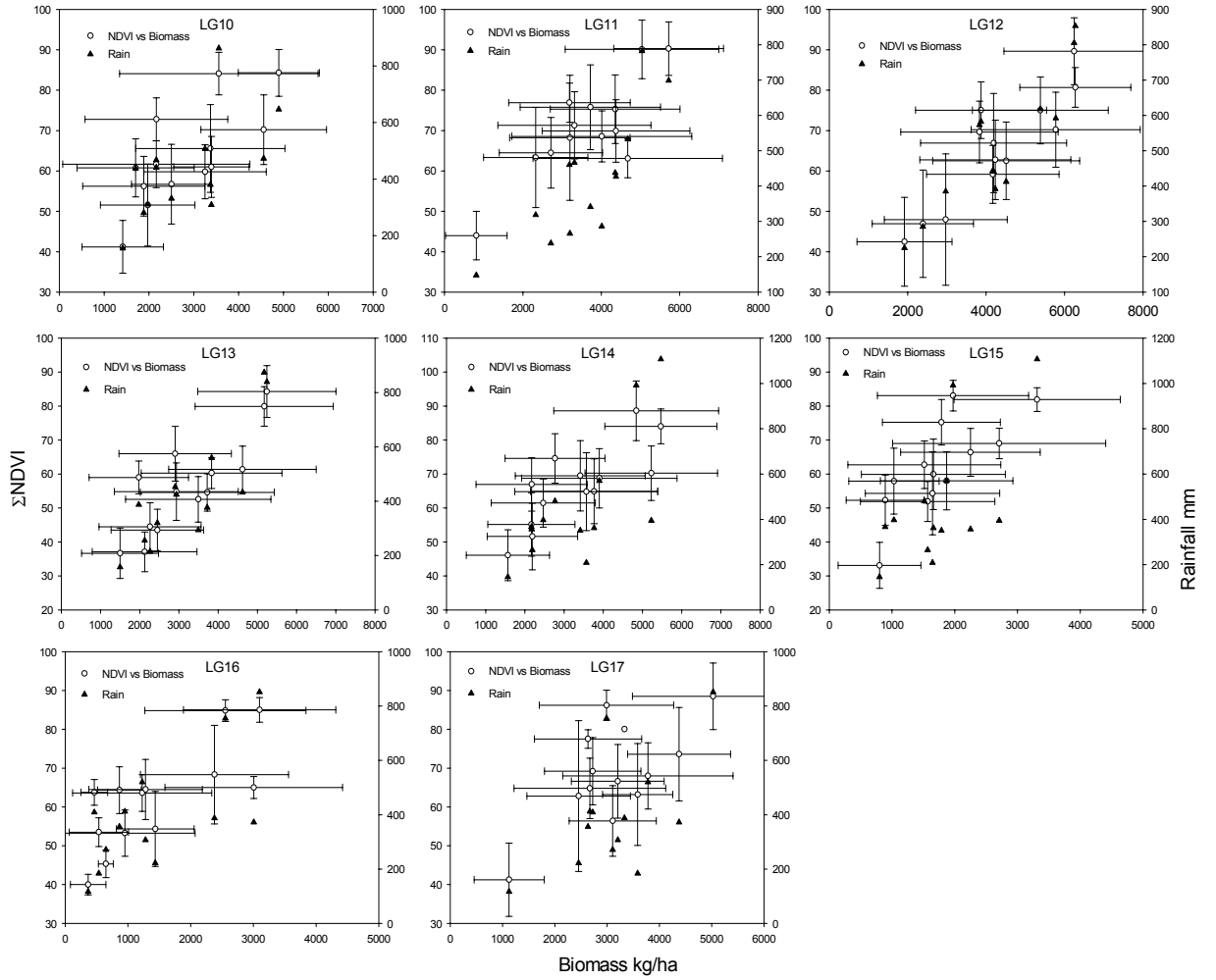


**Figure 2.2 *continue*.** Growth season average  $\Sigma$ NDVI, biomass and rainfall for each landscape group. The landscape groups are described in Table 2.1 and mapped in fig. 2.1b. Error bars indicate  $\pm$  one standard deviation.

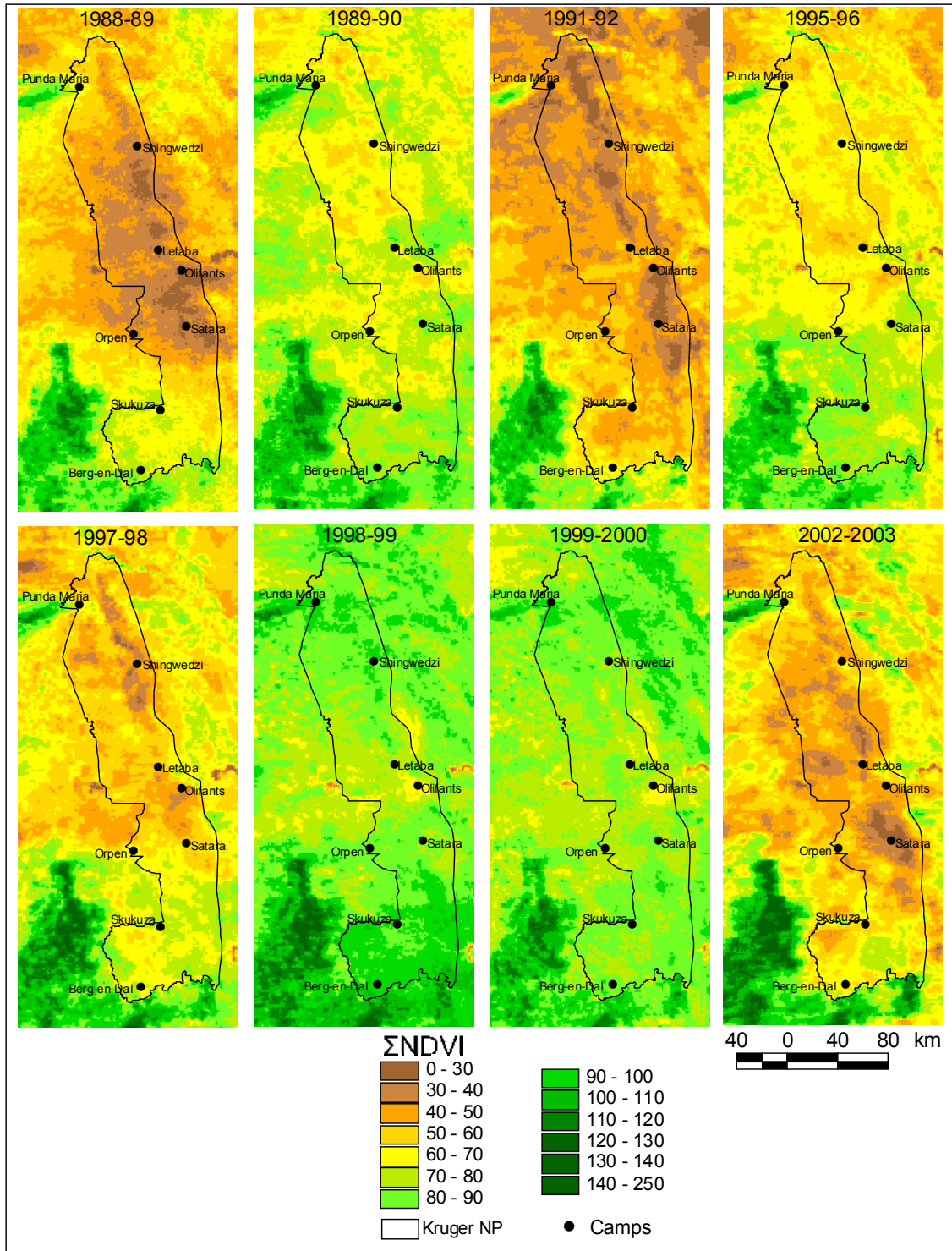


**Figure 2.3** Growth season sum NDVI of Kruger National Park for selected growth seasons.

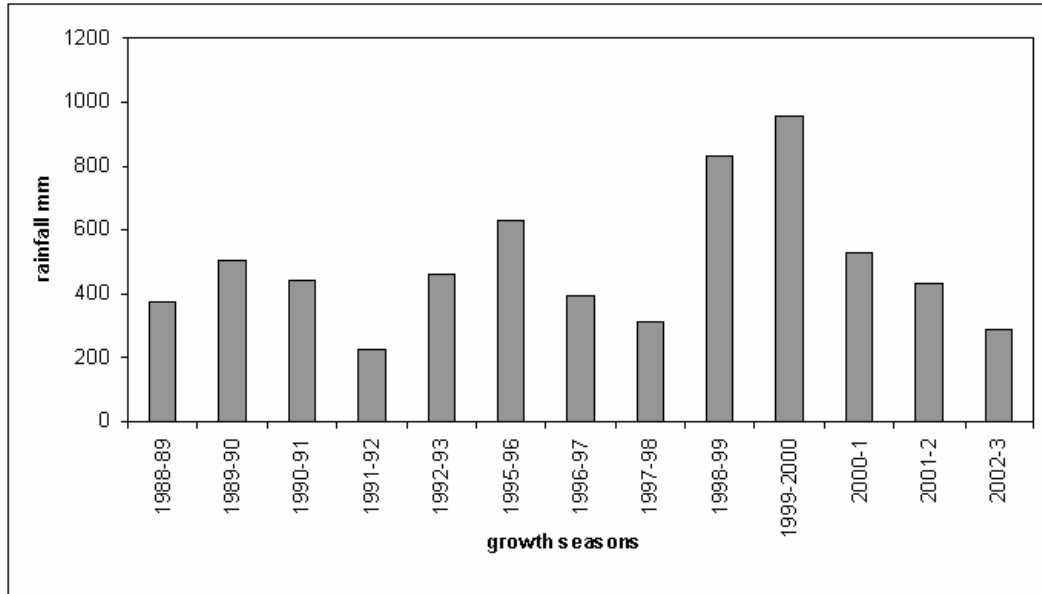


**Figure 2.4** Average growth season rainfall of Kruger National Park, 1989-90 to 2002-2003.

### 2.3.2 $\Sigma$ NDVI-biomass relationship

#### 2.3.2.1 Relationship between $\Sigma$ NDVI and biomass per site, through time.

The coefficients of determination ( $R^2$ ) for the field sites varied from 0.01 to 0.93 with an average of 0.42 (fig. 2.1c). In general  $R^2 > 0.3$  were statistically significant ( $p \leq 0.05$ , degrees of freedom = 7-11). Sites with similar strength of the relationship were somewhat clumped with high values occurring in groups (fig. 2.1c). The reason for this clumped pattern has not yet been determined. Figure 2.5 gives an example of a single field site near Skukuza with a strong  $\Sigma$ NDVI-biomass relationship ( $R^2=0.8$ ). It is clear that rainfall had a very strong influence on the biomass and therefore the  $\Sigma$ NDVI (fig. 2.5).

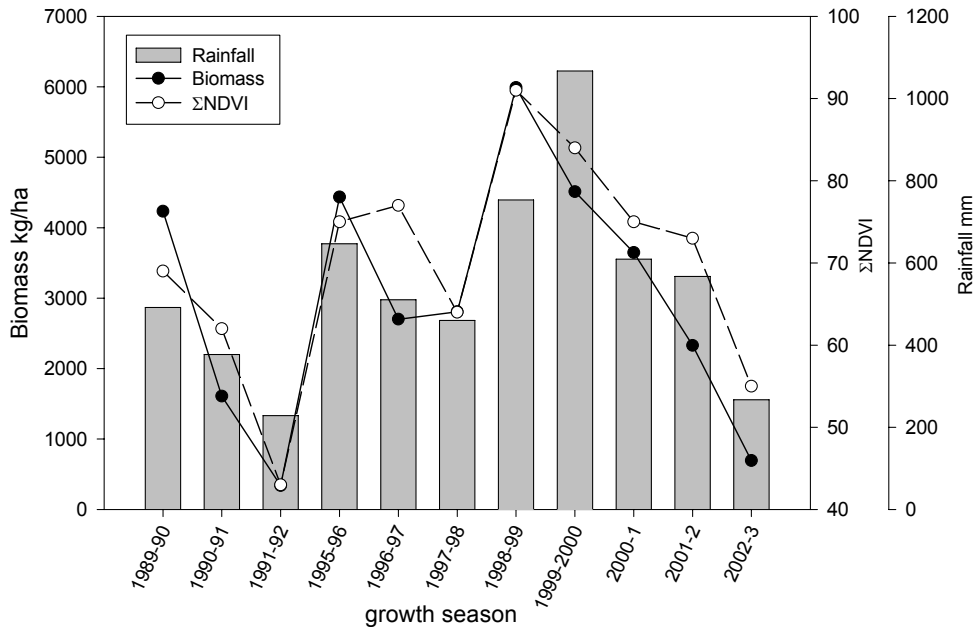


**Figure 2.5** Herbaceous biomass and ΣNDVI for a field site near Skukuza where the rainfall was recorded.

The heterogeneity of the sites, as estimated by the standard deviation of Landsat NDVI, did not appear to be related to the strength of the site's biomass-ΣNDVI (AVHRR) relationship. The sites had coefficients of variance in Landsat NDVI of 8-16%. Using the Landsat imagery, visual inspection of the 700m radius area around sites with low  $R^2$  values did not reveal any obvious landscape features that may have caused weak relationships, except for only two sites which contained a reservoir and bare ground, respectively. Some adjacent sites which had contrasting  $R^2$  values, appeared to have the same landscape pattern according to the Landsat imagery.

Low  $R^2$  values could have been the results of outliers that often have large impacts on the strength of linear relationships determined from the short time series available for the study (9-13 seasons). Senesced material of the previous growth

season, which had not been utilized or decomposed, can also affect the disk pasture meter. No attempt was made to differentiate this “old” material from the material of the current growth season. The ratio of “old” to “new” material depends on the rainfall of the previous and current years and thus varies from year to year. Since senesced material does not contribute to  $\Sigma$ NDVI, but influences the biomass estimates, it may have weakened the  $\Sigma$ NDVI-biomass relationship. Variations in the timing of rainfall can lead to variations in the onset and duration of the actual growth period between growth seasons. This could affect the relationship between the end-of-season measurements and the actual vegetation production, which may further have weakened the  $\Sigma$ NDVI-biomass relationship.

2.3.2.2 Regression between  $\Sigma$ NDVI and biomass, per landscape group, through time.

The coefficients of determination ranged from 0.08 (LG 17) to 0.41 (LG 4), with an average of 0.26 (table 2.3; for all LGs  $p < 0.03$ ). These  $R^2$  values were generally much lower than those calculated for the individual sites (section 2.3.1 ). Thus, grouping data together from different sites within a specific LG may obscure the relationship that exists on a site-to-pixel basis due to landscape variation in the LG. When all the data were grouped together for all growth seasons and all landscape groups, the overall  $R^2 = 0.28$ , which was much lower than the  $R^2 = 0.56$  reported by Prince and Tucker (1986) for a similar analysis in Botswana.

**Table 2.3** Coefficients of determination ( $R^2$ ) for  $\Sigma$ NDVI-biomass relationships for each landscape group and changes in  $R^2$  after adding tree cover to the regression. Tree cover was measured at a total of 100 sites (tree sites).

| Group   | $R^2$ $\Sigma$ NDVI-biomass, |              | $R^2$ $\Sigma$ NDVI-biomass, | $R^2$ $\Sigma$ NDVI-biomass |                   |
|---------|------------------------------|--------------|------------------------------|-----------------------------|-------------------|
|         | all sites                    | % tree cover | tree sites                   | + tree cover                | increase in $R^2$ |
| 1       | 0.17                         | 32.1         | 0.15                         | 0.15                        | 0.00              |
| 2       | 0.26                         | 9.6          | 0.39                         | 0.43                        | 0.04              |
| 3       | 0.27                         | 40.1         | 0.36                         | 0.39                        | 0.03              |
| 4       | 0.41                         | 17.7         | 0.50                         | 0.50                        | 0.00              |
| 5       | 0.11                         | 23.5         | 0.05                         | 0.12                        | 0.07              |
| 6       | 0.24                         | 33.0         | 0.33                         | 0.33                        | 0.00              |
| 7       | 0.21                         | 28.6         | 0.20                         | 0.20                        | 0.00              |
| 8       | 0.31                         | 28.6         | 0.17                         | 0.23                        | 0.06              |
| 9       | 0.40                         | 19.4         | 0.21                         | 0.67                        | 0.46              |
| 10      | 0.11                         | 67.0         | 0.16                         | 0.53                        | 0.37              |
| 11      | 0.37                         | 31.4         | 0.24                         | 0.46                        | 0.22              |
| 12      | 0.39                         | 12.8         | 0.32                         | 0.33                        | 0.01              |
| 13      | 0.31                         | 6.8          | 0.30                         | 0.30                        | 0.00              |
| 14      | 0.33                         | 12.3         | 0.41                         | 0.42                        | 0.01              |
| 15      | 0.12                         | 42.7         | 0.14                         | 0.31                        | 0.17              |
| 16      | 0.36                         | 54.2         | NA                           | NA                          | NA                |
| 17      | 0.08                         | 2.8          | NA                           | NA                          | NA                |
| average | 0.26                         | 27.20        | 0.26                         | 0.36                        | 0.10              |

2.3.2.3 *Influence of tree cover on biomass- $\Sigma$ NDVI relationship.*

The average tree cover for all the sites in KNP was approximately 20%. LGs 8, 9, 10, 11, and 15 showed some increase in  $R^2$  after adding the tree cover to the multiple regression model ( $p < 0.01$ ). There was no clear relationship between the increase in  $R^2$  by adding tree cover to the model and the average tree cover of the LGs (table 2.3). For example, some LGs with tree covers ranging from 0-54% showed no improvement in the  $R^2$  after adding tree cover to the model. These results were expected, since radiative transfer models and field observations have shown that the herbaceous layer in savanna woodlands dominates the signal detected by AVHRR or other sensors, especially during the growth season (Prince, 1987; Fuller *et al.*, 1997).

As described in Botswana (Prince & Tucker, 1986), there appears to be a negative correlation between herbaceous cover and tree cover (fig. 2.6). All the growth seasons showed similar trends to the 1995-96 season which was plotted here (fig. 2.6). The correlation coefficients of the different growth seasons ranged from -0.2 to -0.4 for the relationship between herbaceous biomass and tree cover. Plotting the trend lines of biomass vs.  $\Sigma$ NDVI for all the sites and all the years, grouped into classes according to tree cover, revealed that sites with higher tree cover had higher  $\Sigma$ NDVI values for a specific level of herbaceous biomass (fig. 2.7). The same effect was described by Prince (1991b) and Diallo *et al.* (1991). Therefore, although the tree cover in KNP did not appear to have a major influence on the biomass- $\Sigma$ NDVI relationship, the results suggest that tree cover should not be ignored. Unfortunately measurements of woody vegetation were only conducted at 100 of the sites and therefore the influence of the woody component could not be specified for all sites. It is also uncertain how representative the 0.0005km<sup>2</sup> area sampled in the woody component surveys was of the surrounding 1km<sup>2</sup> landscape.

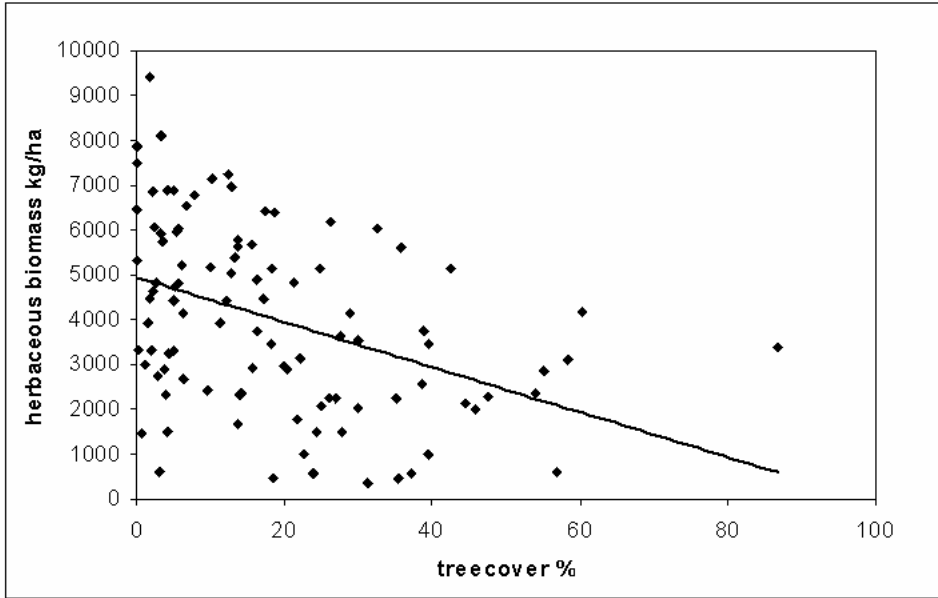


**Figure 2.6** Relationship between herbaceous biomass and percentage tree cover measured at selected field sites (N=100) for the 1995-96 growth season.

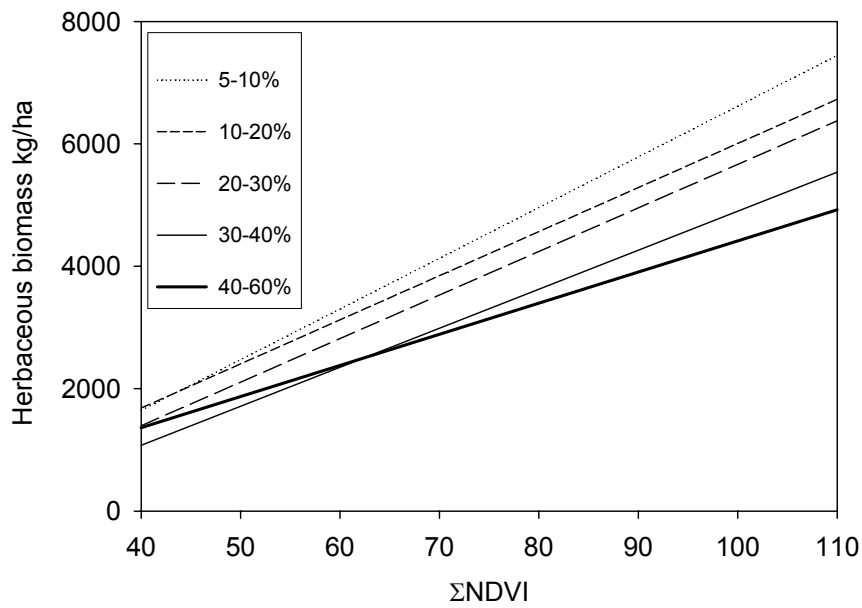


**Figure 2.7** Trend lines of  $\Sigma$ NDVI vs. herbaceous biomass for field sites grouped according to tree cover ranges.

### 2.3.3 *Estimating biomass from $\Sigma$ NDVI*

#### 2.3.3.1 *Predicting biomass using multiple independent variables.*

The  $R^2$  values of the models for the individual growth seasons varied between 0.23 and 0.48, and were all highly significant ( $p < 0.001$ ), with the exception of 2002-3 (table 2.4). The average  $R^2$  of all the growth seasons was 0.36. The amount of variance accounted for by  $\Sigma$ NDVI varied considerably between growth seasons from 0% to 25%. During the three driest growth seasons (1991-92, 2001-2002, 2002-2003, fig. 2.4),  $\Sigma$ NDVI explained the smallest percentages of the variance ( $\leq 4\%$ , table 2.4). For individual growth seasons, the  $\Sigma$ NDVI generally accounted for less variance than reported by similar studies, e.g.  $R^2 = 0.68$  (Diouf & Lambin, 2001). In accordance with the findings of Diouf and Lambin (2001), the relationship between biomass and  $\Sigma$ NDVI changed between growth seasons. When the data for all the growth seasons were analyzed together, and the growth seasons (e.g. 1996-97) added as the final categorical independent variable to the overall multiple regression model, the  $R^2$  increased to 0.5, which was slightly lower, but comparable to the results of similar regression analyses (Prince & Astle, 1986; Prince & Tucker, 1986). The MODIS tree cover accounted for only 1-4% of the variance. Although these contributions were statistically significant ( $p < 0.01$ ), including the MODIS tree cover did not lead to any substantial improvements in the predictive ability of the model (table 2.4).

The landscape groups accounted for 13-30% of the total variation in biomass (table 2.4). This indicates the importance of including landscape group in the predictive model. The average 95% confidence limits over the entire range of the predicted biomass values were  $\pm 700$  kg/ha.

**Table 2.4** Multiple regression analyses to predict biomass from independent variables  $\Sigma$ NDVI, MODIS tree cover and landscape group. Percentage of the total sums of squares explained (and significance levels) by successively adding the variables to models.  $R^2$  and average standard error of maximal model including all variables.

| growth season | variables        | $R^2$ | average standard error | Percentage of total sums of squares | F-value | Pr(f)  |
|---------------|------------------|-------|------------------------|-------------------------------------|---------|--------|
| 1988-89       |                  | 0.41  | 346                    |                                     |         |        |
|               | $\Sigma$ NDVI    |       |                        | 25.3                                | 178.4   | <0.001 |
|               | MODIS tree cover |       |                        | 1.4                                 | 10      | <0.001 |
|               | landscape group  |       |                        | 13.9                                | 6.1     | <0.001 |
| 1989-90       |                  | 0.42  | 352                    |                                     |         |        |
|               | $\Sigma$ NDVI    |       |                        | 24.2                                | 194.9   | <0.001 |
|               | MODIS tree cover |       |                        | 1.8                                 | 14.5    | <0.001 |
|               | landscape group  |       |                        | 16.4                                | 8.2     | <0.001 |
| 1990-91       |                  | 0.38  | 380                    |                                     |         |        |
|               | $\Sigma$ NDVI    |       |                        | 8.2                                 | 60.5    | <0.001 |
|               | MODIS tree cover |       |                        | 2.6                                 | 19.1    | <0.001 |
|               | landscape group  |       |                        | 27.0                                | 12.4    | <0.001 |
| 1991-92       |                  | 0.26  | 301                    |                                     |         |        |
|               | $\Sigma$ NDVI    |       |                        | 4.0                                 | 20.9    | <0.001 |
|               | MODIS tree cover |       |                        | 0.7                                 | 3.9     | 0.04   |
|               | landscape group  |       |                        | 21.9                                | 7.1     | <0.001 |
| 1992-93       |                  | 0.43  | 332                    |                                     |         |        |
|               | $\Sigma$ NDVI    |       |                        | 23.8                                | 187.3   | <0.001 |
|               | MODIS tree cover |       |                        | 3.2                                 | 25      | <0.001 |
|               | landscape group  |       |                        | 16.2                                | 7.9     | <0.001 |
| 1995-96       |                  | 0.42  | 440                    |                                     |         |        |
|               | $\Sigma$ NDVI    |       |                        | 20.9                                | 175.4   | <0.001 |
|               | MODIS tree cover |       |                        | 3.6                                 | 30.6    | <0.001 |
|               | landscape group  |       |                        | 18.3                                | 9.6     | <0.001 |
| 1996-97       |                  | 0.34  | 409                    |                                     |         |        |
|               | $\Sigma$ NDVI    |       |                        | 12.0                                | 88.6    | <0.001 |
|               | MODIS tree cover |       |                        | 3.5                                 | 25.9    | <0.001 |
|               | landscape group  |       |                        | 18.5                                | 8.5     | <0.001 |
| 1997-98       |                  | 0.39  | 372                    |                                     |         |        |
|               | $\Sigma$ NDVI    |       |                        | 22.2                                | 178.8   | <0.001 |
|               | MODIS tree cover |       |                        | 2.2                                 | 17.6    | <0.001 |
|               | landscape group  |       |                        | 15.1                                | 7.5     | <0.001 |

**Table 2.4** *continue*

| growth season | variables                        | R <sup>2</sup> | average standard error | Percentage of total sums of squares | F-value | Pr(f)  |
|---------------|----------------------------------|----------------|------------------------|-------------------------------------|---------|--------|
| 1998-99       |                                  | 0.4            | 439                    |                                     |         |        |
|               | ΣNDVI                            |                |                        | 19.5                                | 164.1   | <0.001 |
|               | MODIS tree cover landscape group |                |                        | 4.2                                 | 35.5    | <0.001 |
| 1999-2000     |                                  | 0.4            | 444                    |                                     |         |        |
|               | ΣNDVI                            |                |                        | 9.1                                 | 52.8    | <0.001 |
|               | MODIS tree cover landscape group |                |                        | 1.9                                 | 10.9    | <0.001 |
| 2000-1        |                                  | 0.28           | 465                    |                                     |         |        |
|               | ΣNDVI                            |                |                        | 13.2                                | 82.48   | <0.001 |
|               | MODIS tree cover landscape group |                |                        | 2.6                                 | 16.02   | <0.001 |
| 2001-2        |                                  | 0.28           | 432                    |                                     |         |        |
|               | ΣNDVI                            |                |                        | 4.2                                 | 22.4    | <0.001 |
|               | MODIS tree cover landscape group |                |                        | 3.6                                 | 19.2    | <0.001 |
| 2002-3        |                                  | 0.23           | 327                    |                                     |         |        |
|               | ΣNDVI                            |                |                        | 0.0                                 | 0.001   | 0.98   |
|               | MODIS tree cover landscape group |                |                        | 19.0                                | 6.6     | <0.001 |
| Average       | Average                          | 0.385          | 381.5                  |                                     |         |        |

**2.3.3.2** *Estimating biomass using smoothed data*

The coefficient of determination increased considerably after performing the regressions on the smoothed data, from an average of R<sup>2</sup>=0.14 to 0.56 (table 2.5). With the exception of the 2002-3 season, all regressions were highly significant, p<0.01 (degrees of freedom = 38-47). The very dry 2002-2003 season had a very weak relationship. When the 2002-2003 season was excluded, the average R<sup>2</sup> for the smoothed data was 0.6, comparable to studies where larger field sites were sampled (Prince & Tucker, 1986; Nicholson *et al.*, 1990; Diallo *et al.*, 1991; Prince, 1991b;

Wylie *et al.*, 1991; Diouf & Lambin, 2001). Based on the 95% confidence intervals associated with the predicted biomass, the error of the prediction was  $\pm 300$  kg/ha around the average biomass measured in a specific growth season (fig. 2.8). Predictions of biomass were less accurate in dry years where biomass values were very low (e.g. 2002-3, 1991-92, 2001-2) (fig. 2.8; table 2.5).

**Table 2.5** Coefficients of determination ( $R^2$ ) for predicting biomass from  $\Sigma$ NDVI using smoothed data.

| growth season | $R^2$ raw data | $R^2$ smoothed data |
|---------------|----------------|---------------------|
| 1988-89       | 0.25           | 0.79                |
| 1989-90       | 0.24           | 0.83                |
| 1990-91       | 0.08           | 0.4                 |
| 1991-92       | 0.04           | 0.4                 |
| 1992-93       | 0.24           | 0.76                |
| 1995-96       | 0.21           | 0.73                |
| 1996-97       | 0.12           | 0.52                |
| 1997-98       | 0.22           | 0.77                |
| 1998-99       | 0.2            | 0.64                |
| 1999-00       | 0.1            | 0.53                |
| 2000-1        | 0.13           | 0.63                |
| 2001-2        | 0.04           | 0.28                |
| 2002-3        | 0.007          | 0.007               |
| average       | 0.14           | 0.56                |

When the smoothed data of all the growth seasons were included in a single regression analysis, the  $\Sigma$ NDVI explained 35% of the variance. This increased to 66% after adding the growth season as a categorical variable, thus allowing different regression lines for each year. These results were in agreement with other studies (Prince & Astle, 1986; Diallo *et al.*, 1991; Diouf & Lambin, 2001) and suggest that separate predictive equations should be developed for each growth season using annual field measurements.

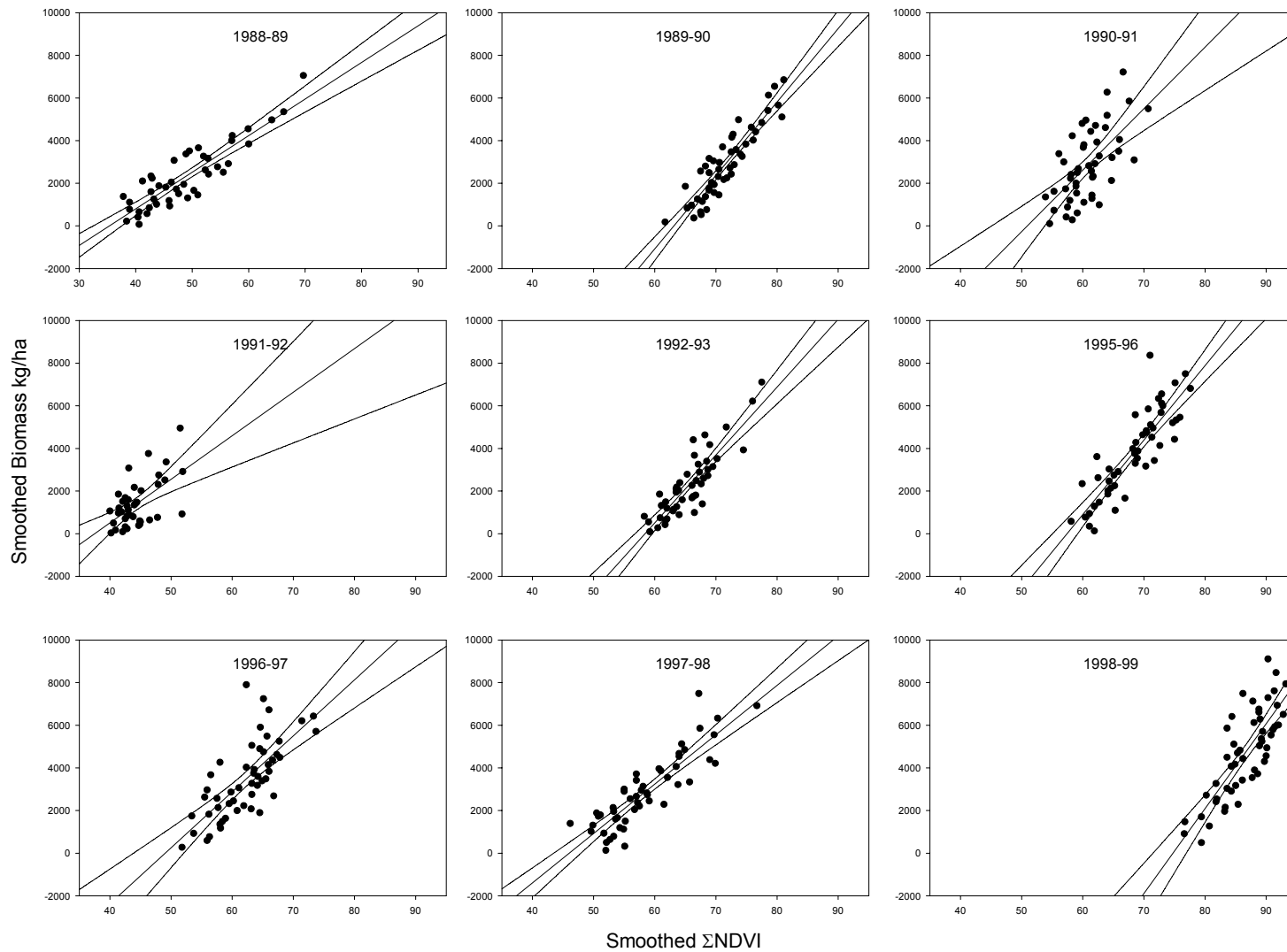


**Figure 2.8** Smoothed biomass and  $\Sigma$ NDVI data of each growth season and their linear regression. The 95% confidence limits are indicated.

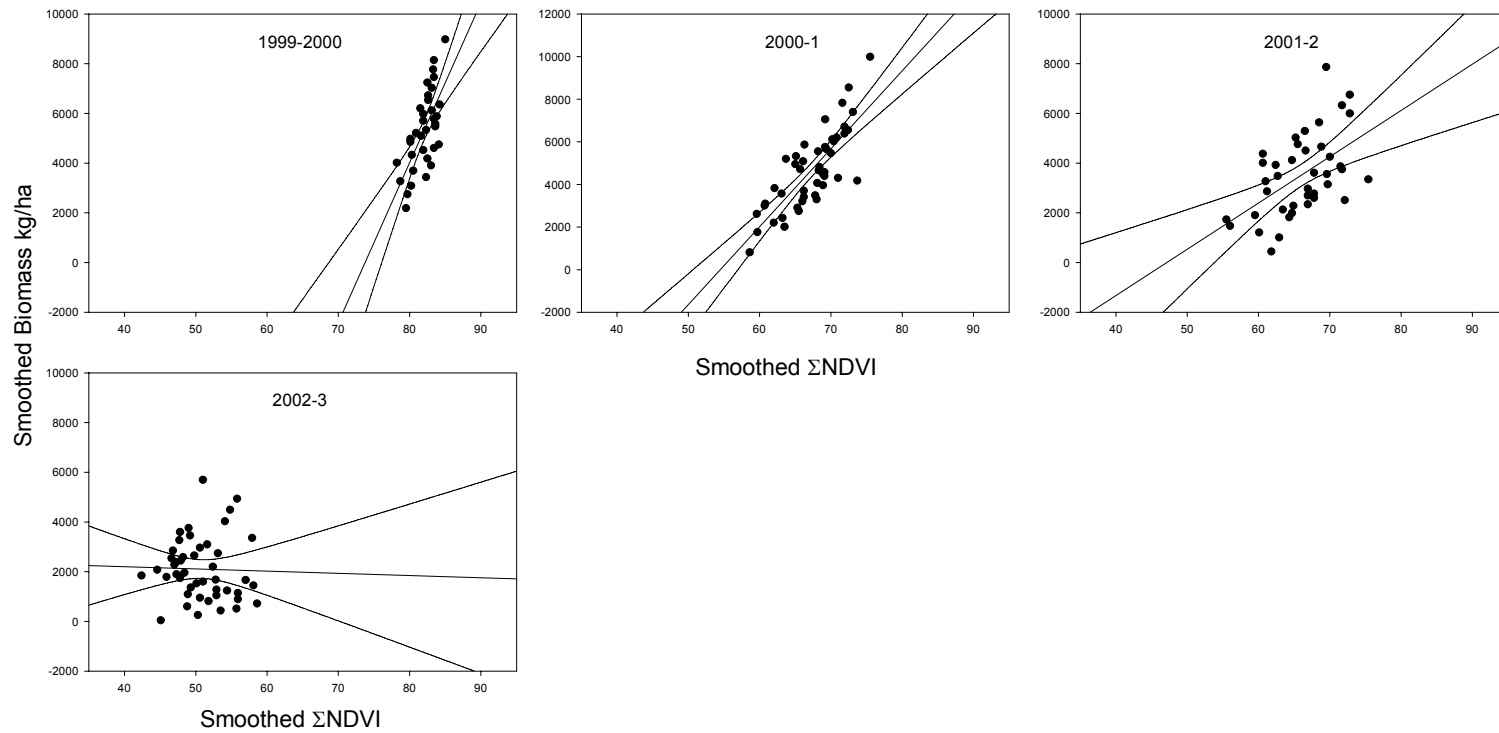


**Figure 2.8 *continue*** Smoothed biomass and  $\Sigma$ NDVI data of each growth season and their linear regression. The 95% confidence limits are indicated.

## 2.4 Conclusions

This study analyzed two unique long-term data sets (1989 to present), i.e. herbaceous biomass measurements at 533 sites and a consistently processed 1km<sup>2</sup> AVHRR NDVI archive, in one of the largest protected areas in the world. The long-term data allowed the  $\Sigma$ NDVI-biomass relationships to be investigated at each individual field site. Although the  $R^2$  values varied greatly, they were moderately high (average  $R^2 = 0.42$ , fig. 2.1c). Landsat imagery enabled highly heterogeneous field sites to be omitted, but did not help to explain why some sites had very weak  $\Sigma$ NDVI-biomass relationships, while similar, adjacent sites had strong relationships. The  $\Sigma$ NDVI-biomass relationship could have been weakened by (i) variations in distribution and intensity of herbivory, (ii) the influence of senescent material from the previous growth season on the biomass measurements and (iii) variations in the onset and duration of actual growth period in relation to the end-of-season biomass measurements.

Growth season mean values for biomass,  $\Sigma$ NDVI and rainfall calculated for each LG were highly correlated (fig. 2.2; table 2.2).  $\Sigma$ NDVI images also clearly reflected the impacts of contrasting rainfall conditions (figs 2.3 and 2.4). Thus, this study demonstrated a relatively strong underlying relationship between biomass, rainfall and  $\Sigma$ NDVI for this new region in accord with studies of other areas (Nicholson *et al.*, 1998; Du Plessis, 1999; Diouf & Lambin, 2001). The KNP biomass estimates can also be compared to other remotely sensed estimates of vegetation activity, e.g. SPOT-VEGETATION derived production estimates (Veroustraete, Sabbe & Eerens, 2002), Global Production Efficiency Model (GLO-PEM) NPP

(Prince & Goward, 1995; Cao *et al.*, 2004), or Moderate Resolution Imaging Spectroradiometer (MODIS) products (Huete *et al.*, 2002; Fensholt *et al.*, 2004).

Although the regression analyses showed that measured tree cover and MODIS estimates of tree cover did not have a major influence on the  $\Sigma$ NDVI-biomass relationship (tables 2.2 and 2.5) (Prince, 1987; Fuller *et al.*, 1997), other results presented here suggest that tree cover should not be ignored when trying to predict herbaceous biomass (figs 2.6 and 2.7). Although the coarse resolution MODIS tree cover data were not useful, more accurate tree cover data derived from higher resolution Landsat ETM+ data and Ikonos data (e.g. Hansen *et al.*, 2002) might be employed to improve herbaceous biomass estimates from the AVHRR data.

The predictive value of the  $\Sigma$ NDVI may have been underestimated in this study, since the biomass measurements were taken from very small sites (50m x 60m) which are shown here to exhibit considerable variability (fig. 2.2). The standard deviation of biomass measured at all the sites in one growth season for a single LG, was approximately 50% of the mean (fig. 2.2). The variability in the biomass can mainly be attributed to local variations in soils and terrain within the LGs. This variability appeared to be the reason for the relatively low  $R^2$  values attained when predicting a growth season's biomass from  $\Sigma$ NDVI using the raw (unsmoothed) data (table 2.5). The regression analyses based on the smoothed data significantly increased the coefficients of determination to values comparable with other studies (table 2.5) (Prince & Tucker, 1986; Nicholson *et al.*, 1990; Diallo *et al.*, 1991; Prince, 1991b; Wylie *et al.*, 1991; Diouf & Lambin, 2001).

The AVHRR  $\Sigma$ NDVI was able to adequately estimate inter-annual variations in the biomass at single sites, but on an annual basis the relationship derived from all the sites was not strong enough for the production of reliable growth season biomass maps. However, the biomass data were sampled from very small field sites that were probably not fully representative of the large area ( $>1\text{km}^2$ ) observed by the AVHRR pixels and as a result the true predictive capability of remote sensing data was not sufficiently tested. A supplementary sampling strategy that consists of a number of biomass measurements over a larger area for each field site (e.g.  $1\text{km}^2$  or larger) is likely to be able to account for the variability in biomass (Zheng *et al.*, 2003) and this would improve the strength of biomass- $\Sigma$ NDVI relationships observed in a single growth season. Therefore, although there is little doubt that the  $\Sigma$ NDVI derived growth season biomass maps should be more reliable than the currently used interpolations of the point measurements; supplementary field sampling will be needed to establish the true accuracy of the biomass maps. KNP management have stated that the desired accuracy of the biomass maps is  $\pm 500$  kg/ha (95% confidence limits) and in the current study the accuracy was  $\pm 700$  kg/ha. It is therefore conceivable that the desired accuracy can be achieved with more appropriate field sampling.

This research has clearly illustrated the ability of  $1\text{km}^2$  AVHRR  $\Sigma$ NDVI to estimated inter-annual changes in vegetation production and should therefore be useful for monitoring primary production as an indicator of land degradation. The historical time-series of  $1\text{km}^2$  AVHRR data can also provide essential spatial information on ecosystem variability and resilience in KNP (Wessels *et al.*, 2004).

KNP has adopted a Strategic Adaptive Management (SAM) program with clear ecosystem management goals based on environmental indicators and their thresholds potential concern (Biggs & Rogers, 2003). It is envisaged that remotely sensed environmental indicators, e.g. measures of vegetation production derived from AVHRR or MODIS data, will be incorporated into KNP's operational monitoring system to assist the SAM program. This approach could be expanded beyond KNP to monitoring and management natural rangelands and combat land degradation throughout SA.

## **Chapter 3. Assessment of the effects of human-induced land degradation in the former homelands of northern South Africa with a 1km AVHRR NDVI time-series.**

### **3.1 Introduction**

Land degradation describes circumstances of reduced biological productivity of the land (UNCCD, 1994; Reynolds & Stafford Smith, 2002b). Vegetation production and biomass have been successfully estimated with the Normalized Difference Vegetation Index (NDVI) derived from satellite data (Deering, 1975; Prince & Tucker, 1986; Tucker & Sellers, 1986; Prince, 1991b; Jury *et al.*, 1997; Myneni *et al.*, 1997). In arid and semi-arid lands seasonal sums of multi-temporal NDVI are strongly correlated with vegetation production (Prince & Tucker, 1986; Prince, 1991b; Nicholson & Farrar, 1994; Nicholson *et al.*, 1998).

Human induced land degradation most likely alters the vegetation cover and function before, for example, increasing the extent of soil erosion or changing the local climate through positive feedbacks (Charney *et al.*, 1977; Xue & Fennessy, 2002). If so, changes in  $f_{PAR}$  should be among the first factors related to primary production that can alert us to degradation. Therefore, remotely sensed NDVI may provide the basis for an early warning of degradation. NDVI derived from the Advanced Very High Resolution Radiometer (AVHRR) has shown to be capable of systematic, repeatable and spatially extensive monitoring of vegetation productivity to assess desertification (Prince & Justice, 1991; Tucker *et al.*, 1991a; Tucker *et al.*,

1991b; Nicholson *et al.*, 1998; Prince *et al.*, 1998; Diouf & Lambin, 2001). The remaining challenge in developing a monitoring approach is how to interpret the NDVI data so that human impacts can be distinguished from both natural spatial variation in the landscape and short-term inter-annual climate variability that is particularly pronounced in SA due to the El Niño-Southern Oscillation (ENSO) phenomenon (Anyamba & Eastman, 1996; Jury *et al.*, 1997; Anyamba *et al.*, 2002). To address this issue we compared a time-series of seasonally integrated 1km AVHRR NDVI of well-known degraded rangelands with non-degraded rangelands with the same climate and soils. The objectives were, (i) quantified the difference in integrated NDVI of degraded and non-degraded areas and (ii) compared the resilience and stability of vegetation production in degraded and non-degraded areas to natural rainfall variability.

### **3.2 Land degradation in the communal lands of South Africa**

As part of SA's effort to develop a National Action Plan in accordance with the UNCCD, Hoffman *et al.* (1999) prepared the "National Review of Land Degradation in South Africa" (NRLD). The NRLD was based on a systematic survey (Liniger & Van Lyden, 1998) of the perceptions of 453 agricultural extension workers and resource conservation technicians about the degradation status of 367 magisterial districts. From these surveys various indices of the severity, extent and rates of different types of degradation (such as reduced vegetation cover, plant species composition and bush encroachment) were estimated. Districts dominated by communal land tenure, i.e. the former homelands, were reported to be moderately to

severely degraded (fig. 3.1) and are therefore a source of major concern (Hoffman & Todd, 2000; Hoffman & Ashwell, 2001).

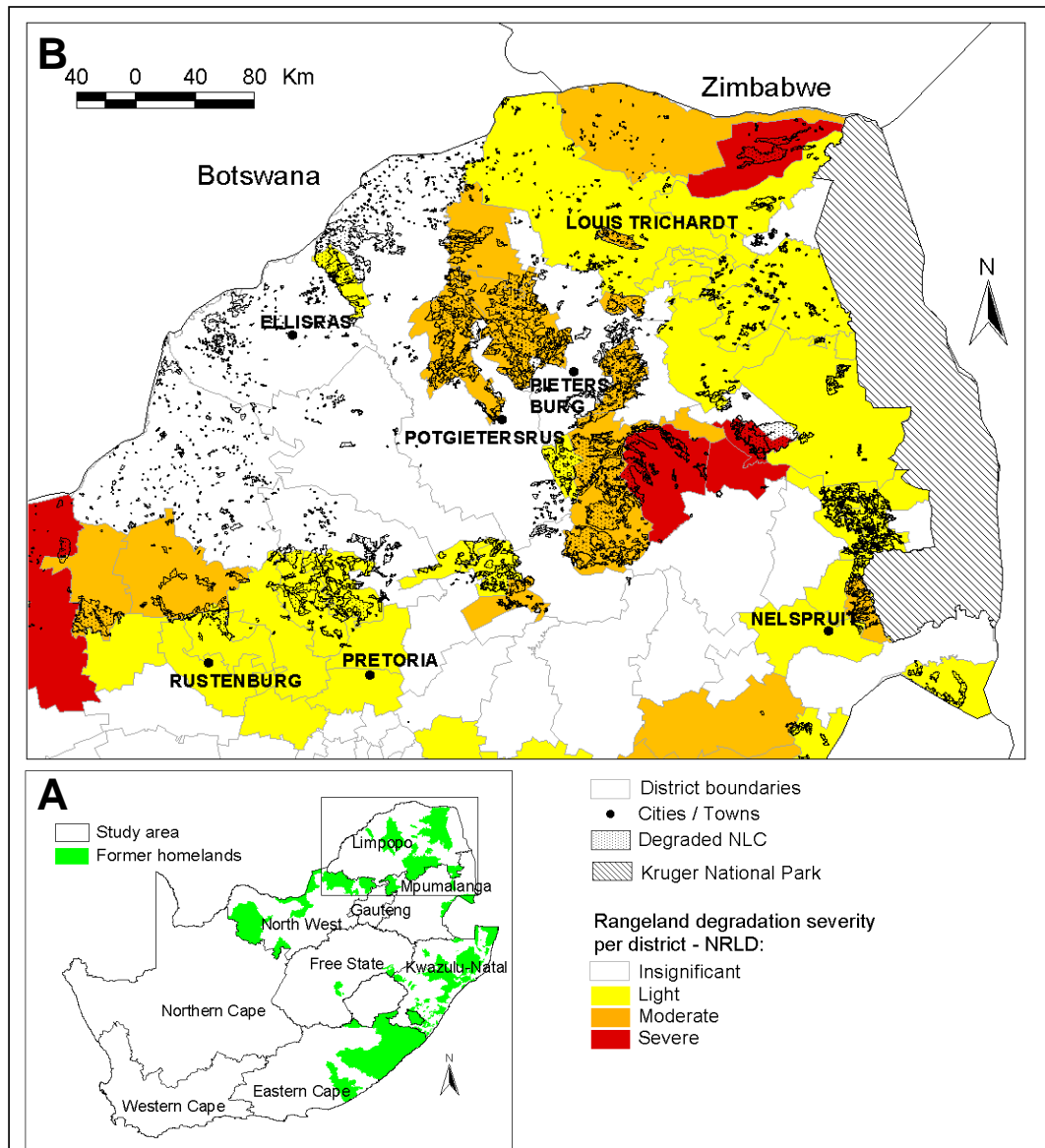


**Figure 3.1** (a) Provinces of South Africa with location of study area and former homelands. (b) Study area indicating severity of rangeland degradation per district according to National Review of Land Degradation (after Hoffman et al. 1999) and degraded areas mapped by the National Land Cover (Fairbanks et al. 2000).

Independently, a National Land Cover map (NLC) was prepared using 1995-96 Landsat TM data, manual photo-interpretation and extensive fieldwork (Fairbanks *et*

*al.*, 2000). 4.8% (5.8 million ha) of the country was mapped as degraded. The degraded classes in the NLC were defined as regions with lower vegetation cover than surrounding areas (Thompson, 1996) and by far the greatest areas of degraded land coincided with the moderate to severely degraded communal lands identified by the NRLD (fig. 3.1).

The current study assessed the vegetation production of areas mapped as degraded by NLC using 1km AVHRR data. Many of these degraded areas are adjacent to apparently non-degraded commercial rangelands, thus allowing the comparison of sites that differ primarily in land management and condition, rather than soils and climate. Because both the NLC and NRLD depended primarily on expert interpretation and thus also considerable subjectivity in the absence of sufficient biophysical measurements, as did the GLASOD program (Oldeman, Hakkeling & Sombroek, 1990), these surveys are not sufficiently repeatable for regular land condition monitoring. However, these two studies greatly facilitate the evaluation of remote sensing based techniques, since there is a severe shortage of empirical ecological studies (e.g. Parsons, Shackleton & Scholes, 1997; Ward, Ngairorue & Kathena, 1998) in the communal areas (Shackleton, 1993).

### **3.3 Materials and Methods**

#### *3.3.1 Study Area*

The north-eastern part of SA, which includes the entire Limpopo Province (formerly Northern Province) as well as parts of the Mpumalanga and North-West Provinces (approx. 200 000 km<sup>2</sup>) was chosen because it includes many of the most

extensive degraded areas according to NLC and NRLC (fig. 3.1)(Botha & Fouche, 2000; Hoffman & Ashwell, 2001). Land use in this region includes commercial and subsistence cultivation, exotic forestry plantations, national parks (e.g. Kruger National Park), private game reserves, commercial cattle ranching and communal grazing. The natural vegetation varies from indigenous forest to open grasslands, but primarily comprises savanna woodlands and thickets. This study was only concerned with areas covered by natural vegetation (according to NLC) that are used for grazing wild and domestic animals. Mean annual precipitation ranges from approx. 300mm along the northern border with Zimbabwe to 1600mm on the escarpment.

### 3.3.2 $1\text{km}^2$ AVHRR NDVI data

AVHRR data from 1985 to 2003 were processed consistently and calibrated to correct for sensor degradation and satellite changes (Rao & Chen, 1995; Rao & Chen, 1996). NDVI was calculated from channel 1 (0.55-0.68  $\mu\text{m}$ ) and channel 2 (0.73-1.1  $\mu\text{m}$ ) bands ( $\text{NDVI} = (\text{ch2} - \text{ch1})/(\text{ch2} + \text{ch1})$ ). Ten day maximum NDVI value composites were calculated to remove residual clouds, reduce atmospheric effects and the influence of varying solar zenith angles (Holben, 1986). A statistical filter was applied to interpolate cloud flagged or atmospherically affected data, identified whenever a relative decrease in the signal of 5% or more was followed within 4 weeks by an equivalent increase (Lo Seen Chong *et al.*, 1993). The 10-day composites were weighted by the number of days in each composite and summed over the entire growing season, October to April (hereafter referred to as  $\Sigma\text{NDVI}$ , fig. 3.2) (Prince, 1991b; Lo Seen Chong *et al.*, 1993; Yang *et al.*, 1998; Diouf & Lambin,

2001). The above-mentioned ten-day compositing, data interpolation and growth season sum procedures all contributed to reducing the atmospheric effects. However, the multi-temporal  $\Sigma$ NDVI data may be influenced by the remaining atmospheric effects (Cihlar *et al.*, 2004). (for more details on AVHRR processing see 2.2.3)

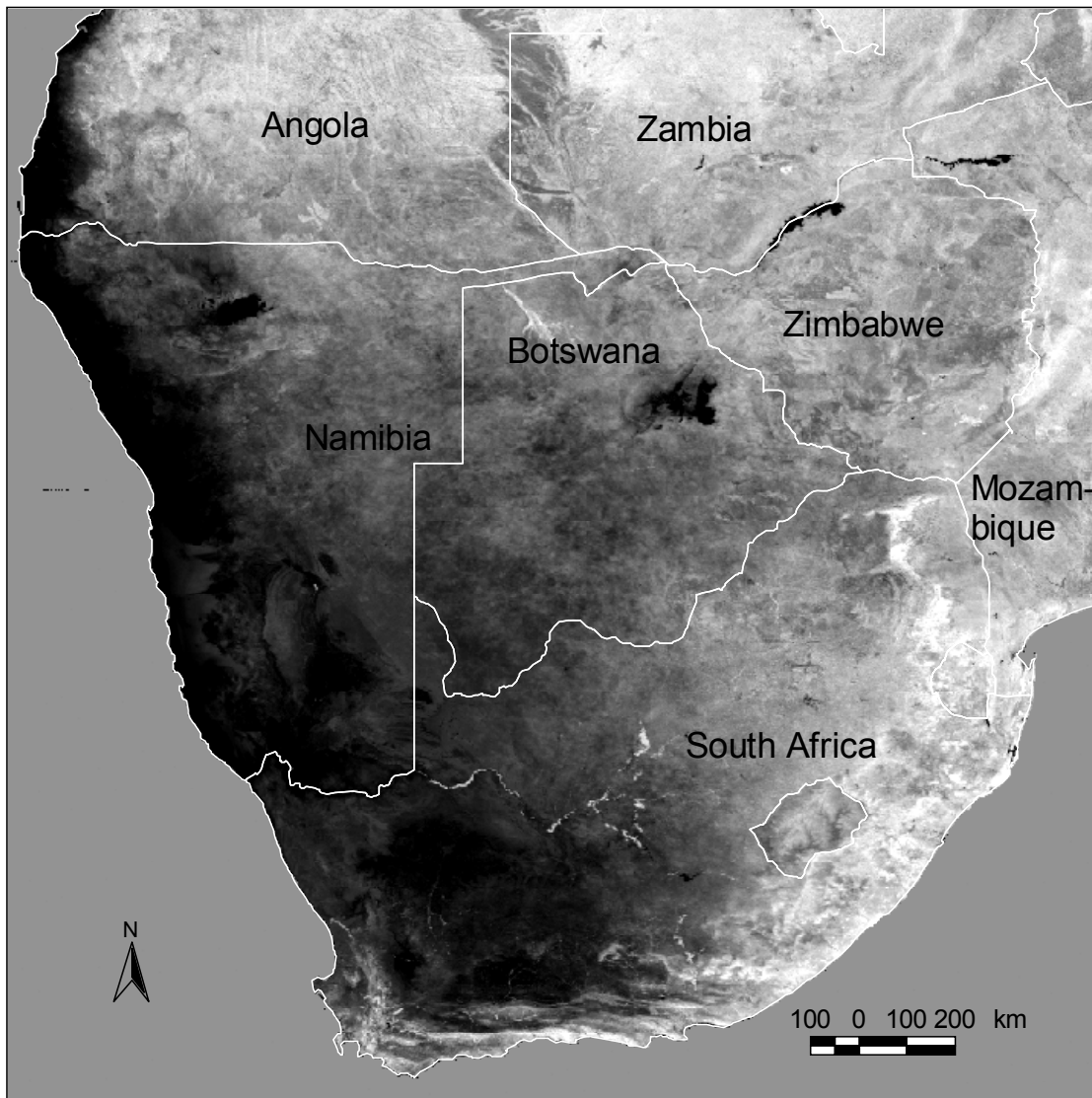


**Figure 3.2** Grayscale  $\Sigma$ NDVI of Southern Africa for 1998-99.

### 3.3.3 *Comparison of degraded and non-degraded rangelands*

For this study the NLC (Fairbanks *et al.*, 2000) was used to identify degraded rangelands (hereafter referred to only as degraded areas) and non-degraded rangelands. The NLC was also used to include only natural vegetation in the analyses and exclude all other land uses (e.g. informal settlements, urban areas, cultivation and commercial forestry). The classification accuracy of the NLC was assessed using field surveys (approximately 1400 sites in the study area) and aerial photography. The overall mapping accuracy for the study area ranged from 75% to 86% with a Kapa index of 68 to 80 and thus provided the best regional reference data currently available (Fairbanks *et al.*, 2000).

In order to isolate the impact of degradation from spatial variation in soils, topography and climate, the study area was stratified into areas with similar environmental characteristics (Bastin, Pickup & Pearce, 1995; Karfs, Applegate & Wallace, 2000). Land capability units (LCUs)(described below), were used for stratification to ensure that areas of contrasting land condition (degraded vs. non-degraded) were comparable in all other respects. The expected  $\Sigma$ NDVI values were estimated as the mean of all the values observed in non-degraded areas of the same LCU.

Non-degraded and degraded areas in the same LCU (hereafter referred to as paired areas) were compared by: (i) testing for differences in spatial mean  $\Sigma$ NDVI values, (ii) calculating the relative degradation impact (RDI) as the difference between the spatial mean  $\Sigma$ NDVI values of paired areas expressed as a percentage of non-degraded mean value, (iii) investigating the relationship between RDI and rainfall, and (iv) comparing the resilience and stability of paired areas in response to

rainfall variation. These comparisons were based on the assumption that the LCUs are sufficiently homogenous so that variations in  $\Sigma$ NDVI could be attributed to human impacts rather than natural landscape, soil and climate variation within the units.

#### 3.3.4 *Land capability units (LCUs) and climate data.*

The LCUs do not consider current vegetation cover, land use or land condition, making it possible to distinguish natural physical variations from human influences. Land capability is a widely used concept in agricultural development and it refers to the ecologically-sustainable suitability of the land for a specific use (e.g. cultivation, grazing or wildlife ranching) (Klingebiel & Montgomery, 1961; Vink, 1975). Land units with similar potential and physical limitations such as, climate or susceptibility to soil erosion, are grouped into land capability classes. The land capability data applied here are used by the SA National Department of Agriculture (NDA) for land use planning purposes (Schoeman *et al.*, 2002). The physical properties used in mapping the land capability units included: (i) terrain: slope length and gradient, (ii) soil: depth, texture, erodibility, internal drainage, mechanical limitations, acidity derived from the comprehensive land type database (Land Type Survey Staff 1977-2000; MacVicar *et al.*, 1977; USDA, 1992), (iii) climate: moisture availability, length of moist and temperate seasons derived from 1km<sup>2</sup> climate surfaces that were modeled from the measurements of a network of approximately 2000 weather stations (Monnik, 2001; Schoeman *et al.*, 2002). Strata were created from individual, contiguous LCU polygons, to reduce the possibility that adjacent polygons may have the same calculated land capability rating, but for very different reasons (fig. 3.3).

Only LCUs containing large degraded areas according to the NLC were considered in this study.

Weather stations falling within or close to each of the selected LCU were identified (fig. 3.3). The average total growing season precipitation (Oct-Apr) was calculated for all stations located in or near each LCU (N= 1-10).

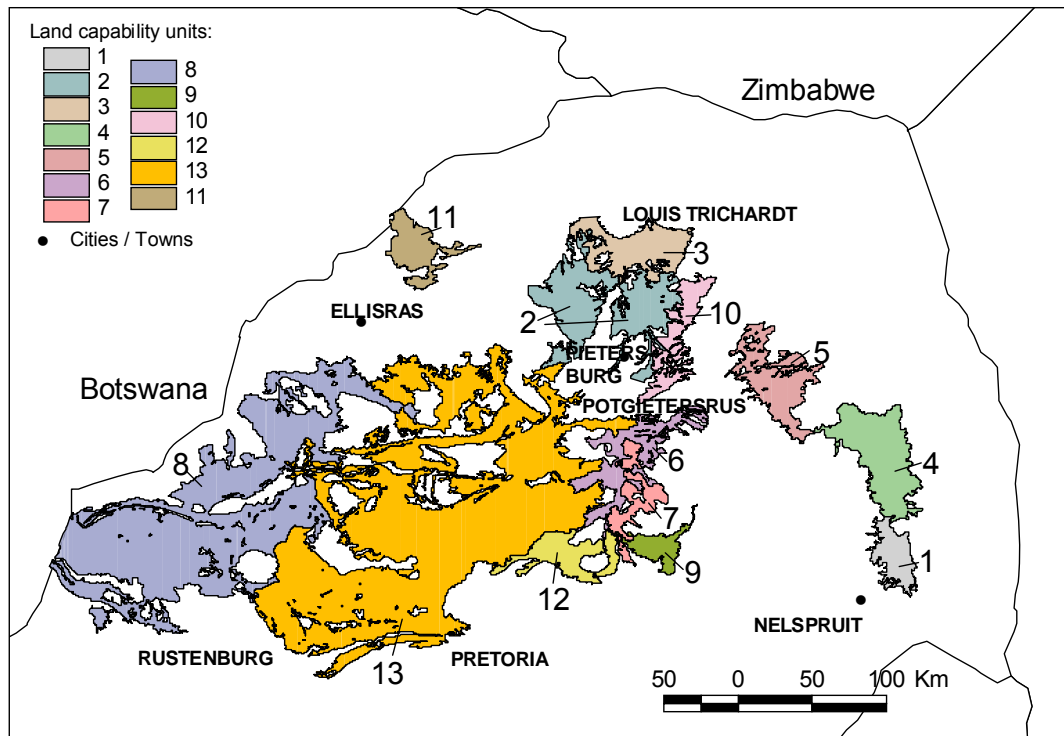


**Figure 3.3** Selected land capability units (LCU) and weather stations used to calculate mean growth season rainfall for each LCU.

### 3.3.5 Testing for differences in $\Sigma$ NDVI of non-degraded and degraded areas

The non-parametric Wilcoxon's rank sum test was applied to test if the median difference between annually paired non-degraded (nd) and degraded (d)  $\Sigma$ NDVI was larger than zero ( $H_1: \Sigma\text{NDVI}_{\text{nd}} - \Sigma\text{NDVI}_{\text{d}} > 0$ ). Resulting P-values indicate the

probability that the median differences were equal to zero ( $H_0: \Sigma NDVI_{nd} - \Sigma NDVI_d = 0$ ) (table 3.1).

### 3.3.6 *Relative degradation impact.*

The means of all the  $\Sigma NDVI$  pixel values in the degraded or non-degraded parts of a specific LCU were first calculated. The relative degradation impact (RDI) was then calculated as the difference between the non-degraded (nd) mean  $\Sigma NDVI$  and degraded (d) mean  $\Sigma NDVI$  expressed as a percentage of the non-degraded mean  $\Sigma NDVI$  value for a specific growth season (1).

$$RDI = (\Sigma NDVI_{nd} - \Sigma NDVI_d) / \Sigma NDVI_{nd} * 100 \quad (1)$$

For every growth season this provided a measure of the impact of degradation relative to the expected non-degraded mean value for each LCU. This variable non-degraded baseline effectively accounted for inter-annual variability in growing conditions experienced by the paired areas.

### 3.3.7 *$\Sigma NDVI$ - rainfall relationship*

To investigate the relationship between  $\Sigma NDVI$  and growth season rainfall ( $Rainfall_t$ ), correlation coefficients and linear regression models were computed for every LCU. The potential influence of inter-annual lags in vegetation response to rainfall was examined by calculating the correlation between the preceding growth season's rainfall ( $Rainfall_{t-1}$ ) and  $\Sigma NDVI_t$ . Where this correlation was positive, multiple regression models were computed with the dependent variable  $\Sigma NDVI_t$  being determined by the corresponding growth season's rainfall ( $Rainfall_t$ ) and the preceding growth season's rainfall ( $Rainfall_{t-1}$ ).

### 3.3.8 RDI – rainfall relationship

Comparisons of remote sensing data for dry and wetter years have been used to measure the recovery or resilience of vegetation along grazing gradients as a measure of degradation (Pickup & Chewings, 1994; Bastin *et al.*, 1995; Pickup *et al.*, 1998; Dube & Pickup, 2001). Degraded areas are expected to be those where grazing gradients do not diminish following good rainfall. In Australia and Botswana, where this method has been applied, the driver of degradation is the increase in grazing intensity closer to livestock water supplies (Pickup *et al.*, 1998; Dube & Pickup, 2001), while in the current study abrupt boundaries occur between degraded and non-degraded areas, often owing to boundaries between communal and commercial rangelands. Following the general approach of the resilience method (Pickup *et al.*, 1998), we analyzed the inter-annual relationship between RDI and rainfall to ascertain if RDI decreases or remains the same in years with higher rainfall. We therefore tested if the degraded areas were resilient enough to reduce or eliminate the RDI with increased rainfall.

### 3.3.9 Ecological Stability

Ecological stability refers to the ability of a system to remain the same while external conditions change (Noy-Meir & Walker, 1986). We compared the stability of degraded and non-degraded areas by calculating the percentage departure of a pixel's  $\Sigma$ NDVI value for a specific growth season from the long-term mean value for that pixel. Stability consists of, (a) resistance or the ability of vegetation to stay

unchanged during a growth season of reduced rainfall and, (b) resilience or the ability to recover from the preceding dry growth season after higher rainfall in the following growth season (Grimm & Wissel, 1997; Carpenter *et al.*, 2001; Walker *et al.*, 2002). More stable areas would be expected to have a lower negative percentage departure (higher resistance) in dry year and a higher positive percentage departure in wet year (higher resilience). A non-parametric Wilcoxon's rank sum test was applied to test whether non-degraded areas have higher stability than paired degraded areas across all growth seasons:

$$H_0: m = 0; \quad H_1: m > 0$$

$$m = \text{median } D_{nd} - D_d$$

$D_{nd}$  = percentage departure from long-term average for non-degraded areas

$D_d$  = percentage departure from long-term average for degraded areas

Therefore we tested if non-degraded areas showed smaller negative departure from their long-term mean ( $D_{nd}$ ) than degraded areas ( $D_d$ ) (resistance during drier years) or if non-degraded areas showed larger positive departures ( $D_{nd}$ ) than degraded areas ( $D_d$ ) in wetter years following dry years (resilience). The percentage departure therefore measures  $\Sigma NDVI$  relative to the long-term average of that particular pixel, while the above-mentioned RDI measures the difference between paired non-degraded and degraded areas for a specific year relative to the non-degraded values of the same year. All the years were included in one analysis to investigate stability through time, since both higher resistance and higher resilience of non-degraded areas result in  $m > 0$  and paired areas ( $D_{nd}$  and  $D_d$ ) mostly had the same signs, i.e. deviated from the long-term average in the same direction in any given growth season. In

isolated cases where  $D_{nd}$  and  $D_d$  had opposite signs, the departures were close to zero and therefore excluded from the Wilcoxon's test. The inter-annual coefficient of variation in  $\Sigma NDVI$  provided another measure of ecological stability of paired areas (Noy-Meir & Walker, 1986).

### 3.4 Results

#### 3.4.1 Differences between non-degraded and degraded areas

Degraded areas had lower  $\Sigma NDVI$  than their paired non-degraded area across all growth seasons and LCUs (fig. 3.4a) with very few exceptions (e.g. LCU 11 and LCU 1 during the very dry 1991-92 and 2002-03 growth seasons). The degree of overlap in values for degraded vs. non-degraded areas (indicated by error bars in fig. 3.4a) also varied between LCUs and there was still substantial variation in most LCUs (fig. 3.4a). Figure 3.5 gives the average  $\Sigma NDVI$  (1995-2000) for the non-degraded areas of each LCU to illustrate the differences between LCUs (coefficient of variance = 12.7%) and emphasizes the importance of detailed stratification.

P-values derived from the Wilcoxon's test denote the probability that the median difference in  $\Sigma NDVI$  between paired areas was equal to zero ( $H_0: m = 0$ ) (table 3.1). LCUs 2, 5, 6, 7, 9, 10, 12, 13 had P-values < 0.05 indicating a 95% probability that non-degraded areas have significantly higher  $\Sigma NDVI$  values. Two other LCUs (1 and 3) had probabilities of 83 and 85% respectively, while non-degraded areas in LCUs 8 and 11 were not significantly different (table 3.1).

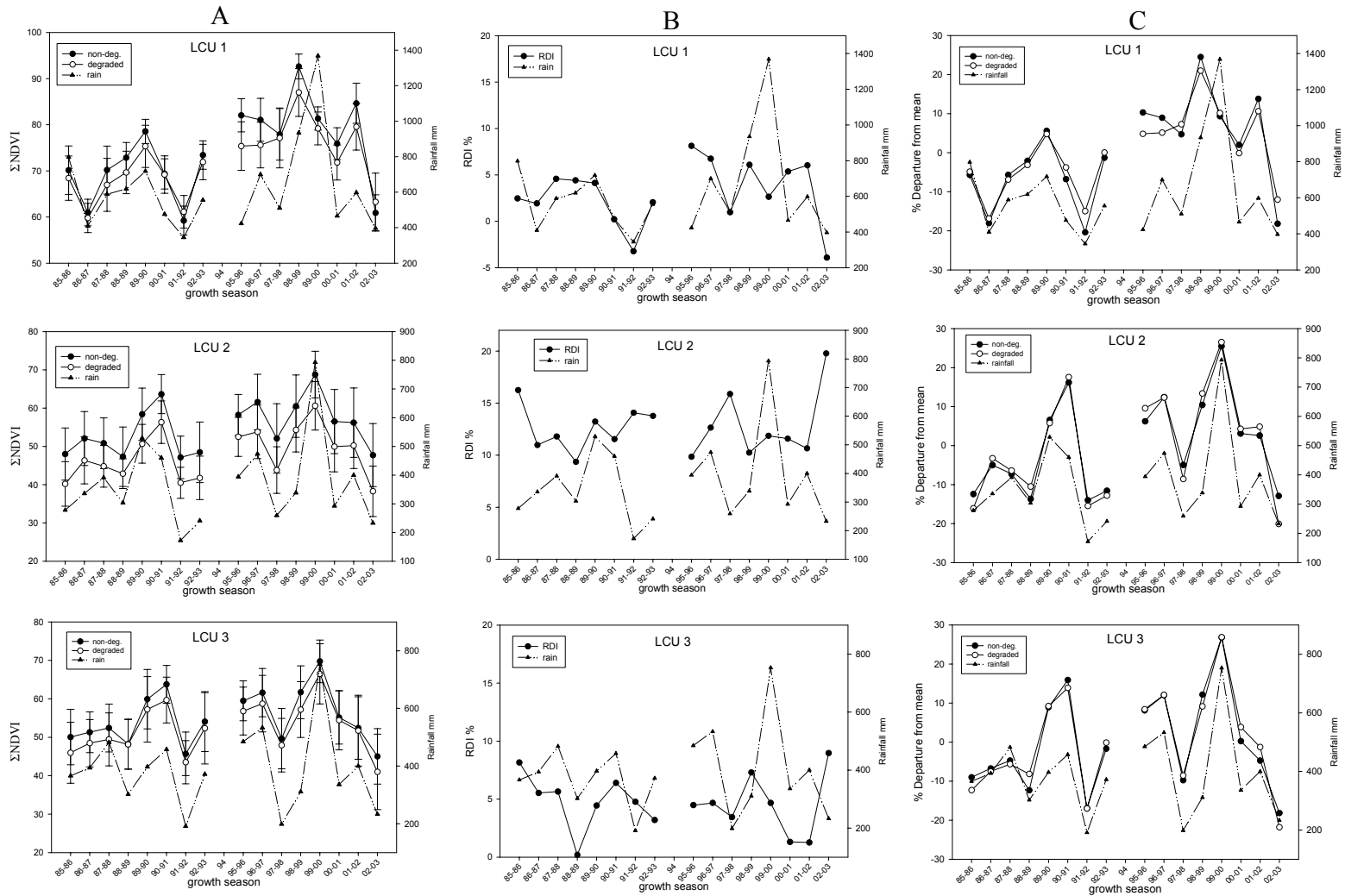


**Figure 3.4** (a)  $\Sigma$ NDVI and rainfall per growth season for each land capability unit (LCU). Error bars indicate standard deviation. (b) Relative degradation impact (RDI) and rainfall per growth season. (c) Departures from long-term mean  $\Sigma$ NDVI and rainfall per growth season.

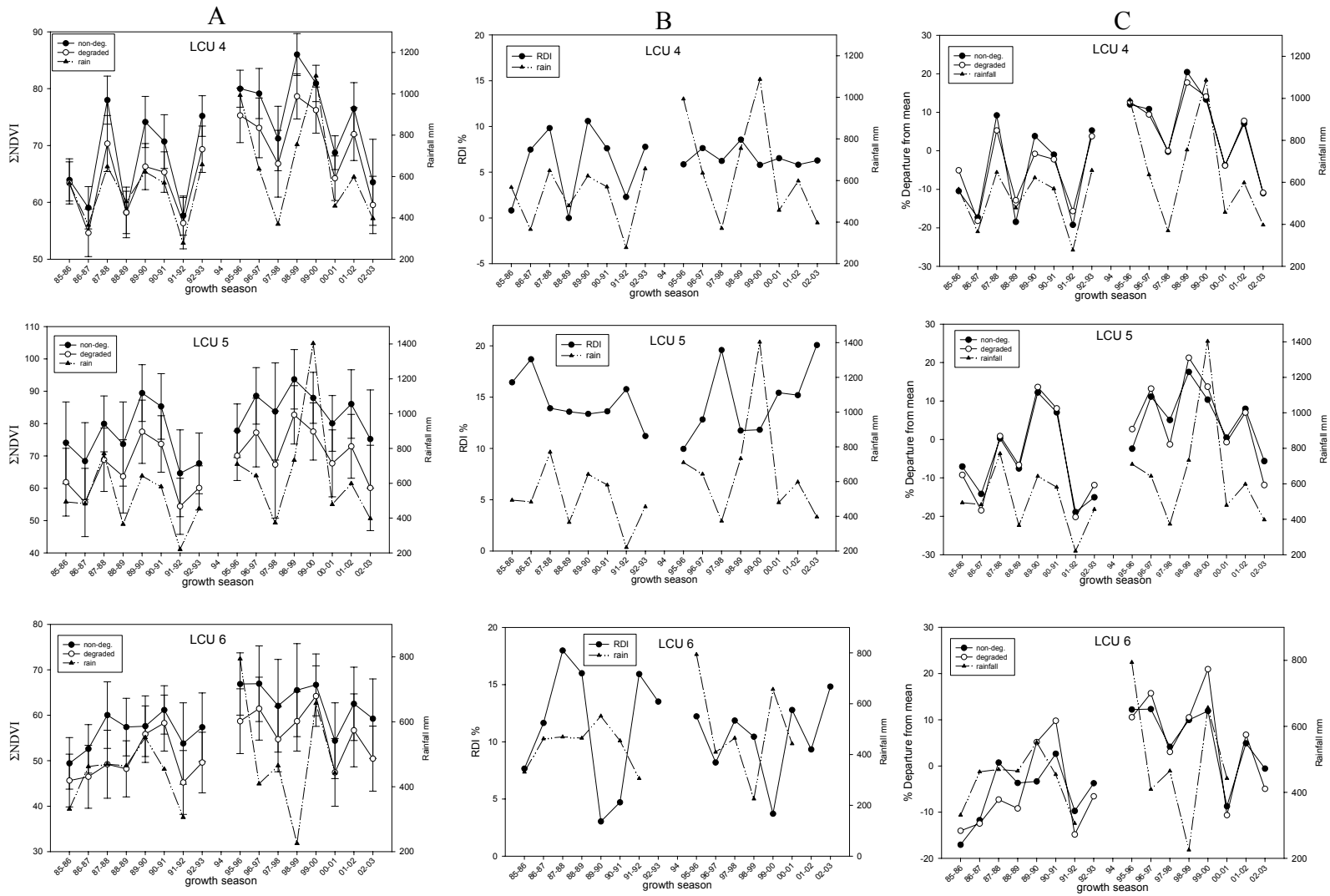


Figure 3.4 continue.

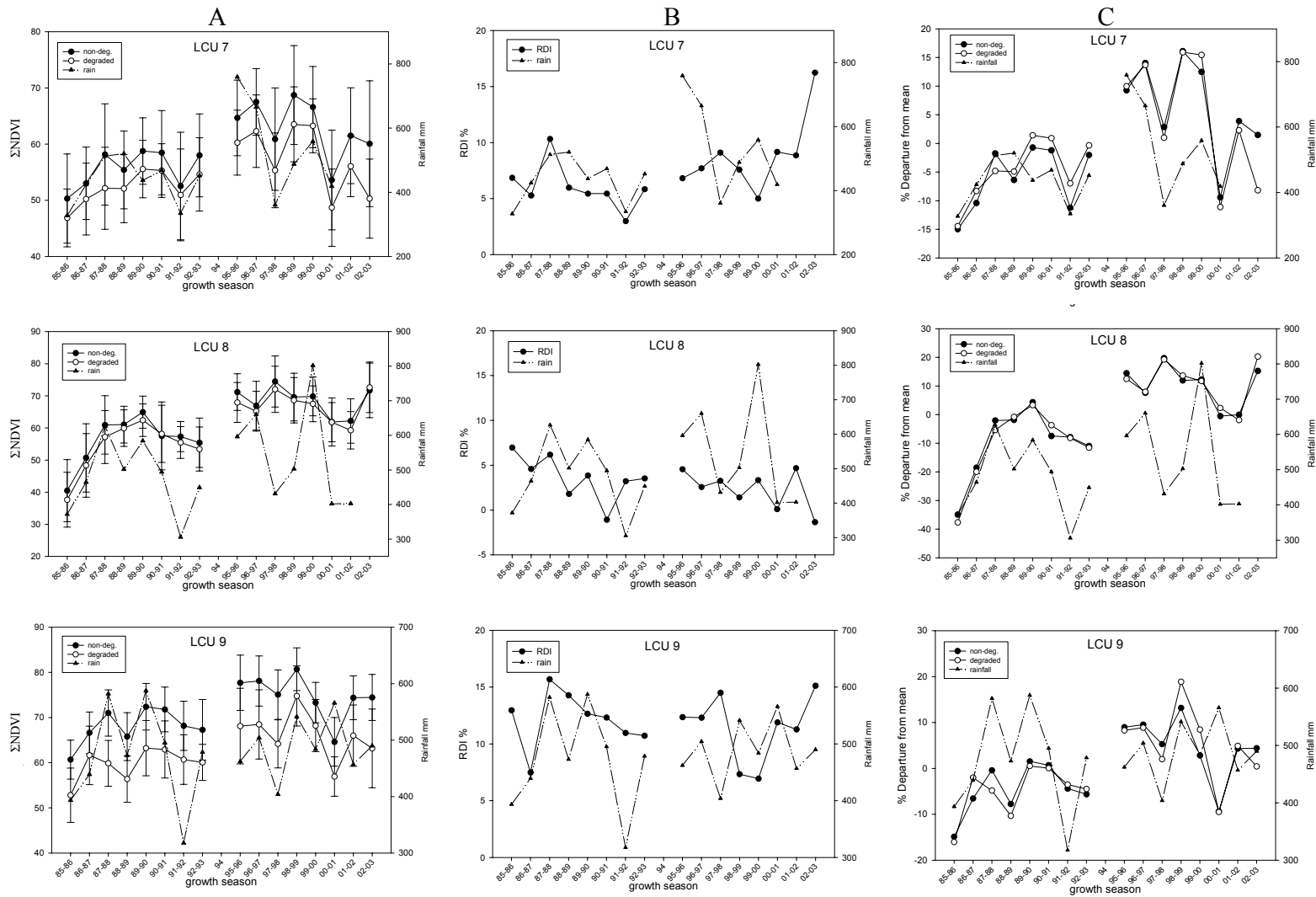


Figure 3.4 continue

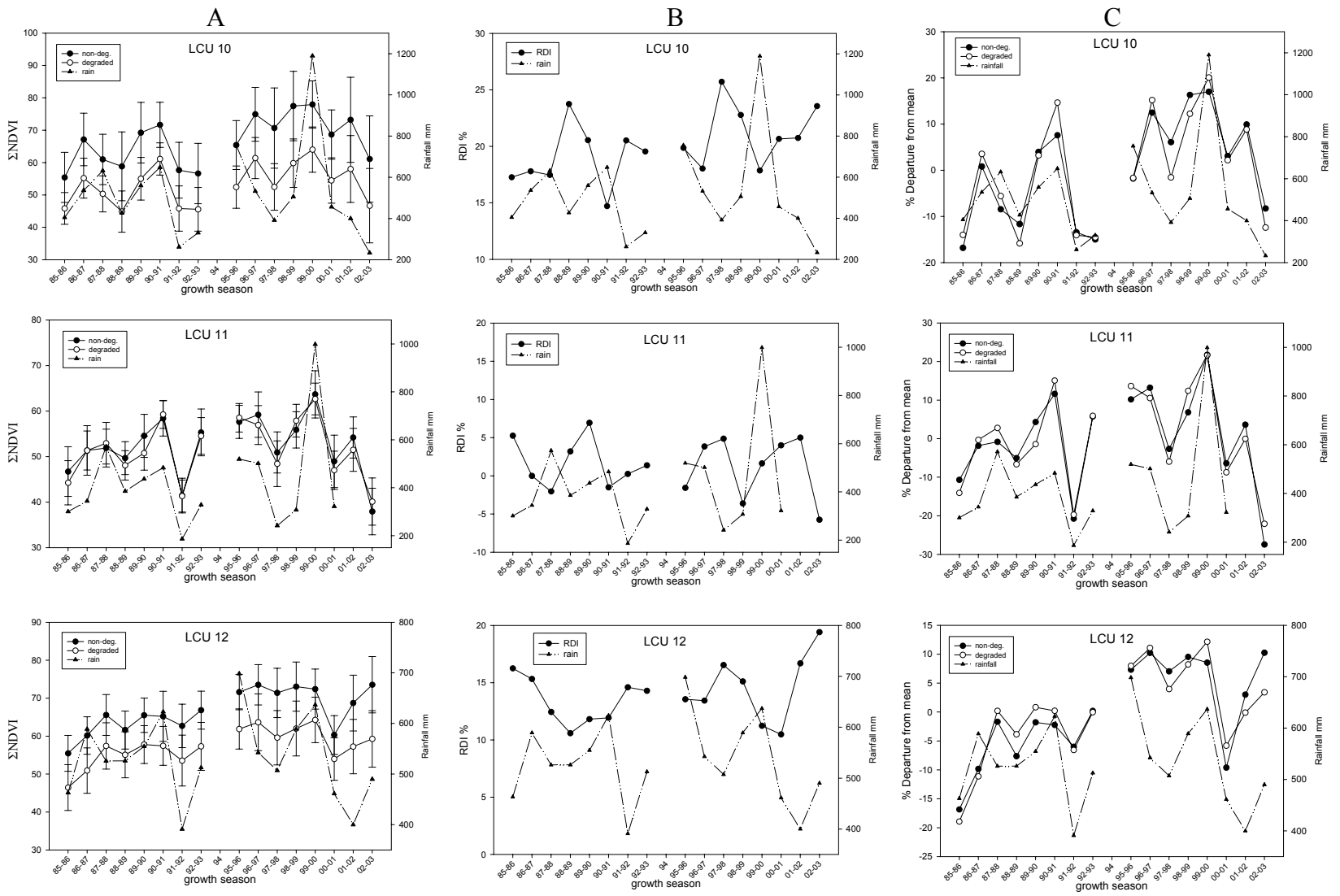


Figure 3.4 continue

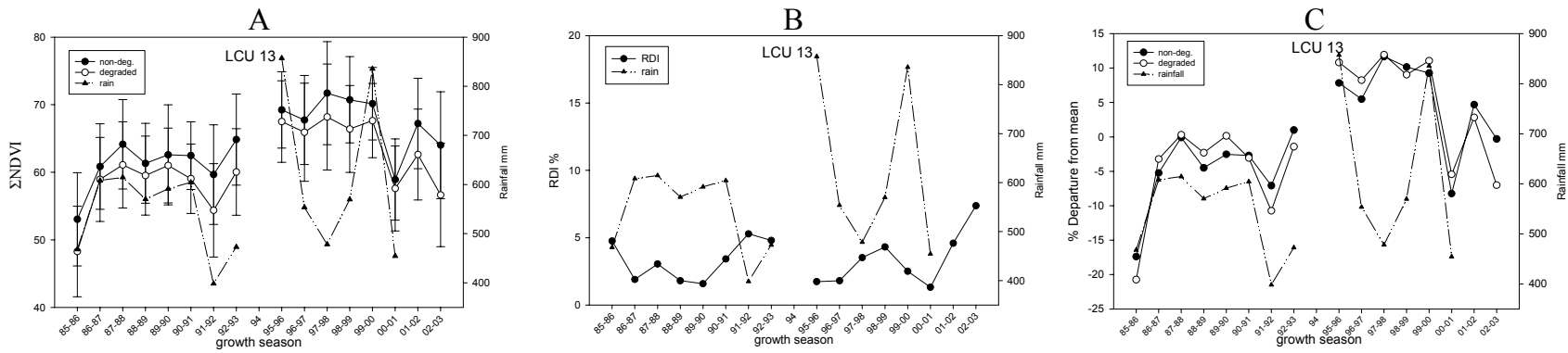


Figure 3.4 continue

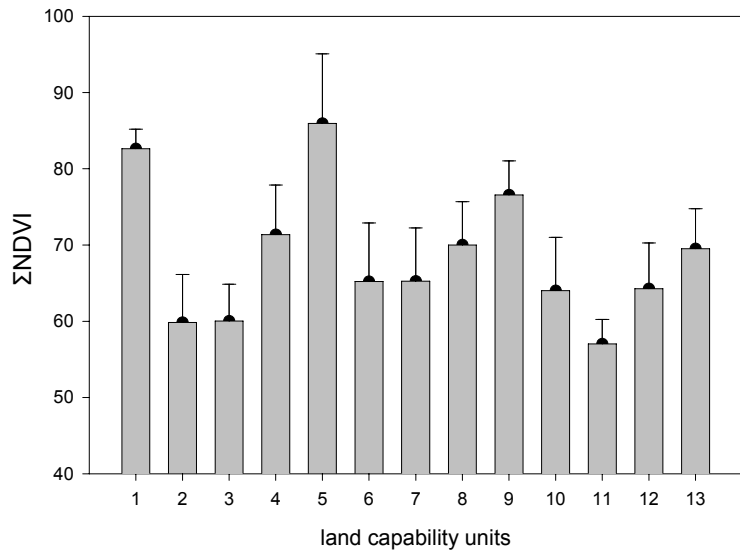


Figure 3.5 Average non-degraded ΣNDVI of land capability units, for 1995 to 2000. Error bars indicate standard deviation.

**Table 3.1.** Results of analyses of  $\Sigma$ NDVI for non-degraded (n) and degraded areas (d) of land capability units.

| land capability unit                                      | 1      |        | 2      |       | 3      |       | 4      |        | 5      |        | 6      |       | 7     |       |
|---|--------|--------|--------|-------|--------|-------|--------|--------|--------|--------|--------|-------|-------|-------|
| land condition  | n      | d      | n      | d     | n      | d     | n      | d      | n      | d      | n      | d     | n     | d     |
| Average $\Sigma$ NDVI 1985 to 2003                        | 74.5   | 72.0   | 54.8   | 47.9  | 55.0   | 52.4  | 71.4   | 66.9   | 79.8   | 68.2   | 59.6   | 53.2  | 59.3  | 54.9  |
| Standard deviation $\Sigma$ NDVI<br>(1985 to 2003)        | 8.9    | 7.0    | 6.4    | 6.3   | 6.8    | 6.5   | 8.5    | 7.0    | 8.4    | 8.1    | 5.2    | 5.9   | 5.4   | 5.0   |
| Coefficient of variance $\Sigma$ NDVI                     | 12.0   | 9.8    | 11.8   | 13.2  | 12.4   | 12.4  | 12.0   | 10.5   | 10.5   | 11.9   | 8.8    | 11.1  | 9.1   | 9.2   |
| Max. $\Sigma$ NDVI  | 92.6   | 87.0   | 68.8   | 60.6  | 69.7   | 66.5  | 86.0   | 78.6   | 93.7   | 82.7   | 66.9   | 64.2  | 68.7  | 63.5  |
| Min. $\Sigma$ NDVI  | 59.2   | 59.8   | 47.1   | 38.3  | 45.0   | 41.0  | 57.7   | 54.6   | 64.6   | 54.4   | 49.4   | 45.2  | 50.3  | 46.9  |
| Mean annual RDI   | 3.0    |        | 12.7   |       | 4.7    |       | 6.2    |        | 14.6   |        | 10.9   |       | 7.4   |       |
| Mean annual rainfall                                      | 780.0  |        | 455.6  |       | 472.9  |       | 718.1  |        | 718.9  |        | 529.0  |       | 554.1 |       |
| P-value: Wilcoxon's test                                  |        |        |        |       |        |       |        |        |        |        |        |       |       |       |
| $\Sigma$ NDVI non-deg. vs. deg.                           | 0.170  |        | 0.005  |       | 0.140  |       | 0.069  |        | 0.001  |        | 0.003  |       | 0.016 |       |
| R <sup>2</sup> RDI vs. rainfall                           | 0.040  |        | 0.060  |       | 0.030  |       | 0.057  |        | 0.244  |        | 0.039  |       | 0.019 |       |
| Correlation RDI vs. rainfall                              | 0.200  |        | -0.257 |       | 0.180  |       | 0.240  |        | -0.490 |        | -0.199 |       | 0.140 |       |
| Correlation $\Sigma$ NDVI vs. rainfall                    | 0.557  | 0.609  | 0.830  | 0.816 | 0.779  | 0.773 | 0.769  | 0.827  | 0.575  | 0.654  | 0.398  | 0.408 | 0.688 | 0.674 |
| R <sup>2</sup> $\Sigma$ NDVI vs. rainfall                 | 0.311  | 0.371  | 0.690  | 0.666 | 0.600  | 0.598 | 0.592  | 0.684  | 0.330  | 0.428  | 0.159  | 0.167 | 0.474 | 0.454 |
| P-value: R <sup>2</sup> $\Sigma$ NDVI vs. rainfall        | 0.038  | 0.020  | 0.000  | 0.000 | 0.001  | 0.001 | 0.001  | 0.000  | 0.019  | 0.005  | 0.177  | 0.166 | 0.006 | 0.008 |
| Correlation $\Sigma$ NDVI vs. rainfall $t_{-1}$           | -0.033 | -0.352 | 0.095  | 0.079 | -0.308 | -0.24 | -0.149 | -0.100 | 0.045  | -0.006 | 0.117  | 0.073 | 0.299 | 0.200 |
| R <sup>2</sup> $\Sigma$ NDVI vs. rainfall<br>(multi-year) | NA     | NA     | 0.743  | 0.731 | NA     | NA    | NA     | NA     | 0.340  | 0.424  | 0.021  | 0.090 | 0.420 | 0.378 |

**Table 3.1 cont.** Results of analyses of  $\Sigma$ NDVI for non-degraded (n) and degraded areas (d) of land capability units.

| land capability unit                                      | 8     |       | 9     |        | 10     |       | 11     |       | 12     |        | 13     |       |
|---|-------|-------|-------|--------|--------|-------|--------|-------|--------|--------|--------|-------|
| land condition  | n     | d     | n     | d      | n      | d     | n      | d     | n      | d      | n      | d     |
| Average $\Sigma$ NDVI 1985 to 2003                        | 62.2  | 60.5  | 71.4  | 63.0   | 66.7   | 53.3  | 52.4   | 51.6  | 66.7   | 57.4   | 64.3   | 60.9  |
| Standard deviation $\Sigma$ NDVI<br>(1985 to 2003)        | 8.5   | 8.8   | 5.3   | 5.3    | 7.2    | 6.2   | 6.4    | 6.3   | 5.4    | 4.5    | 4.9    | 5.3   |
| Coefficient of variance $\Sigma$ NDVI                     | 13.7  | 14.6  | 7.4   | 8.3    | 10.9   | 11.6  | 12.2   | 12.3  | 8.2    | 7.9    | 7.6    | 8.6   |
| Max. $\Sigma$ NDVI  | 74.5  | 72.7  | 80.7  | 74.8   | 77.9   | 64.0  | 63.7   | 62.6  | 73.5   | 64.3   | 71.7   | 68.2  |
| Min. $\Sigma$ NDVI  | 40.5  | 37.6  | 60.7  | 52.8   | 55.4   | 44.9  | 37.9   | 40.1  | 55.5   | 46.5   | 53.0   | 48.3  |
| Mean annual RDI   | 3.0   |       | 11.8  |        | 20.1   |       | 1.4    |       | 14.0   |        | 3.4    |       |
| Mean annual rainfall                                      | 594.0 |       | 535.9 |        | 663.2  |       | 491.8  |       | 612.8  |        | 643.8  |       |
| P-value: Wilcoxon's test                                  |       |       |       |        |        |       |        |       |        |        |        |       |
| $\Sigma$ NDVI non-deg. vs. deg.                           | 0.294 |       | 0.000 |        | 0.000  |       | 0.348  |       | 0.000  |        | 0.040  |       |
| R <sup>2</sup> RDI vs. rainfall                           | 0.005 |       | 0.005 |        | 0.145  |       | 0.016  |       | 0.034  |        | 0.228  |       |
| Correlation RDI vs. rainfall                              | 0.070 |       | 0.075 |        | -0.380 |       | -0.126 |       | -0.180 |        | -0.470 |       |
| Correlation $\Sigma$ NDVI vs. rainfall                    | 0.495 | 0.463 | 0.252 | 0.202  | 0.537  | 0.649 | 0.758  | 0.721 | 0.199  | 0.340  | 0.491  | 0.577 |
| R <sup>2</sup> $\Sigma$ NDVI vs. rainfall                 | 0.245 | 0.215 | 0.060 | 0.040  | 0.289  | 0.420 | 0.570  | 0.520 | 0.039  | 0.119  | 0.241  | 0.333 |
| P-value: R <sup>2</sup> $\Sigma$ NDVI vs. rainfall        | 0.060 | 0.080 | 0.360 | 0.460  | 0.030  | 0.006 | 0.001  | 0.003 | 0.450  | 0.189  | 0.070  | 0.030 |
| Correlation $\Sigma$ NDVI vs. rainfall <sub>t-1</sub>     | 0.267 | 0.309 | 0.011 | -0.083 | 0.094  | 0.1   | -0.385 | -0.46 | -0.223 | -0.081 | -0.230 | -0.06 |
| R <sup>2</sup> $\Sigma$ NDVI vs. rainfall<br>(multi-year) | 0.313 | 0.361 | 0.020 | 0.011  | 0.344  | 0.486 | NA     | NA    | NA     | NA     | NA     | NA    |

### 3.4.2 *Relative degradation impact (RDI)*

The average RDI values (table 3.1) indicate that the  $\Sigma$ NDVI of degraded areas were between 1% and 20% lower than the non-degraded areas. LCUs 5, 10 and 12 had the highest average RDI values of 14.6%, 20.1% and 14.0% respectively. LCUs 1, 8 and 11 had the lowest average RDI values of 3%, 3% and 1.4% respectively. The average RDI of all the LCUs was approximately 9%, indicating the average reduction in  $\Sigma$ NDVI caused by degradation. When LCUs 1, 8 and 11 were excluded the average RDI was 11.4%. In most cases the RDI did not show any obvious directional trends through entire time-series (fig. 3.4b). Although degradation may have intensified in specific parts of an LCU, this did not increase the RDI, which was calculated for all the pixels in each LCU. LCUs 2, 5, 6, 7, 9, 10, 12 and 13 showed an increase in RDI from the 1999-2000 to the 2002-2003 growth season, but this may be attributed to a sharp decrease in rainfall during this period (discussed below).

### 3.4.3 *$\Sigma$ NDVI - rainfall relationship*

The average growth season rainfall for the selected weather stations (N = 151) within the study area (fig. 6) indicate that the study period captured the most extreme rainfall years in the past 35 years. 1991-92, 1994-95 and 1997-98 were amongst the driest El Niño seasons, while 1999-2000 and 1995-96 were, respectively, the wettest and third wettest growth seasons. The 2001-02 and 2002-03 growth seasons have been very dry (fig. 6). In general, the late 80's were below average rainfall and, since the early 90's, oscillations between wet and dry years have been more extreme than

any other period in the 35 year record (fig. 6). The rainfall has a coefficient of variance of 30% overall and 40% since 1990 and therefore rainfall is highly variable in the study area.

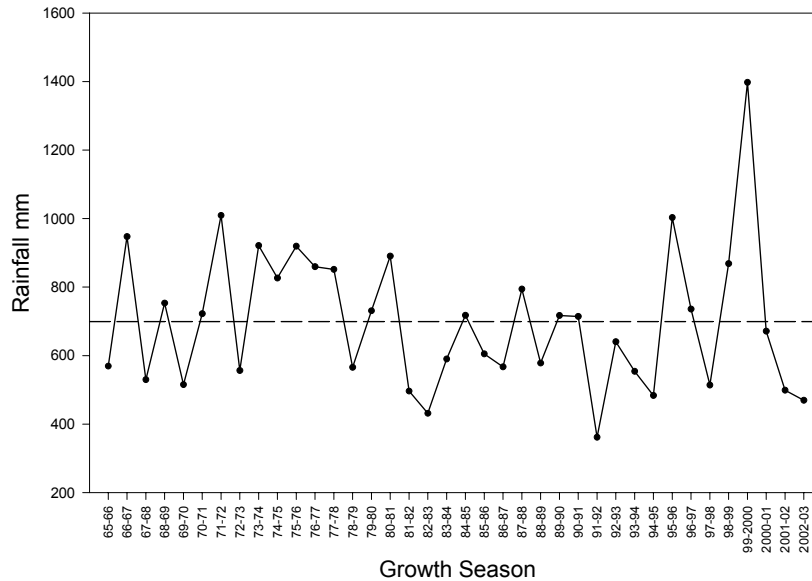


**Figure 3.6** Mean growth season rainfall for all weather stations (N=151) in study area for 1965 to 2003.

The differences between  $\Sigma$ NDVI of contrasting rainfall years are shown in fig. 3.7. The areas of consistent high  $\Sigma$ NDVI (dark green in fig. 7) are indigenous forest and exotic forestry plantations along the escarpment (north-south) and the Soutpansberg mountain range (east-west). There was a close spatial coincidence of reduced  $\Sigma$ NDVI in areas mapped as degraded by NLC, especially those northwest of Pietersburg and southeast of Potgietersrus (fig. 3.7c). Many of the large areas with low  $\Sigma$ NDVI outside the NLC degraded polygons are subsistence cultivation and not rangeland (fig. 3.7c).

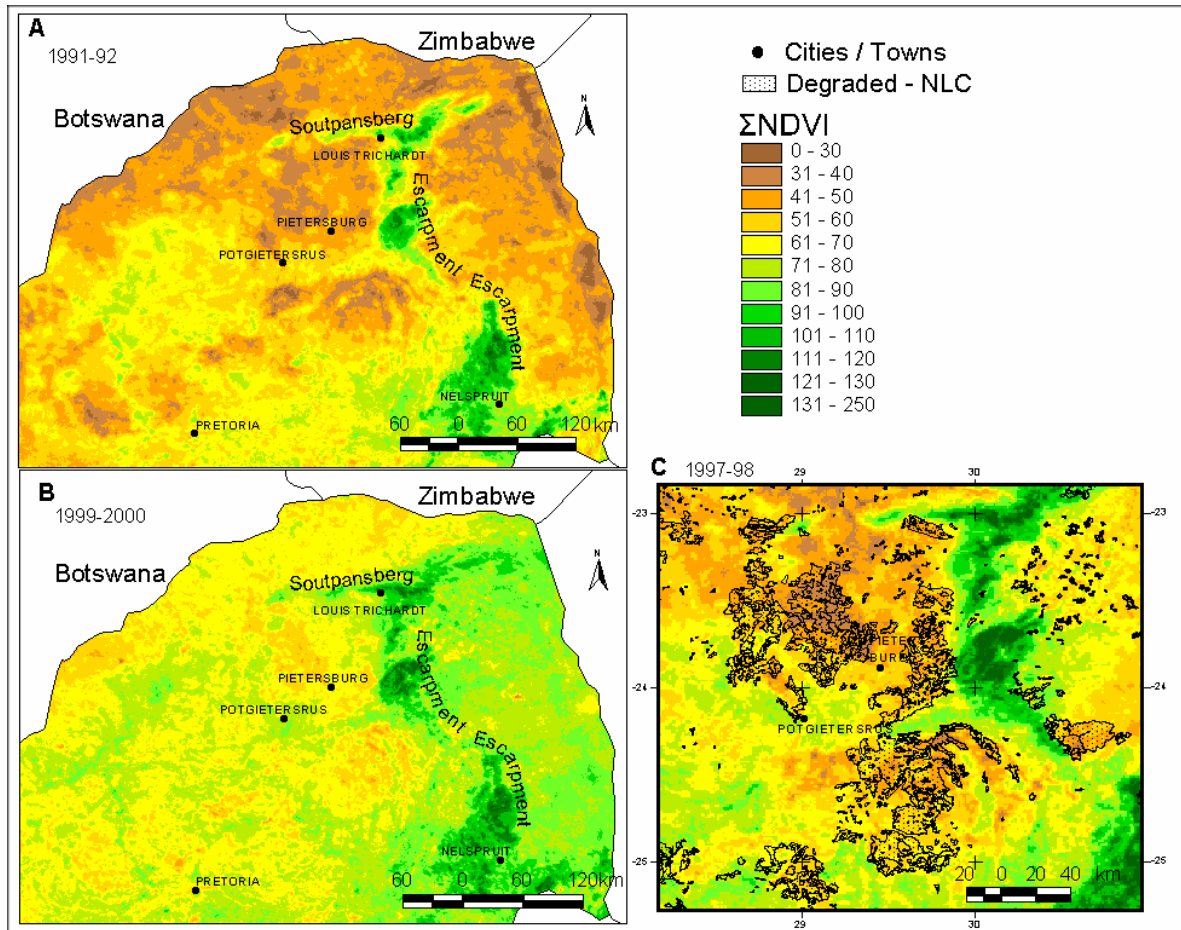


**Figure 3.7** ΣNDVI of study area for (a) 1991-92 and (b) 1999-2000. (c) ΣNDVI for central parts of study area (1997-98) overlaid with degraded areas mapped by National Land Cover (NLC).

The 1991-92 El Niño caused reduced ΣNDVI values for most LCUs (fig. 3.4a). The effects of the 1997-98 El Niño event (Anyamba, Tucker & Eastman, 2001) and transition to the 1999-2000 La Niña conditions (Anyamba *et al.*, 2002) on ΣNDVI are clearly visible in fig. 3.4a and figs 3.7b,c. Although the 1997-98 El Niño events did not result in severe drought over the entire region (Anyamba *et al.*, 2002), most LCUs (2, 3, 4, 5, 6, 7, 9,10, 11) showed a marked decline in ΣNDVI (fig. 3.4a). The southern part of the study area and the corresponding LCUs 8, 12 and 13 did not show a decline in ΣNDVI during the 1997-98 El Niño event (fig. 3.4a and fig. 3.7c).

The 1999-2000 La Niña event caused the highest rainfall in recent history and very high  $\Sigma$ NDVI values (fig. 3.4a and fig. 3.7b). The reduction in  $\Sigma$ NDVI showed by LUC1 in 1999-2000 (fig. 3.4a) was most likely caused by the severe flooding in the area.

Variation in growth season precipitation appears to be the proximate cause of the substantial inter-annual variation in  $\Sigma$ NDVI (fig. 3.4a). Degraded areas and paired non-degraded areas showed similar increases in  $\Sigma$ NDVI following good rainfall, although the  $\Sigma$ NDVI values of degraded areas remained consistently lower than those of non-degraded areas of the same growth season (fig. 3.4a). LCUs 2, 3, 4, and 11 showed the strongest relationship between  $\Sigma$ NDVI and  $\text{Rainfall}_t$ , with  $R^2 \geq 0.5$  ( $p \leq 0.001$ ) and LCUs 1, 5, and 7 had moderately strong  $\Sigma$ NDVI -  $\text{Rainfall}_t$  relationships ( $R^2 \geq 0.3$ ,  $p < 0.05$ ) (table 3.1).

LCUs 1, 3, 4, 11, 12 and 13 showed negative correlations between  $\Sigma$ NDVI- $\text{Rainfall}_{t-1}$ . This unexpected negative relationship was caused by the contrast between the rainfall of successive growth seasons, which often oscillated between very wet and very dry (fig. 3.4a). Adding the preceding year's rainfall ( $\text{Rainfall}_{t-1}$ ) to the multiple regression models only slightly increased the percentage of the variance in  $\Sigma$ NDVI accounted for in LCUs 2, 8, and 10. This may indicate that these LCUs experienced a small degree of inter-annual lag effects between rainfall and vegetation response (table 3.1).

#### 3.4.4 RDI – rainfall relationship

Several LCUs (2, 5, 6, 7, 9, 10) exhibited a common pattern of a peak in RDI during the very dry 1997-1998 El Niño season and a subsequent decrease in RDI following the high rainfalls of 1998-1999 and 1999-2000 growth seasons (fig. 3.4b). This was followed by an increase of RDI during the dry 2001-02 and 2002-03 growth seasons (fig. 3.4b). This indicated that the relative degradation impact was most pronounced during the dry periods (1997-98 and 2002-2003) and decreased to some extent during the exceptionally high rainfall growth season (1999-2000). In the same fashion several LCUs (2, 3, 5, 11, 12, 13) showed a common pattern of elevated RDI during the very dry 1985-86 and 1986-87 growth seasons followed by a reduction in RDI corresponding with higher rainfall in 1987-88 (fig. 3.4b).

A regression analysis between rainfall and the RDI for all growth seasons showed that only LCUs 5 and 13 had an  $R^2 \geq 0.2$ . For LCUs 2, 5, 6, 10, 11, 12 and 13 the correlations were negative (although weak) indicating that the magnitude of the difference slightly decreases during higher rainfall years (fig. 3.4b). The low  $R^2$  values suggests that, for most of the LCUs, the RDI values, i.e. magnitude of difference between degraded and non-degraded, was not strongly related to the rainfall.

#### 3.4.5 Ecological Stability

In agreement with the pattern of slightly smaller RDI in wetter years, the degraded areas in LCUs 5, 6, 7, 9, 10, 12 exhibited slightly less resistance during the 1997-1998 El Niño, but slightly more resilience in 1998-1999 or in the 1999-2000 La

Niña (fig. 3.4c). The degraded and non-degraded areas generally showed very similar departures (fig. 3.4c). The results of the Wilcoxon's test showed that, overall, there were no significant difference in the departures and thus the stability of paired degraded and non-degraded areas. The inter-annual coefficient of variation of  $\Sigma$ NDVI ranged from 7% to 14%, with an average of approximately 10% for all the LCUs (table 3.1). The coefficients of variation of paired areas were very similar with the biggest difference being 1.9% (table 3.1), suggesting that degraded and non-degraded areas exhibited the same level of inter-annual variation.

### **3.5 Discussion**

Relative degradation impacts (RDI) across all LCUs ranged from 1% to 20% with an average of 9%, while inter-annual coefficient of variation  $\Sigma$ NDVI ranged from 8% to 14% with an average of 10.7% (table 3.1). The 12.7 % coefficient of variance of mean  $\Sigma$ NDVI across all LCUs (fig. 3.5) indicates that landscape variability was a large source of natural background variation that was addressed through detailed stratification (Bastin *et al.*, 1995; Dube & Pickup, 2001).

LCUs 5, 10 and 12 showed the highest RDI values and thus showed the biggest degradation impact. LCUs 2, 5, 10, and 13 showed weak to moderate negative correlation between RDI and rainfall (table 3.1), indicating that the degradation impacts were slightly reduced with higher rainfall (fig. 3.4b). This is in accordance with other studies in Botswana and Australia where vegetation resilience was investigated using the grazing gradient method (Bastin *et al.*, 1995; Pickup *et al.*,

1998; Dube & Pickup, 2001). In this study, however, the RDI never reached zero as a result of high rainfall (fig. 3.4b).

The relationship between  $\Sigma$ NDVI and  $\text{Rainfall}_t$  was generally not as strong as those reported elsewhere (Malo & Nicholson, 1990; Nicholson *et al.*, 1998; Diouf & Lambin, 2001). For some LCUs (i.e. 2, 3, 4, 7 and 11) the  $R^2$  values were relatively high (approx. 0.5,  $p < 0.01$ ) (table 3.1) and comparable to those reported in the Sahel (Prince *et al.*, 1998). Different LCUs also demonstrated considerable variation in the strength of the relationship between  $\Sigma$ NDVI and  $\text{Rainfall}_t$ . There was no clear relationship between the long-term mean annual rainfall of an LCU and the strength of the  $\Sigma$ NDVI and  $\text{Rainfall}_t$  relationship (table 3.1). In the current study the primary objective was not to relate rainfall to  $\Sigma$ NDVI of pixels around the weather station as in most previous studies, but rather to relate the rainfall to all the pixels in the LCU. This could have reduced the strength of the observed relationship depending on how representative weather stations were of the climate of the specific LCU they were assigned to. Furthermore, the timing and distribution of precipitation throughout the growth season influences vegetation production, but was not analyzed here. Since  $\Sigma$ NDVI of all growth seasons may not have been affected equally by the atmosphere, this may have further reduced the  $\Sigma$ NDVI-rainfall correlation. Only three LCUs (2, 8 and 10) showed a slight influence of the preceding growth season's rainfall on  $\Sigma$ NDVI. Therefore, in contrast with previous studies (Goward & Prince, 1995; Prince *et al.*, 1998; Diouf & Lambin, 2001) there was no strong evidence of inter-annual lag periods in the effects of rainfall on vegetation activity.

The results suggest that degraded areas were no less stable in  $\Sigma$ NDVI than were non-degraded areas (fig. 3.4c). The inter-annual coefficients of variation in  $\Sigma$ NDVI of paired areas were within 2% of one another (table 3.1), indicating similar variability (Noy-Meir & Walker, 1986). The ecological stability, as measured by the percentage departures from long-term mean of each pixel, showed no difference between degraded and non-degraded paired areas (fig. 3.4a). Although the lack of atmospheric correction of the AVHRR data may otherwise complicate the inter-annual comparison of  $\Sigma$ NDVI, it should not influence the comparison of ecological stability of paired areas, since these adjacent areas should experience the same atmospheric effects during any given growth season. Both non-degraded and degraded areas showed remarkable resilience whenever droughts were followed by good rainfall (fig. 3.4a). The influence of rainfall was so pronounced that the  $\Sigma$ NDVI of degraded areas in wet years was often much higher than that of non-degraded paired areas in drier years (fig. 3.4a). Although the degraded areas appear to be in a different stable ecological state, they have not changed to a radically different low biomass state, as described elsewhere (Noy-Meir, 1975; Holmgren & Scheffer, 2001). Communal lands have continuously supported large numbers of livestock without any of the catastrophic declines in total numbers predicted during the past six decades (Tapson, 1991; Shackleton, 1993). Apart from instances where livestock declines were attributed to severe drought (Shackleton, 1993), degraded communal areas appear to be functionally stable.

Several definitions of land degradation are based on the loss of resilience and a permanent, irreversible decline in forage output (Abel & Behnke, 1996; Scheffer *et*

*al.*, 2001; Folke *et al.*, 2002). According to these definitions, the above-mentioned results suggest that the areas mapped as degraded by NLC are not necessarily degraded. However, rangeland degradation can more specifically be expressed in terms of productivity, defined as forage production per unit rainfall (Pickup, 1996; Abel, 1997; Walker *et al.*, 2002). In any given year and for a specific amount of rainfall, degraded areas showed lower  $\Sigma$ NDVI (fig. 3.4a) and thus reduced productivity. Although some of the results suggest the relative impact of the degradation decreased slightly following high rainfall, the degradation impact never disappeared, not even after the very strong 1999-2000 La Niña event (Anyamba *et al.*, 2002) (fig. 3.4b). The degraded areas showed an equivalent capacity to recover, but very rarely reached the same levels of productivity as those attained by paired non-degraded areas (fig. 3.4a). In contrast to previous studies, which used AVHRR NDVI, where apparent “desertification” in Africa could mainly be attributed to droughts (Tucker *et al.*, 1991a; Nicholson *et al.*, 1998; Prince *et al.*, 1998; Diouf & Lambin, 2001), the reductions in  $\Sigma$ NDVI discussed here can be attributed to human-induced land degradation. The relative degradation impact remained fairly consistent for a test period of 16 growth seasons, despite exceptionally high rainfall in the late 90’s. This might suggest that the reduced productivity has become permanent or very difficult to reverse (Prince, 2002). However, unless the high grazing pressure in communal lands can be removed for a number of years using exclusion plots, the irreversibility of these impacts cannot be unequivocally established (Shackleton, 1993; Prince, 2002).

Since there is a perception that communal rangelands are moderately to severely degraded (fig. 3.1) (Hoffman & Ashwell, 2001) it may seem surprising that average

RDI (i.e. the percentage difference in  $\Sigma$ NDVI values of degraded and non-degraded areas) of all the LCUs is only 9%, with a maximum of 20% (table 3.1). Within the context of net primary production (NPP) models (e.g. Prince & Goward, 1995) this would suggest that, if the general climate (air temperature, rainfall and relative humidity) of the paired areas were the same, the  $f_{\text{PAR}}$  and therefore the NPP of degraded areas were on average only 9% less (RDI in table 3.1).

There are a number of potential explanations for this apparent disparity in the perceived and the remotely sensed degradation impacts. (i) The detailed stratification applied here allowed a more precise pairing of comparable areas with similar soils and climate, while human observations may compare degraded areas to dissimilar areas with higher potential productivity (Ward, Ngairorue & Apollus, 2000). (ii) Qualitative human perceptions of rangeland condition are often based on single annual observations of standing biomass. Biomass is largely determined by grazing intensity and this can be up to four times higher in communal areas (Shackleton, 1993), hence a lower standing crop is expected. In contrast, NDVI gives a continuous measure of the photosynthetically active radiation absorbed by the vegetation, which may be more closely related to NPP than single observations of accumulated standing biomass that do not account for large differences in herbivory (Scurlock *et al.*, 1999). Much of this uncertainty stems from the lack of sufficient field data or any coordinated long-term field campaigns to compare degraded and non-degraded areas (Shackleton, 1993). (iii) In addition, the AVHRR data cannot detect observed changes in species composition towards unpalatable or annual grass species (Parsons *et al.*,

1997; Hoffman & Ashwell, 2001), since these changes are not always associated with a reduction in herbaceous production (Kelly & Walker, 1977).

The results nevertheless clearly indicate that there has not been a radical shift to a very different state or a catastrophic reduction in ecosystem function within areas mapped as degraded by the NLC (Holmgren & Scheffer, 2001; Scheffer *et al.*, 2001; Folke *et al.*, 2002). Instead, degradation impacts were reflected as reductions in productivity that varied along a continuum from slight to severe depending on the specific LCU (Tongway & Hindley, 2000). In general we can conclude that although the degraded areas are functionally stable and resilient, they show consistent, moderate reductions in forage production per unit rainfall. These results highlight the importance of multi-temporal analyses of ecosystem function to understanding land degradation, which has often been limited to a binary degraded/non-degraded classification.

Land redistribution and restitution programs could potentially subject areas currently under commercial management to the socio-economic driving forces of land degradation (Dean *et al.*, 1996; Fox & Rowntree, 2001; Shackleton *et al.*, 2001) as in Zimbabwe (Prince, 2004). Therefore there is an urgent need for a reliable national monitoring procedure. There have been isolated efforts to map land degradation for specific study areas in SA with Landsat TM (Kiguli, Palmer & Avis, 1999; Tanser & Palmer, 1999; Botha & Fouche, 2000). Provincial-scale natural resource audits based on Landsat TM mapping of vegetation cover, field surveys of plant species composition and soil erosion assessments in SA (e.g. Wessels *et al.*, 2000) and elsewhere (e.g. Pickup, Chewings & Nelson, 1993; Pickup & Smith, 1993; Karfs *et*

*al.*, 2000) have proven to be slow, costly and not sufficiently repeatable for timely national-scale monitoring. Coarse resolution satellite data, for example the AVHRR, SPOT Vegetation and Moderate Resolution Imaging Spectroradiometer (MODIS) sensors provide daily observations and will therefore have to play a central role in monitoring vegetation dynamics and land degradation in SA. Such a coarse resolution remote sensing based monitoring approach can direct attention to areas where high resolution remote sensing and field surveys are needed.

## **Chapter 4. Can the impacts of human-induced land degradation be distinguished from the effects of rainfall variability?**

### **4.1 Introduction**

Vegetation production in arid and semi-arid regions is closely related to the long-term average precipitation (Rosenzweig, 1968; Rutherford, 1980) and inter-annual rainfall variability (Le Houérou, Bingham & Skerbek, 1988), especially in southern Africa which is strongly affected by the El Niño-Southern Oscillation (ENSO) phenomenon (Jury *et al.*, 1997; Anyamba *et al.*, 2002; Cao & Prince, 2005). Short-term variability in primary production makes it exceedingly difficult to distinguish long-term change as a result of human-induced land degradation from the effects of periodic droughts (Pickup *et al.*, 1998; Dahlberg, 2000; Dube & Pickup, 2001; Prince, 2002). Human impacts are further obscured by spatial variability in topography, soil types, vegetation types and land use.

Land degradation has a broad range of definitions that essentially describe circumstances of reduced biological productivity of the land (UNCCD, 1994; Reynolds & Stafford Smith, 2002b). According to the United National Convention to Combat Desertification (UNCCD) definition, land degradation can be caused by both human and climate factors (UNCCD, 1994). A number of studies have shown that the perceived desertification in the Sahel (e.g. Lamprey, 1975) can largely be attributed to variations in rainfall rather than human-induced land degradation (Tucker *et al.*,

1991a; Nicholson *et al.*, 1998; Prince *et al.*, 1998). These studies demonstrated that there was neither a progressive southwards march of the Sahara desert, nor large-scale expansion of less productive land (Tucker *et al.*, 1991a; Nicholson *et al.*, 1998). In order to successfully combat land degradation, according to the UNCCD, signatory countries need spatial monitoring systems that are able to distinguish human impacts on vegetation production from the impacts of rainfall variability (Pickup, 1996).

Various methods have been used to monitor changes in vegetation function based on multi-temporal Advanced Very High Resolution Radiometer (AVHRR) data (Hellden, 1991; Tucker *et al.*, 1991b; Lambin & Strahler, 1994). The results are often dominated by erratic rainfall, temporary modifications in seasonality and abrupt land cover changes (Lupo, Reginster & Lambin, 2001), which all mask any land degradation that is more subtle and gradual. Two methods are explored to distinguish human-induced land degradation from inter-annual variability in rainfall; (i) Rain-Use Efficiency ( $RUE = NPP/Rainfall$  or  $NDVI/Rainfall$ ) and (ii) negative trends in the differences between the observed  $\Sigma NDVI$  and the  $\Sigma NDVI$  predicted by the rainfall using regressions calculated for each pixel (residual trends method - RESTREND). Both these methods are based on the concept that land degradation causes reductions in vegetation production per unit rainfall as a result of soil erosion, soil degradation, changes in vegetation species composition and increased run-off of water (Pickup, 1996; Walker *et al.*, 2002).

It has been suggested that rain-use efficiency (RUE), the ratio of net primary productivity (NPP) to precipitation, can normalize the inter-annual variability in NPP caused by rainfall variability and consequently provide an index of degradation that is

independent of the effects of rainfall (Nicholson *et al.*, 1998; Prince *et al.*, 1998). Field experiments have shown that degraded rangelands have reduced RUE (Le Houérou, 1984; Noy-Meir, 1985; Le Houérou *et al.*, 1988; Snyman, 1998; Illius & O'Connor, 1999; O'Connor, Haines & Snyman, 2001). Therefore, RUE has been proposed as a regional indicator of productivity and land degradation, since it can be derived from remote sensing estimates of production (e.g. Normalized Difference Vegetation Index, NDVI) and rainfall data (Tucker, Justice & Prince, 1986; Justice *et al.*, 1991a; Nicholson & Farrar, 1994; Pickup, 1996; Nicholson *et al.*, 1998; Prince *et al.*, 1998; Diouf & Lambin, 2001).

Evans and Geerken (2004) described a method that allows individual production-rainfall relationships to be developed for each pixel; after which negative trends in the production-rainfall relationship are used to facilitate the detection of potential human-induced land degradation. Analysis of the rainfall-production relationship for every pixel accommodates the effects of local variations in slope, soil and vegetation which all have a major influence on the nature of this relationship (Justice *et al.*, 1991a). The residual trends method (RESTREND) uses the entire time-series to derive a production-rainfall relationship, which is then used to predict annual production based on rainfall. Using the same time-series, it then identifies areas with negative trends in the difference between the observed and predicted production (residual=observed-predicted). Although natural ecological processes, such as the lag effects of successive dry years (Goward & Prince, 1995), can potentially produce negative trends in the residual, this method assumes that human impacts are one of the primary causes. Ideally the rainfall-production relationship should be derived

from a time-series containing no degradation and a full range of rainfall conditions, after which trends in the residuals of an independent time-series could be used to detect reduction in production caused by factors other than rainfall, such as degradation. Unfortunately such an independent, non-degraded reference period does not exist, since degradation may have occurred at any time, from before the beginning to the end of the satellite record (1981 to present). However, as will be discussed below, this does not prevent the calculated trends in the residuals from being used as an indicator of degradation (Evans & Geerken, 2004).

A serious problem that has inhibited studies of land degradation, is the lack of undisputed, large areas of land that have been degraded and as a result studies often end in discussion about the degree or even the reality of degradation (Prince *et al.*, 1998). Although the result of a policy that has caused extensive human suffering, the homelands in SA and communal lands in Zimbabwe (Prince, 2004) provide an extraordinarily valuable, if unintended experiment on the effects of long-term heavy utilization of the land that can be compared to adjacent, non-degraded, commercial areas that are equivalent in all other respects (e.g. soils, local climate and topography). The objectives of this study were to (i) characterize the relationship between rainfall and satellite-derived estimates of growth season production (NPP and sums of NDVI), (ii) compare the RUE values of known degraded and non-degraded areas with the same climate and soils in the north-eastern South Africa (SA), (iii) evaluate the inter-annual variability of the RUE values to determine if RUE is a robust index that can be mapped to monitor land degradation, and (iv) evaluate the ability of the RESTRENDS method to detect degradation.

#### 4.1.1 Remote sensing estimates of vegetation production

In arid and semi-arid lands seasonal sums of multi-temporal NDVI are strongly correlated with vegetation production (Prince & Tucker, 1986; Prince, 1991b; Nicholson & Farrar, 1994; Nicholson *et al.*, 1998). This is because phenological adjustments and intra-seasonal drought generally induce changes in leaf display and hence NDVI, rather than leaf persistence with physiological adjustments. Thus NDVI data derived from the AVHRR sensor have been widely used to assess desertification (Prince & Justice, 1991; Tucker *et al.*, 1991a; Tucker *et al.*, 1991b; Nicholson *et al.*, 1998; Prince *et al.*, 1998; Diouf & Lambin, 2001).

Satellite data can be used in production efficiency models to estimate net primary productivity (NPP) at global or regional scales (Prince, 1991a; Prince & Goward, 1995; Gower *et al.*, 1999; Running *et al.*, 1999; Behrenfeld *et al.*, 2001). These models are based on the concept of light-use efficiency, and they use the strong linear relationship between NDVI and the fraction of photosynthetically active radiation (PAR) absorbed by the plant ( $f_{PAR}$ ) to set the upper limit for unstressed NPP (Monteith, 1977; Sellers *et al.*, 1997; Schloss *et al.*, 1999). Spatial data for stress factors such as air temperature, vapor pressure deficit and soil moisture are used in various ways to convert the potential gross production into actual NPP (Cramer *et al.*, 1999; Gower *et al.*, 1999).

In this study both 1km resolution AVHRR  $\Sigma$ NDVI and modeled 8km resolution NPP were used to estimate vegetation production. The former has the advantages of computational simplicity and higher spatial resolution, while the latter

has the advantage of taking various climatic factors (e.g. rainfall and air temperature) into account to estimate actual NPP. Not all aspects of degradation are necessarily associated with reductions in biomass accumulation (Kelly & Walker, 1977; Parsons *et al.*, 1997), for example changes in species composition and soil erosion although, as Prince (2002) argues, these are phenomena of different scales than the regional scales considered here. Remotely sensed vegetation production may be the single most useful indicator of land degradation at regional and decadal scales (Prince, 2002).

## **4.2 Materials and Methods**

### *4.2.1 Study area - Summer rainfall region of South Africa*

The analyses were based on the summer growth season (October to April) excluding the winter rainfall region (April to September) along the western coast and the year-round rainfall region on the southern coast of SA (fig. 4.1a). The summer rainfall regions include the Nama Karoo, Savanna, Grasslands and Thicket biomes (Low & Rebelo, 1996)(fig. 4.1b) and therefore the vast majority of South African rangelands. Mean annual precipitation varies greatly along an east-west gradient from 1000mm along the east coast and escarpment to only 200mm in the Northern Cape Province (fig. 4.1c). Exotic forestry plantations are located along the high rainfall areas of the escarpment and parts of the Kwa-Zulu Natal Province. Dryland crop cultivation is largely limited to the grassland biome (Fairbanks *et al.*, 2000), while cattle, game, sheep and goat livestock farming is the dominant land use throughout the rest of the summer rainfall region.

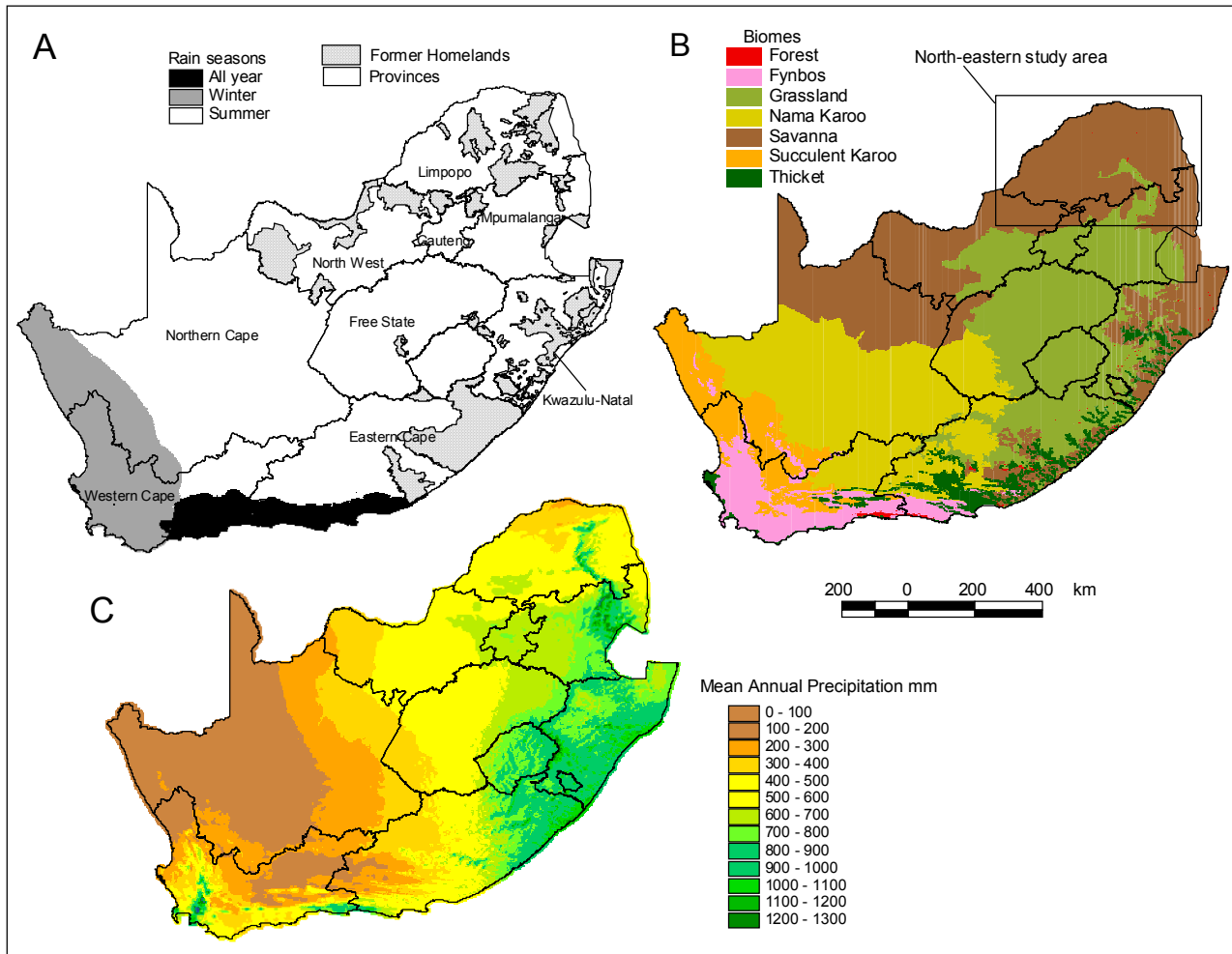


**Figure 4.1** (a) Rain seasons and former homelands, (b) biomes and (c) average rainfall of South Africa.

#### 4.2.2 NPP – GLO-PEM

The Global Production Efficiency Model (GLO-PEM) (Prince & Goward, 1995; Goetz *et al.*, 2000; Cao *et al.*, 2004) calculates gross primary production (Pg) from the product of incident photosynthetically active radiation (PAR), the fraction of PAR absorbed by the plant ( $f_{PAR}$ )(function of remotely sensed NDVI) and potential conversion efficiency or light use efficiency ( $\epsilon_g^*$ ) (Kumar & Monteith, 1982). The potential unstressed efficiency  $\epsilon_g^*$  of assimilation is further reduced by the environmental stress terms: air temperature ( $\delta_{Ta}$ ), vapor pressure deficit ( $\delta_{VPD}$ ) and soil moisture stress ( $\delta_M$ ).

$$Pg = PAR \cdot f_{PAR} \cdot \epsilon_g^* \cdot (\delta_{Ta} \delta_{VPD} \delta_M)$$

$$NPP = Pg \cdot R_m \cdot R_g$$

The total above and below-ground net primary production (NPP) is obtained by multiplication of Pg by the constant fraction of growth respiration ( $R_g$ ) and air temperature dependent maintenance respiration ( $R_m$ ) calculated for standing biomass pools, estimated using maps of percentage tree cover (DeFries, Townshend & Hansen, 1999). (For further details on the most recent version of the GLO-PEM model and input data used see Goetz *et al.*, 2000; Cao *et al.*, 2004).

Total growth season NPP (October to April of following year) was calculated from the 10-day NPP estimates for 1981-82 to 1999-2000 (N=19). The spatial patterns of total above and below-ground NPP predicted by the GLO-PEM model agreed very well with the above-ground NPP estimated by Schultze (1997) using Rosenzweig's (1968) approach. For details on AVHRR processing and  $\Sigma$ NDVI see section 2.2.3.

#### 4.2.3 *Rainfall data*

The rainfall data were recorded by a network of approximately 1800 weather stations managed by the South African Weather Service and ARC-ISCW (Monnik, 2001). For each station the long-term mean rainfall was calculated for every 10-day period of the year. Ten-day climatological mean rainfall surfaces were then created using multiple linear regression models with independent variable layers such as altitude, distance from ocean, local variation in elevation, latitude, longitude (Malherbe, 2001). To produce a date-specific, 10-day rainfall surface, the percentage of the 10-day long-term mean rainfall received during the specific period was calculated for every weather station. These percentage deviations were interpolated using inverse distance weighting. The resulting deviation layers were then multiplied by the long-term 10-day mean rainfall layers (Malherbe, 2001). The individual rainfall maps were subjected to stringent quality control to remove errors that may have been caused by, for example, incorrect weather station data. The total sum of summer growth season rainfall (October to April; hereafter referred to as only as rainfall) was used here, since it has a strong relationship with growth season sum NDVI ( $\Sigma$ NDVI)(Prince *et al.*, 1998; Yang *et al.*, 1998; Wang, Price & Rich, 2001).

#### 4.2.4 *Relationship of NPP and $\Sigma$ NDVI with rainfall*

The relationships of rainfall with NPP and  $\Sigma$ NDVI were characterized using linear regression for every pixel. The coefficients of determination ( $R^2$ ) were mapped to show geographical patterns of the NPP-rainfall and  $\Sigma$ NDVI-rainfall relationships.

The relationships between the inter-annual variability of estimates of vegetation production and that of rainfall were also investigated. The coefficient of variation (CV = standard deviation/mean) of each pixel was calculated for rainfall, NPP and  $\Sigma$ NDVI (Le Hou rou *et al.*, 1988; Schulze, 1997). Pixel values of the three CV layers were extracted at 1500 random points throughout the study area. A linear regression analysis based on these values was used to characterize the relationships between the CVs of rainfall and NPP, and rainfall and  $\Sigma$ NDVI.

#### 4.2.5 Comparison of $\Sigma$ NDVI-RUE of degraded and non-degraded areas.

This analysis was carried out in north-eastern SA which includes the entire Limpopo Province and parts of the Mpumalanga and North-West Provinces (approximately 200 000 km<sup>2</sup>)(fig. 4.1b). The region includes extensive degraded rangelands in the former homelands and current communal lands (Botha & Fouche, 2000; Hoffman & Ashwell, 2001). The National Land Cover map (NLC) (Fairbanks *et al.*, 2000) was used to map degraded and non-degraded rangelands. The NLC was produced using visual interpretation of 1995-96 Landsat TM data and extensive fieldwork (Fairbanks *et al.*, 2000). The degraded classes in the NLC were defined as regions with higher surface reflectance and lower vegetation cover compared to surrounding areas of similar vegetation (Fairbanks *et al.*, 2000).

In order to isolate the impact of degradation from spatial variation in soils, topography and climate, the study area was stratified using land capability units (LCUs). Land capability is a widely used concept in agricultural development and it refers to the suitability of the land for a specific use (Klingebiel & Montgomery,

1961). Land units with similar potential and physical limitations (e.g. climate or susceptibility to soil erosion) were grouped into land capability classes (fig. 4.2)(Schoeman *et al.*, 2002; Wessels *et al.*, 2004). Paired degraded and non-degraded areas in the same LCU were compared in terms of their RUE.

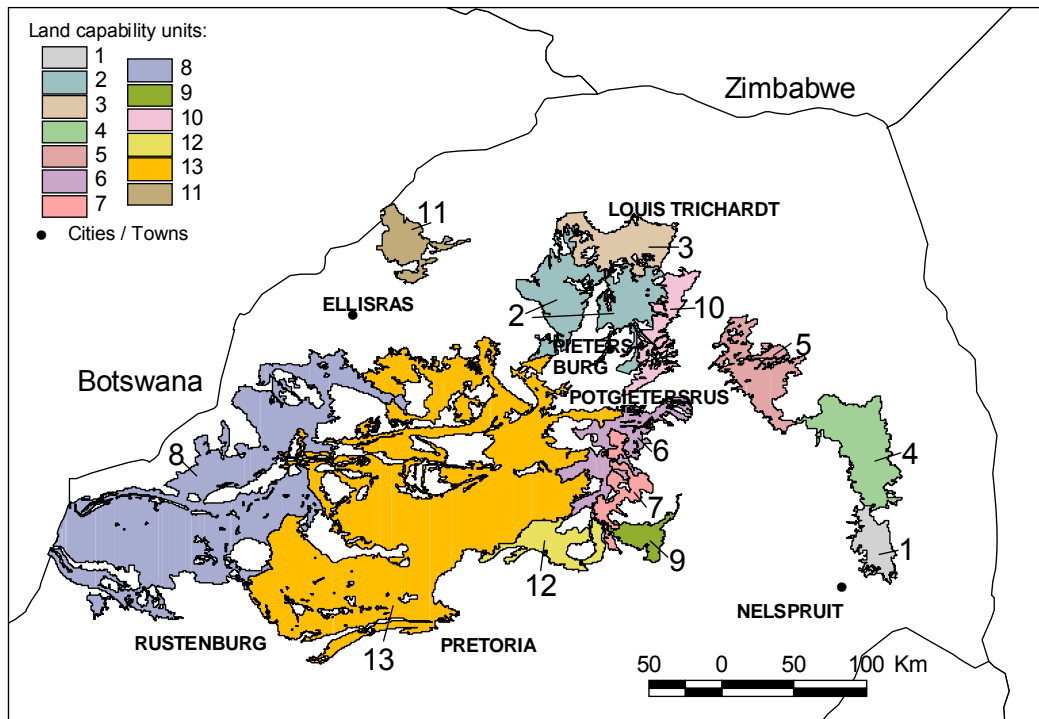


**Figure 4.2** Selected land capability units (LCU) containing degraded areas in north-eastern South Africa.

The RUE for a specific growth season (N=16) was estimated as the ratio  $\Sigma\text{NDVI} / \text{Rainfall}$  (hereafter referred to as  $\Sigma\text{NDVI-RUE}$ ). The spatial average  $\Sigma\text{NDVI-RUE}$  was calculated for each paired area and every growth season (N=16). A non-parametric Wilcoxon's rank sum test was applied to test if the median difference between annually paired non-degraded (nd) and degraded (d) RUE values was larger than zero ( $H_1: \Sigma\text{NDVI-RUE}_{\text{nd}} - \Sigma\text{NDVI-RUE}_{\text{d}} > 0$ ). Resulting P-values indicate the

probability that the median differences were equal to zero ( $H_0: \Sigma \text{NDVI-RUE}_{\text{nd}} - \Sigma \text{NDVI-RUE}_{\text{d}} = 0$ )

The average slopes and intercepts of the  $\Sigma \text{NDVI}$ -rainfall regressions were calculated for all the pixels in paired degraded and non-degraded areas to provide another measure of the mean rain-use efficiency (Rutherford, 1980; Illius & O'Connor, 1999).

#### *4.2.6 Variability of NPP-RUE in time and space.*

RUE maps were calculated using the NPP and growth season rainfall (hereafter referred to as NPP-RUE). The NPP-RUE maps for successive growth seasons were compared to test their value as an index of land degradation. NPP-RUE values were regressed on time, i.e. growth seasons 1-19 (1981-82 to 1999-2000) for each pixel to identify areas that had significant trends in NPP-RUE values.

#### *4.2.7 Identifying long-term trends in $\Sigma \text{NDVI}$*

$\Sigma \text{NDVI}$  values were similarly regressed on time, i.e. growth seasons 1-16 (1985-86 to 2002-3, excluding 1993-94 and 1994-95), for each pixel. Pixels with significant negative slopes indicate areas that experienced a negative temporal trend in growth season biomass production (Evans & Geerken, 2004).

#### *4.2.8 Detecting negative trends in the $\Sigma$ NDVI-rainfall relationships – RESTREND method.*

The long-term trends in  $\Sigma$ NDVI identified in the above-mentioned analyses contain a significant climate signal that needs to be removed to allow climate trends to be distinguished from human-induced land degradation (Archer, 2004; Evans & Geerken, 2004). Regressions between  $\Sigma$ NDVI and growth season rainfall were calculated for every pixel. To control the effect of inter-annual variation in precipitation, the differences between the observed  $\Sigma$ NDVI and the  $\Sigma$ NDVI predicted by the rainfall were calculated and the residuals (observed-predicted) regressed on time. Trends in these residuals over time may indicate changes in  $\Sigma$ NDVI that were not due to the effect of rainfall in the current year and therefore may facilitate the identification of human impacts (Evans & Geerken, 2004; Geerken & Ilaiwi, 2004).

### **4.3 Results and discussion**

#### *4.3.1 Relationship of NPP and $\Sigma$ NDVI with rainfall*

The rainfall-NPP and rainfall- $\Sigma$ NDVI relationships differed in strength, but showed very similar patterns (fig. 4.3). The rainfall-NPP relationship was generally the stronger one, as expected, since rainfall affects the physiological as well as the leaf area components of NPP. Critical t-values calculated for every pixel indicated that, in general, all the regressions with  $R^2 > 0.3$  were significant. The strongest relationships ( $R^2 = 0.6-0.9$ ) were evident in north-eastern Mpumalanga and in most of the Limpopo Province (figs 4.3a, b). Using field data from world-wide semi-arid areas, Le Hou  rou

*et al.* (1988) found slightly lower  $R^2$  values of between 0.25 and 0.4, but Snyman (1998) reported similar values for the Free State, SA.

In general, the drier areas (<500mm e.g. Northern Cape, North-West, Limpopo Provinces) had the strongest, while the wetter areas (>700mm e.g. Lesotho, Kwa-Zulu-Natal, Mpumalanga Highveld) had the weakest relationships (figs 4.3a, b). The areas with very low  $R^2$  values in Limpopo and Mpumalanga provinces occurred on the wet escarpment and the Soutpansberg mountains that are covered by indigenous forests and commercial plantations of exotic trees. Low  $R^2$  values were evident for the irrigated cultivation along the Orange River and some dry land cultivation in western Free State.

For approximately half of the drier (<700mm) parts of the study area the strength of the rainfall-ΣNDVI was comparable to those reported in the literature (Malo & Nicholson, 1990; Nicholson *et al.*, 1998; Prince *et al.*, 1998; Yang *et al.*, 1998; Diouf & Lambin, 2001). Some dry areas had very weak relationships that are not related to specific land uses or vegetation types (e.g. Northern Cape; figs 4.3a, b) and may have been caused by extreme rainfall values. Extreme rainfall values are often the result of storms that produce high rainfall in a very short period at the end of a summer growing season, sometimes followed by a lagged response of vegetation to this high rainfall in the following growth season (Goward & Prince, 1995).

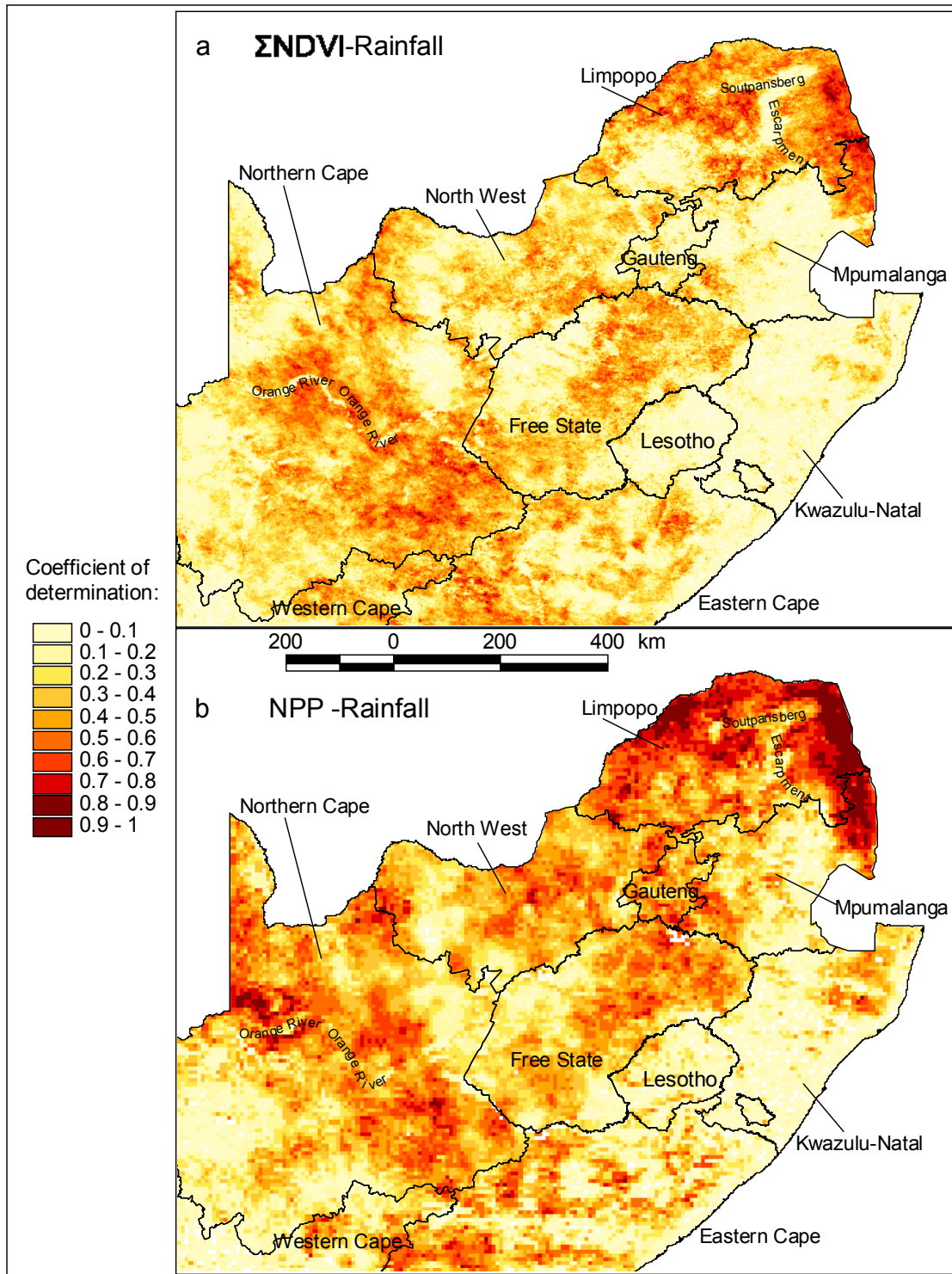


**Figure 4.3** Maps of coefficients of determination for (a)  $\Sigma$ NDVI-rainfall and (b) NPP-rainfall regressions for the summer rainfall region of South Africa.

The regional patterns of the CVs of rainfall,  $\Sigma$ NDVI and NPP (fig. 4.4) were similar, with an eastward decrease over SA and the lowest values along the wet east coast. There were moderate to strong linear relationships between the CVs of rainfall vs.  $\Sigma$ NDVI ( $R^2=0.366$ ) and rainfall vs. NPP ( $R^2=0.58$ ). All three CV maps had their highest values in the drier Northern Cape, Western Cape and Limpopo Provinces. The CVs for  $\Sigma$ NDVI and NPP were very high (>30%) in north-eastern Mpumalanga (Lowveld) and eastern Limpopo provinces, in the region occupied by Kruger National Park (fig. 4.4). Thus areas with high rainfall variability also experienced high variability in vegetation production (Le Hou  rou, 1984; Le Hou  rou *et al.*, 1988; Schulze, 1997).

There was a strong negative relationship between mean annual precipitation and the CVs of rainfall ( $R^2=0.85$ ), NPP ( $R^2=0.5$ ) and  $\Sigma$ NDVI ( $R^2=0.3$ )(figs 4.1c, 4.4). The CV of rainfall was more than double that of NPP in the eastern half of SA (fig. 4.4). Prince *et al.* (1998) also reported lower inter-annual variability in  $\Sigma$ NDVI than in rainfall. However, this does not agree with field measurements that suggest 50% greater variation in production than rainfall (Le Hou  rou *et al.*, 1988; O'Connor *et al.*, 2001). Therefore, it appears that remote sensing estimates of vegetation production may underestimate the variability of production as measured in the smaller field sites (Diouf & Lambin, 2001).

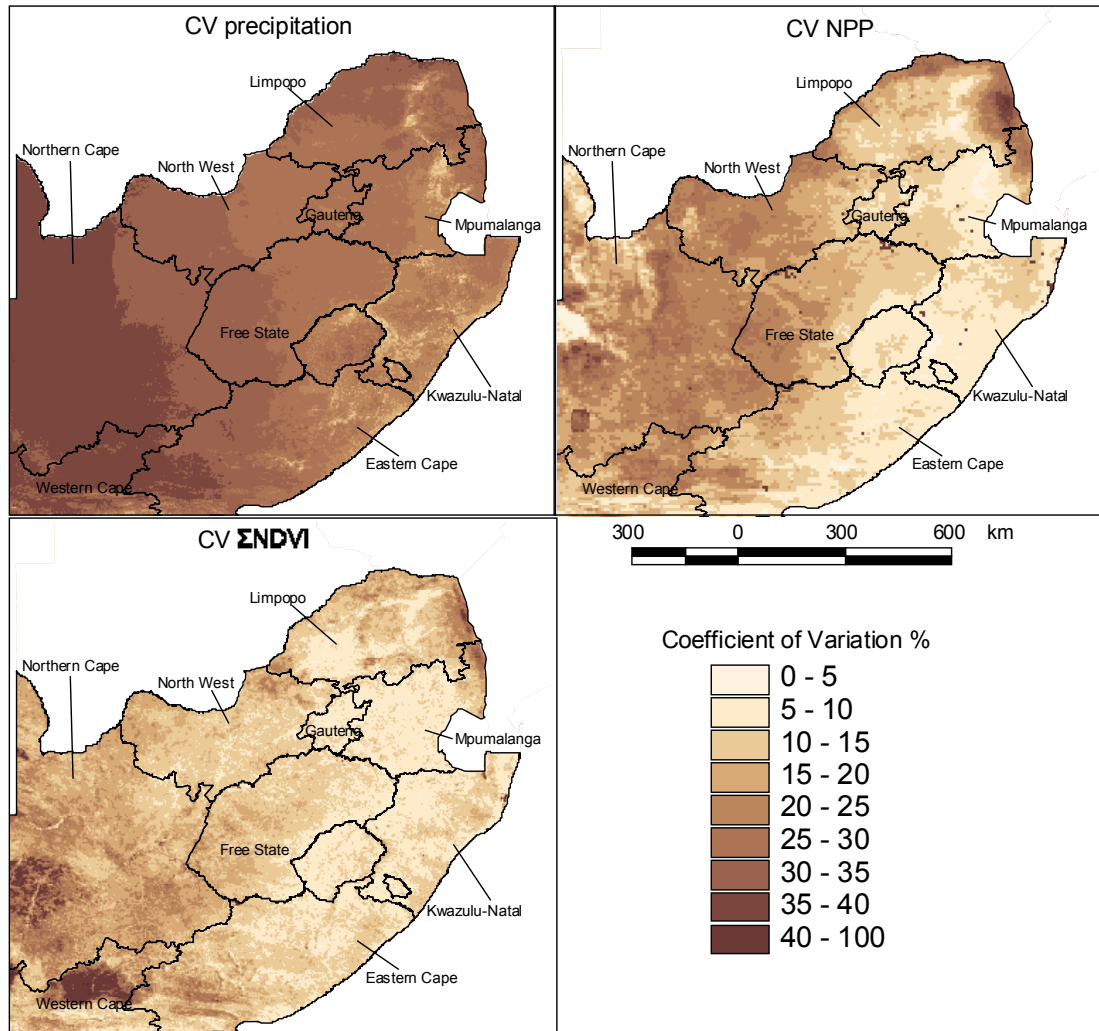


**Figure 4.4** Coefficients of variation for precipitation (after Schulze 1997) NPP and  $\Sigma$ NDVI of the summer rainfall region of South Africa.

#### 4.3.2 Comparison of $\Sigma$ NDVI-RUE of degraded and non-degraded areas.

The  $\Sigma$ NDVI-RUE of degraded areas was consistently lower than that of paired non-degraded areas for most LCUs (fig. 4.5), with the exception of a few seasons in LCUs 1 and 11. In a Wilcoxon's test of the probability that the median difference in  $\Sigma$ NDVI-RUE between paired areas was equal to zero ( $H_0: m = 0$ ), LCUs 2, 5, 7, 9, 10, and 12 had P-values  $< 0.05$  indicating significantly higher  $\Sigma$ NDVI-RUE values in

non-degraded areas. LCUs 4 and 13 had slightly lower probabilities (92 and 93% respectively). LCUs 1, 3, 6, 8 and 11 were not significantly different.

$\Sigma$ NDVI-RUE values were inversely related to rainfall; the highest  $\Sigma$ NDVI-RUE values were observed in the very low rainfall 1991-92 and 1997-98 seasons. The  $\Sigma$ NDVI-RUE values did not show any clear trend through time, but rather fluctuated between growth seasons in step with variations in rainfall.

The intercepts of the regressions of  $\Sigma$ NDVI on rainfall for the non-degraded areas were consistently higher than those of the degraded paired areas, while the slopes were approximately equal (table 4.1). This agreed with the findings in Zimbabwe (Kelly & Walker, 1977) and SA where heavily utilized rangelands were compared with rangelands in good condition (Illius & O'Connor, 1999). This indicated that the forage production of degraded areas was consistently less for a given amount of rainfall, although the degraded areas had the same inter-annual variability and hence similar resilience (Wessels *et al.*, 2004).

**Table 4.1** Average slope and intercept for  $\Sigma$ NDVI-Rainfall relationship in degraded and non-degraded areas of each land capability unit (LCU). The number of pixels varied between degraded and non-degraded areas of each LCU.

| LCU | Slope        |          | Intercept    |          |
|-----|--------------|----------|--------------|----------|
|     | Non-degraded | Degraded | Non-degraded | Degraded |
| 1   | 0.019        | 0.014    | 61.3         | 61.5     |
| 2   | 0.033        | 0.033    | 41.0         | 34.5     |
| 3   | 0.037        | 0.035    | 40.3         | 38.3     |
| 4   | 0.027        | 0.020    | 54.5         | 52.4     |
| 5   | 0.018        | 0.023    | 67.5         | 53.3     |
| 6   | 0.039        | 0.042    | 40.0         | 34.3     |
| 7   | 0.039        | 0.036    | 39.7         | 37.4     |
| 8   | 0.029        | 0.028    | 45.8         | 44.4     |
| 9   | 0.026        | 0.027    | 54.8         | 47.1     |
| 10  | 0.014        | 0.020    | 57.8         | 42.7     |
| 11  | 0.033        | 0.030    | 38.3         | 38.7     |
| 12  | 0.025        | 0.022    | 52.0         | 44.8     |
| 13  | 0.018        | 0.025    | 53.7         | 46.9     |

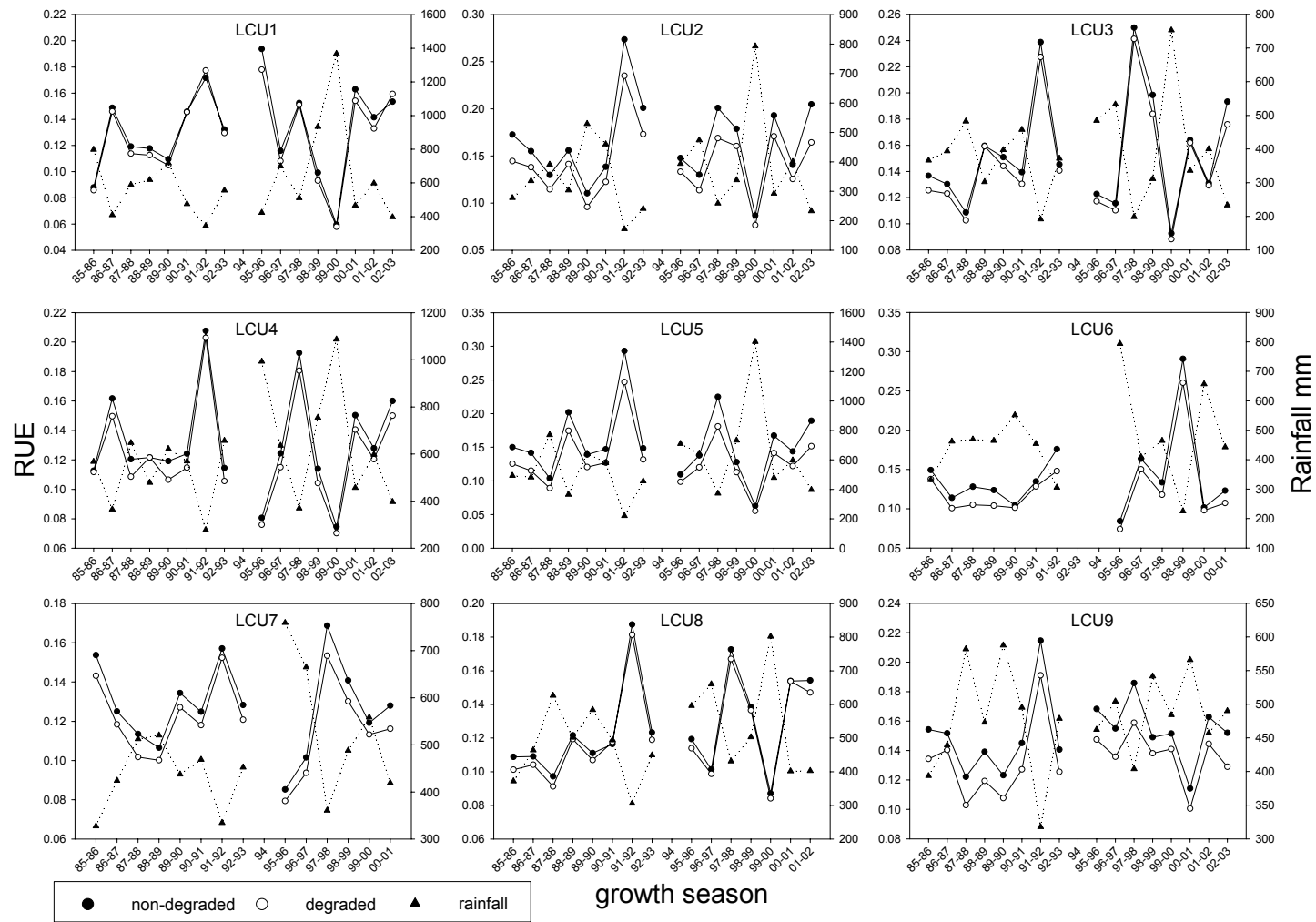


**Figure 4.5** Average  $\Sigma$ NDVI-RUE of degraded and non-degraded rangelands per growth season, in specified land capability units (LCUs) in north-eastern SA. The locations of the LCUs are shown in Figure 4.2.

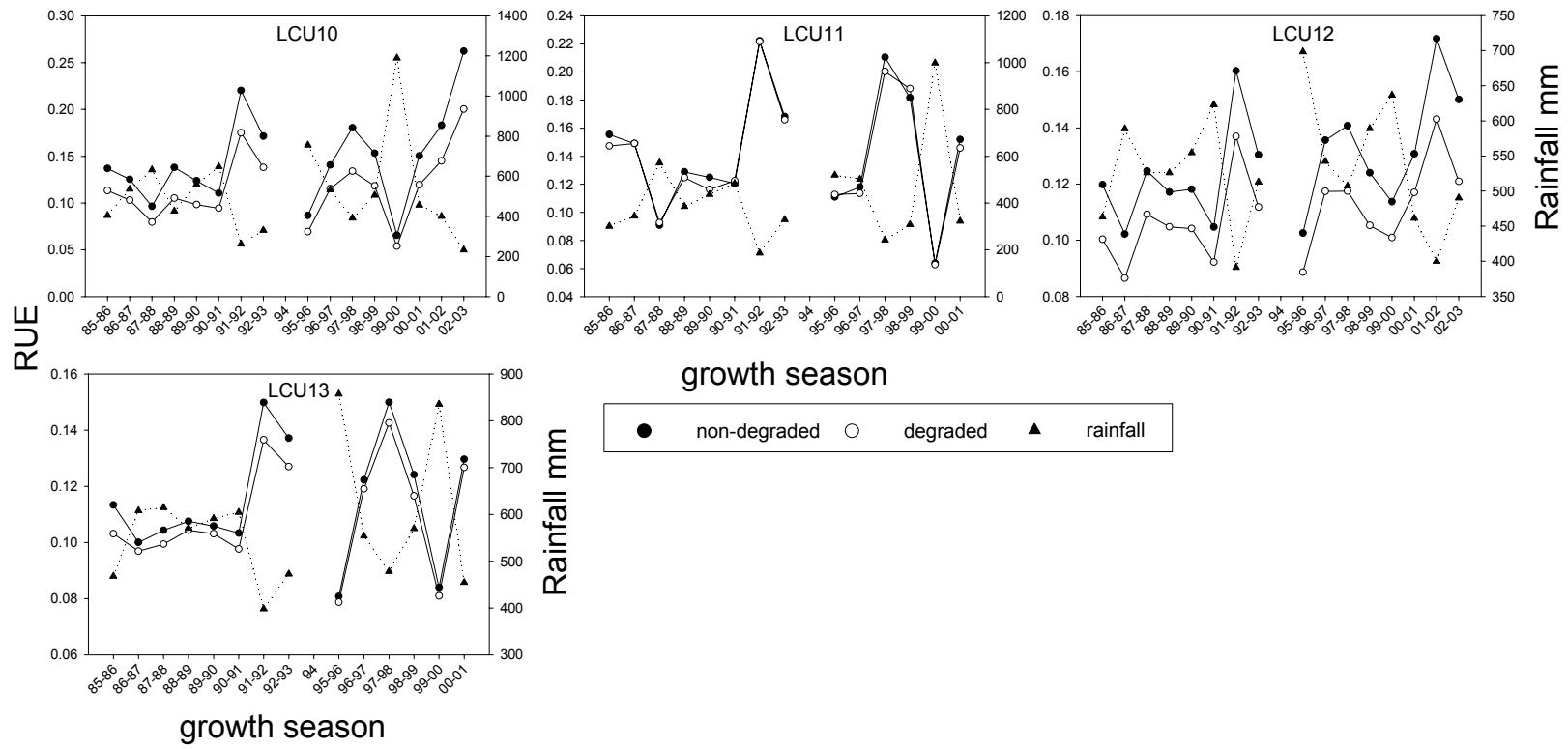
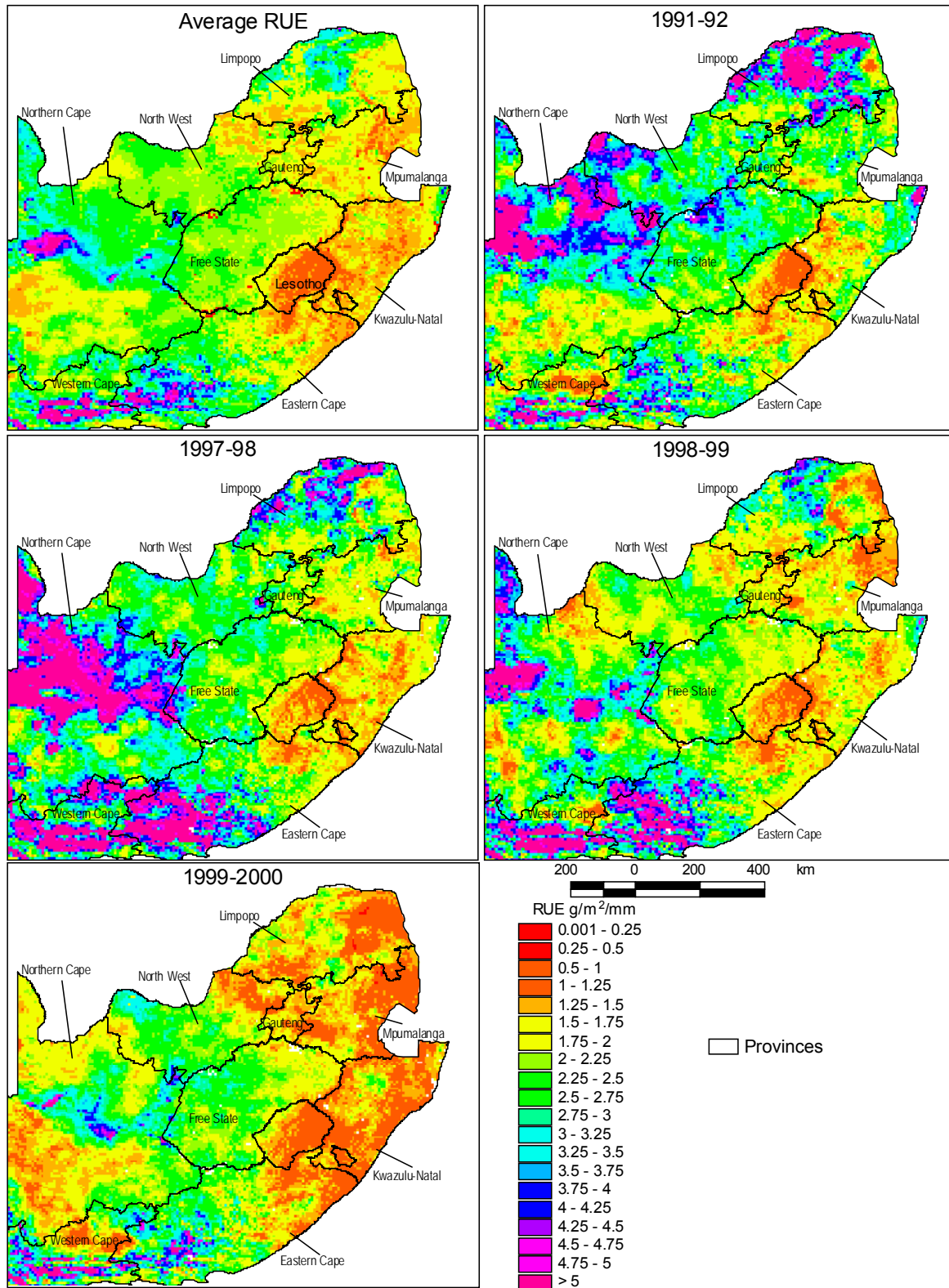


Figure 4.5. continue

#### 4.3.3 Variability of NPP-RUE through time and space.

The average NPP-RUE (1981-82 to 1999-2000) was lowest in the mountains of Lesotho and the escarpment in the Mpumalanga and Limpopo provinces, probably because although these areas experience high rainfall, there is extensive surface run-off due to steep topography (fig. 4.6). Very high average NPP-RUE values were found along the Orange River in the Northern Cape Province probably caused by irrigated cultivation in an otherwise very dry region. The average NPP-RUE was the highest in some of the driest rangelands of SA (<350mm), i.e. northern Limpopo and northern Northern Cape Provinces (figs 4.1c, 4.6, 4.7). This does not completely agree with the findings of Le Houérou (1984), who found that RUE decreased with increasing aridity due to the fact that the proportion of “inefficient” rains increased in very dry sites. However, in agreement with another study in the Sahel (Prince *et al.*, 1998), RUE varied over a narrow range at high rainfall but, at low rainfall the mean and range of RUE increased (fig. 4.7). This could be the result of overestimation of very low NPP values by satellite observations (Prince, 1991b), or an upward shift in the RUE in desert margin vegetation (Prince *et al.*, 1998).

There was considerable inter-annual variation in NPP-RUE as a result of large fluctuations in growth season rainfall (fig. 4.6). In 1991-92 and 1997-98, both El Niño years (Anyamba *et al.*, 2002; Anyamba *et al.*, 2003), there were very high NPP-RUE values over parts of the Northern Cape and Limpopo Provinces, which were caused by very low rainfall. In the 1999-2000 La Niña year (Anyamba *et al.*, 2002) there were very low NPP-RUE values in the eastern part of the country associated with exceptionally high rainfall.



**Figure 4.6** Average NPP-RUE, 1991-92 NPP-RUE and 1997-98 to 1999-2000 NPP-RUE. Note that the NPP includes both above and below ground production.

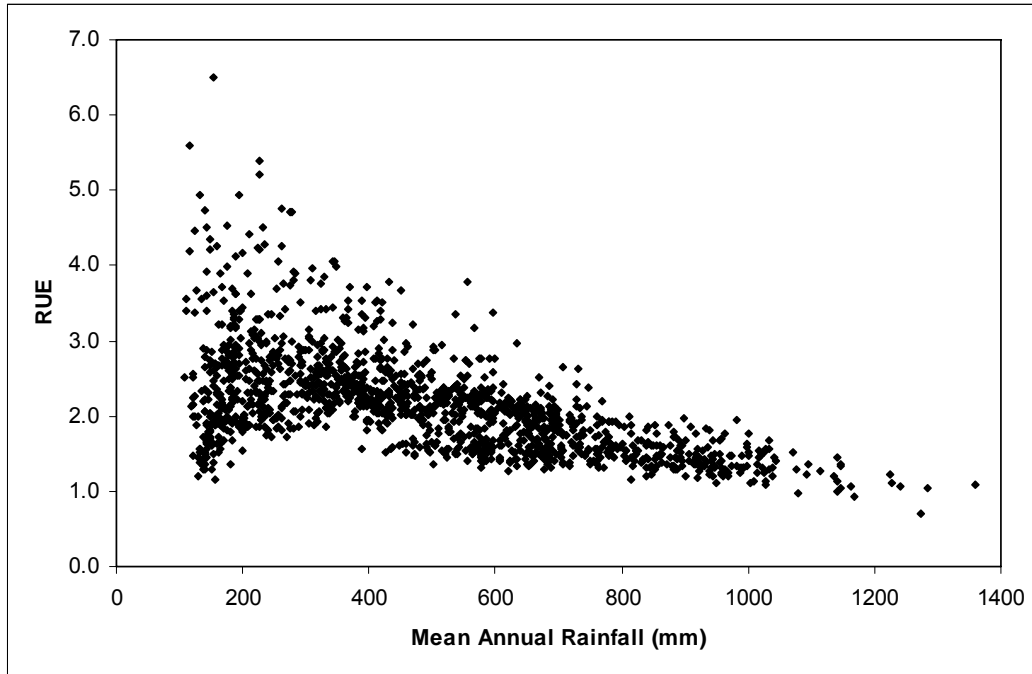


**Figure 4.7** Average NPP-RUE of 1500 random points plotted against average rainfall for the summer rainfall region of South Africa.

The temporal trend of NPP-RUE had negative values over large areas of the Limpopo, Northern Cape and Mpumalanga Provinces (figs 4.6, 4.8). NPP-RUE was often high in growth seasons with very low rainfall and low NPP (e.g. fig. 4.9, 1982-83, 1991-92) and low in growth seasons with high rainfall and high NPP (e.g. fig. 4.9, 1998-99, 1999-2000). The correlation between annual RUE and rainfall was also calculated for each pixel and confirmed a strong negative correlation (average  $r = -0.82$ ) across the entire SA. Thus the NPP-RUE ratio does not provide an index of degradation that is independent of the effects of rainfall.

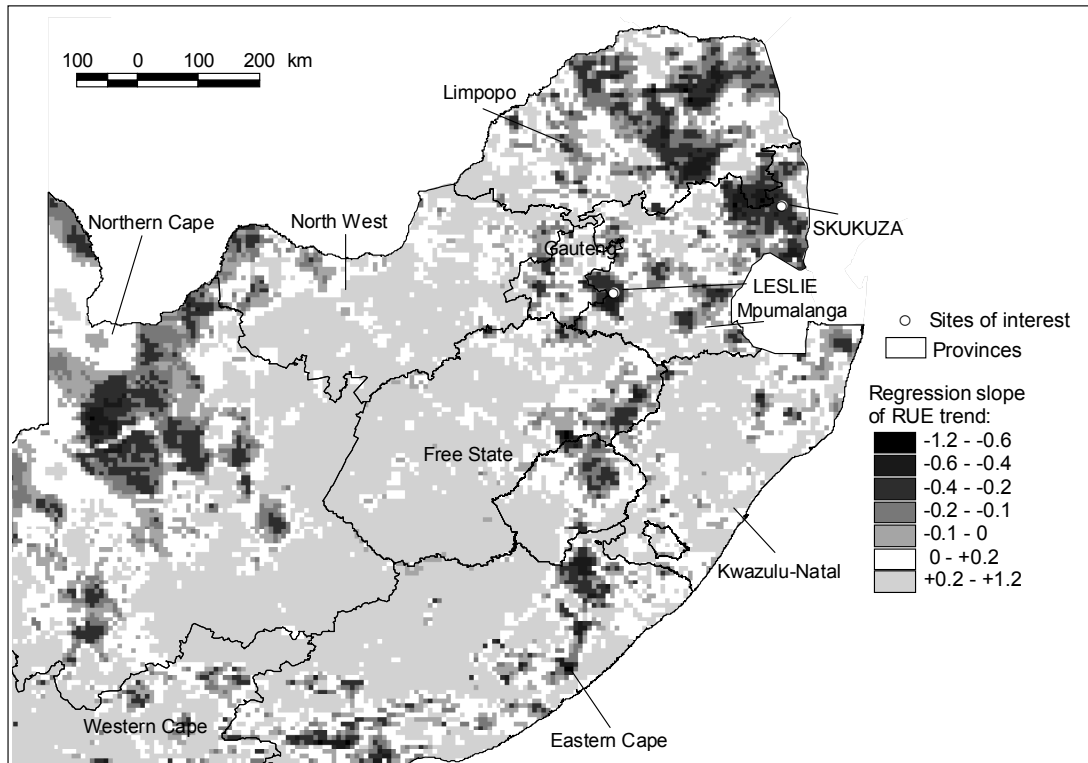


**Figure 4.8** Map of slope of the NPP-RUE-time regression indicating positive or negative trends. The locations of two sites are indicated for which NPP, rainfall and RUE values are given in figure 4.9.

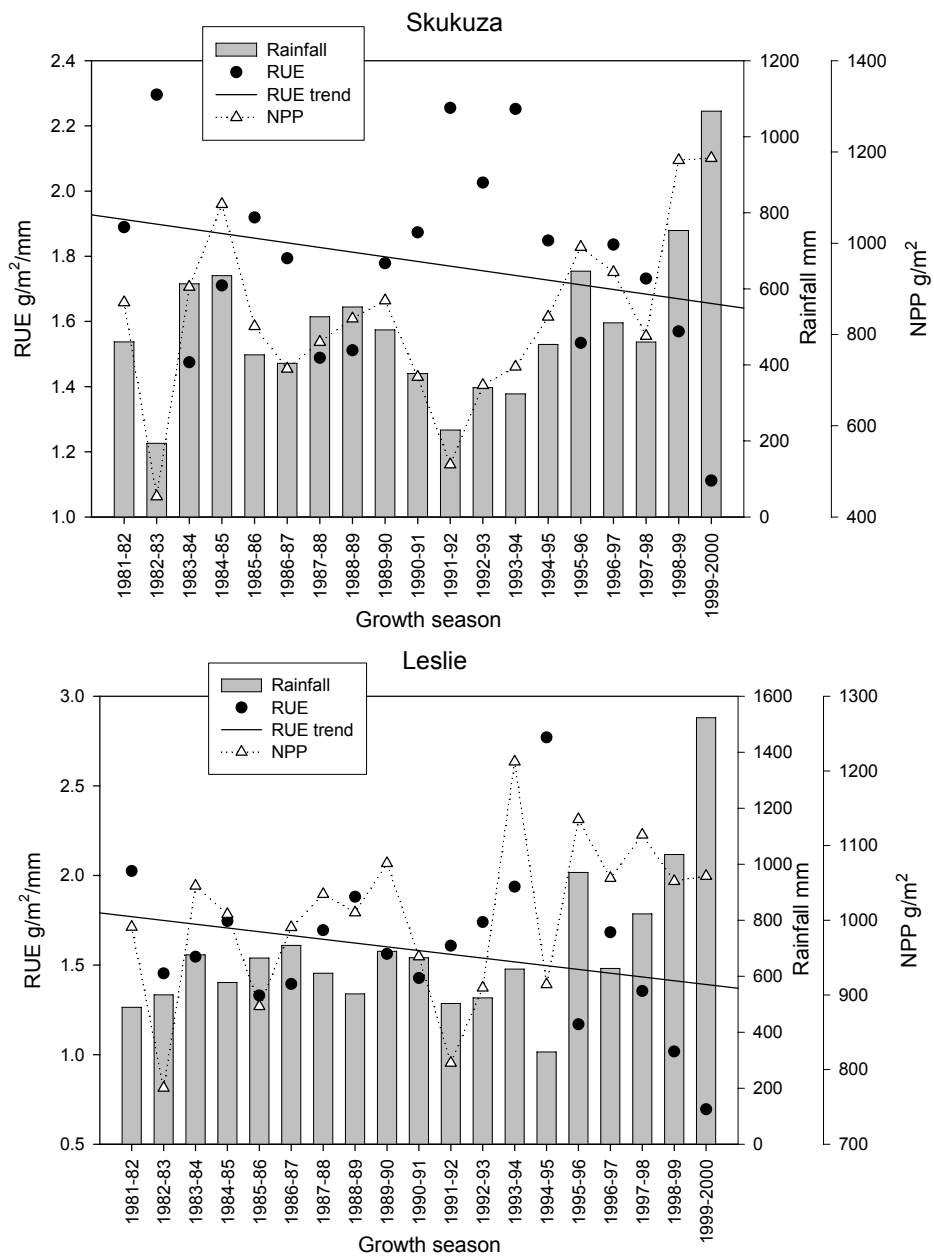


**Figure 4.9** NPP-RUE profile for two locations with negative trends in figure 4.8.

#### 4.3.4 Identifying long-term trends in $\Sigma$ NDVI

Most of eastern SA showed a positive trend in  $\Sigma$ NDVI through time (fig. 4.10), although the Nama Karoo biome (fig. 4.1b) and most of the western Northern Cape Province had negative trends (fig. 4.10a). These widespread phenomena are unlikely to have been

caused by human factors and are more likely due to wetter conditions over the eastern half of SA during the late 90's, as opposed to drier condition during this periods across western SA.

Small areas that had negative trends within areas that otherwise had positive trends may indicate changes in land cover or land condition during the study period (Geerken & Ilaiwi, 2004). Areas in the Gauteng province which had strong negative trends in  $\Sigma$ NDVI (fig. 4.10a) appeared to be the result of the expansion of informal settlements (e.g. Hammaskraal), mining operations and urban areas on the outskirts of Pretoria and Johannesburg (Fairbanks *et al.*, 2000). Areas with negative trends in the Mpumalanga Highveld appeared to be associated with coal mining operations and harvesting of forestry plantations.

Isolated patches within the degraded former homelands of the Limpopo Province had negative trends, while most of these areas had positive trends, just like the surrounding non-degraded rangelands (fig. 4.10a). This may indicate that much of the extensive land degradation in the former homelands of Limpopo Province occurred before the period examined here, i.e. prior to 1985 (Hoffman & Ashwell, 2001; Wessels *et al.*, 2004).

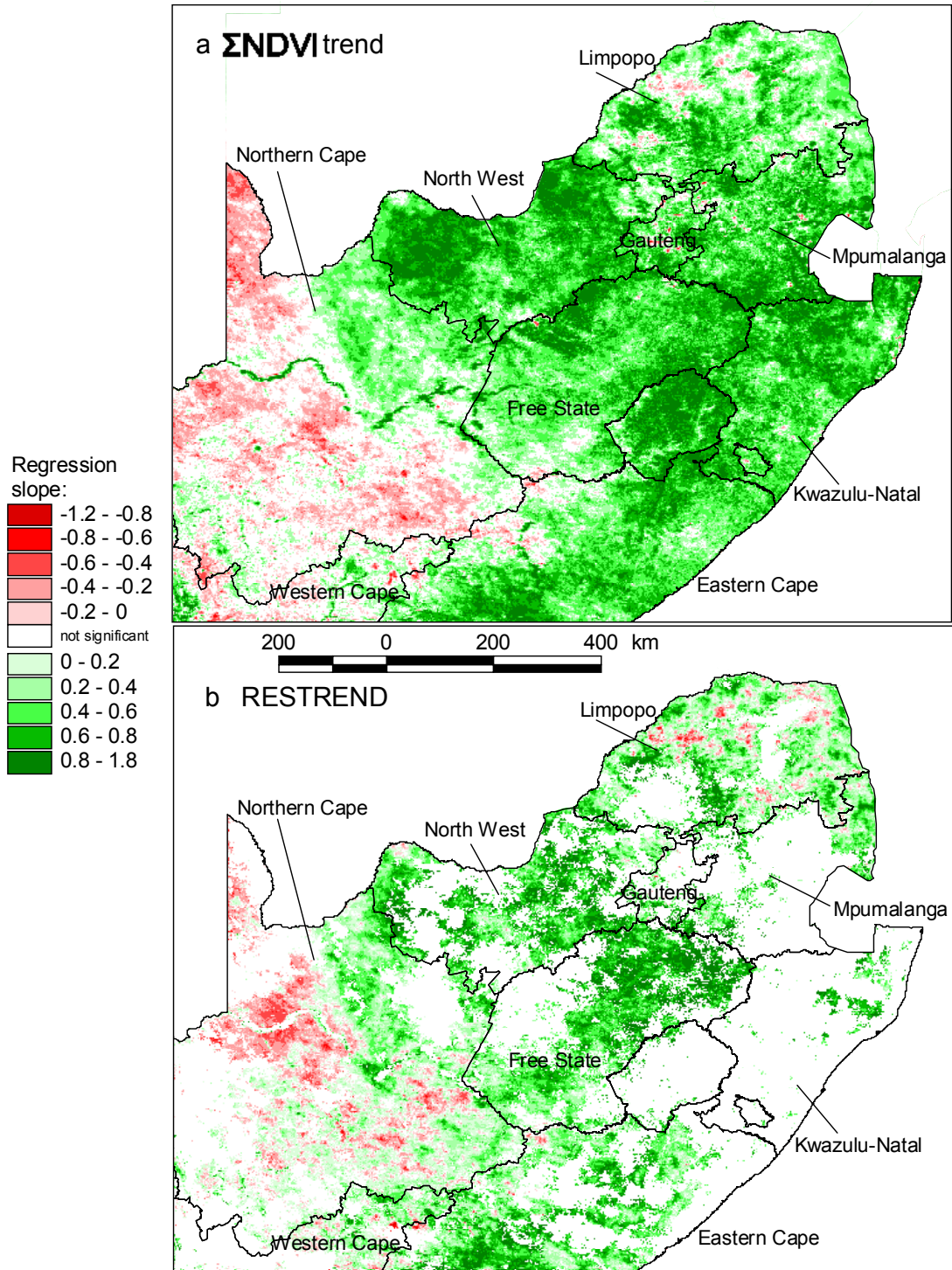


**Figure 4.10** (a) Map of slope of the  $\Sigma$ NDVI-time regression indicating positive or negative trends. (b) Map of slope of the residual-time regression. The residuals were calculated as the difference between the observed  $\Sigma$ NDVI and predicted  $\Sigma$ NDVI using the linear  $\Sigma$ NDVI-rainfall relationships. Pixels without statistically significant slopes were omitted (white).

#### 4.3.5 Detecting negative trends in the $\Sigma$ NDVI-rainfall relationships – RESTREND

Most of SA showed positive trends of residuals with time and therefore an apparent increase in forage production per unit rainfall (fig. 4.10b). There were similarities in the geographic patterns of the residual (fig. 4.10b) and the  $\Sigma$ NDVI trends (fig. 4.10a). Areas with negative trends in  $\Sigma$ NDVI in the

Limpopo Province (fig. 4.10a) also had negative residual trends (fig. 4.10b). However, more and larger areas had negative residual trends suggesting that, although such areas showed increases in  $\Sigma$ NDVI with time, it was lower than that predicted by the rainfall. The correlation between annual residuals and rainfall was calculated for each pixel and, in contrast to RUE, the residuals were not correlated with rainfall ( $r < |1|$ ).

A number of areas in Limpopo Province showed negative residual trends, for example, the area of commercial rangelands north of the Soutpansberg near the town of Alldays (fig. 4.11, area 1 fig. 4.12).

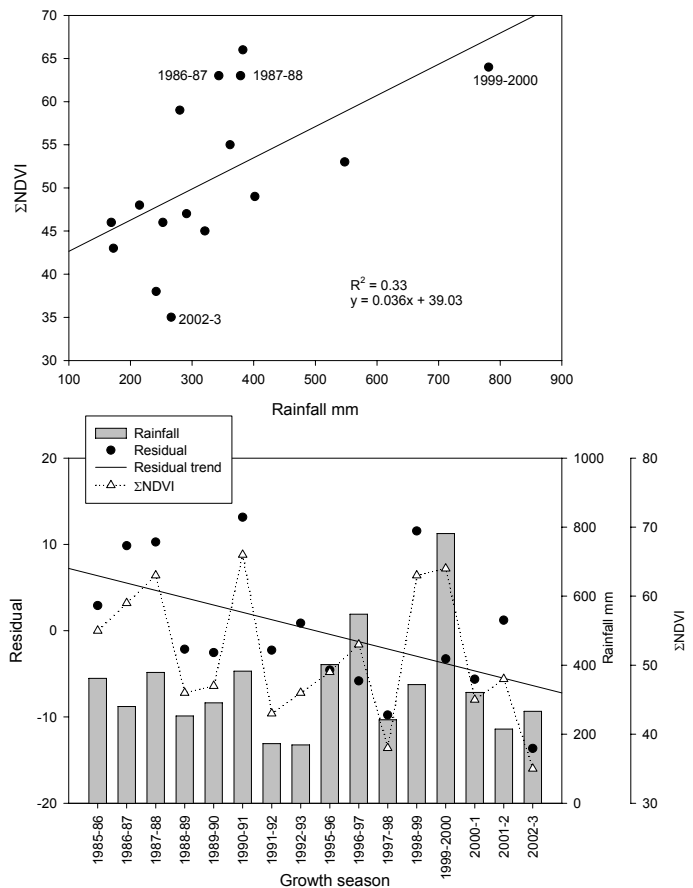


**Figure 4.11** Linear regression of  $\Sigma$ NDVI and rainfall (top panel). Trend of residuals plotted against  $\Sigma$ NDVI and rainfall per growth season for a typical pixel in area 1 of fig. 4.12 (bottom panel).

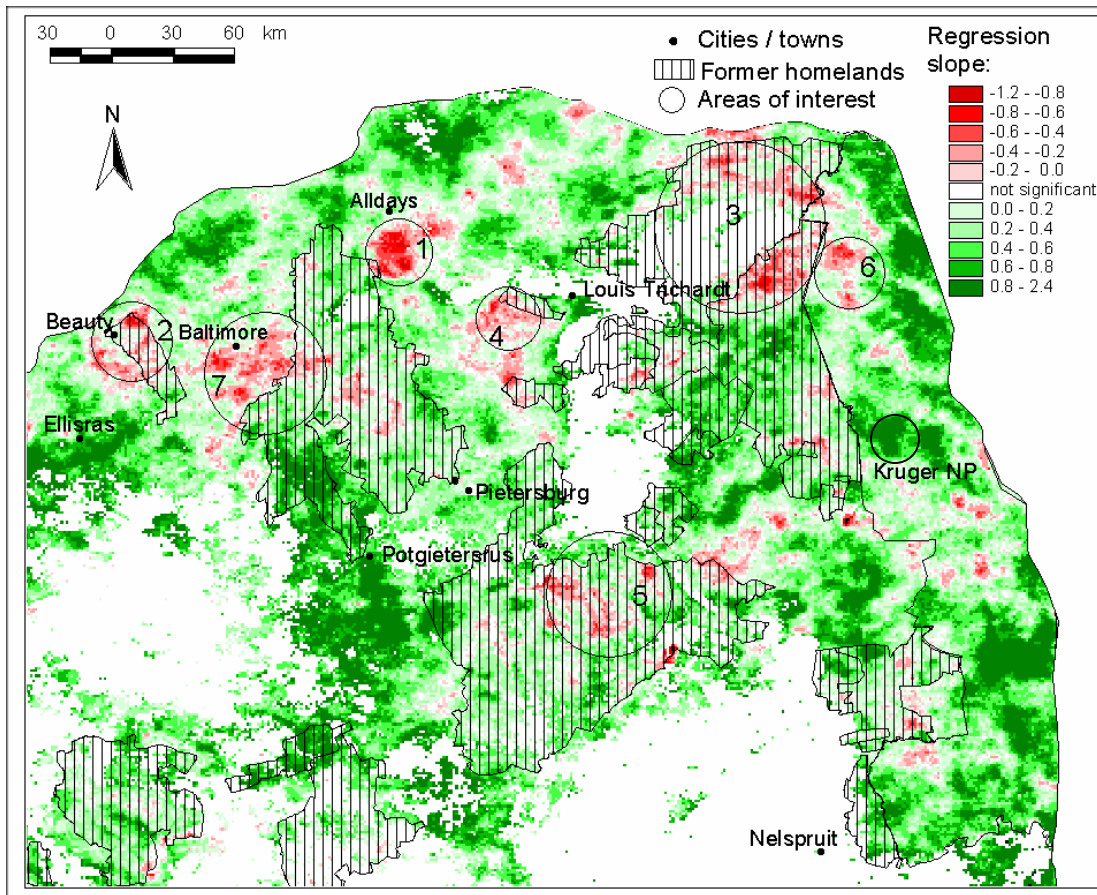


**Figure 4.12** Enlargement of Figure 10a for north-eastern SA with former homelands and areas of interest showing negative trends (circles). Map of slope of the residual-time regression. The residuals were calculated as the difference between the observed  $\Sigma$ NDVI and predicted  $\Sigma$ NDVI using the linear  $\Sigma$ NDVI-rainfall relationships. Pixels without statistically significant slopes were omitted (white).

Areas around the town of Beauty in the former Lebowa homeland had negative residuals in and around areas mapped as degraded by the NLC (area 2 fig. 4.12). Parts of the former Venda and Gazankulu homelands along the western boundary of Kruger National Park (KNP) had negative residual trends that might be caused by expanding land degradation, informal settlements, and subsistence cultivation (area 3 fig. 4.12).

The degraded areas in the Dzanani district (also part of former Venda homeland) west of Louis Trichardt appeared to be expanding and had negative residual trends (area 4 fig. 4.12). This was the result of lower than predicted  $\Sigma$ NDVI in the last two growth seasons of the time series which may have been exacerbated by the accumulative lag effects of three successive dry years (fig. 4.13)(Goward & Prince, 1995). Exceptionally high rainfall also caused negative residuals during the 1999-2000 growth season.

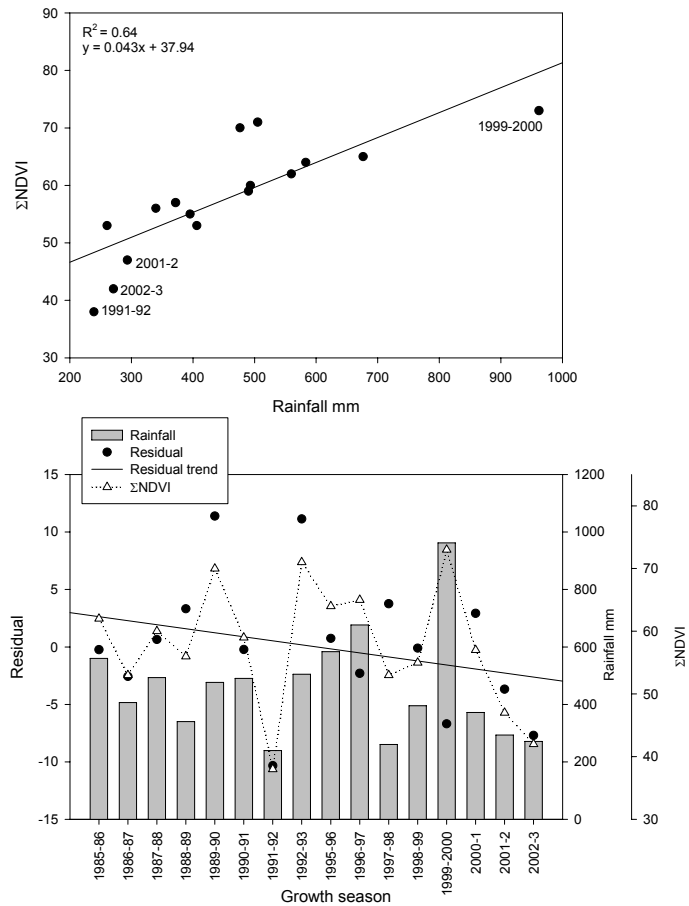


**Figure 4.13** Linear regression of  $\Sigma$ NDVI and rainfall (top panel). Trend of residuals plotted against  $\Sigma$ NDVI and rainfall per growth season for a typical pixel in area 4 of fig. 4.12 (bottom panel).

Other areas with negative residual trends occurred in the former Lebowa homeland and appeared to be associated with degraded rangelands identified by the NLC (area 5 fig. 4.12).

A very large area south-east of the town of Baltimore showed negative trends that could be attributed to abandoned agricultural fields, rangeland degradation and expanding informal settlements (area 7 fig. 4.12). Isolated patches within KNP showed negative trends (area 6 fig. 4.12) that were caused by negative residuals in the very wet 1999-2000 and the dry 2002-3 growing seasons (fig. 4.14). Large areas had strong positive residual trends and in KNP (fig. 4.12) it was caused by negative residuals

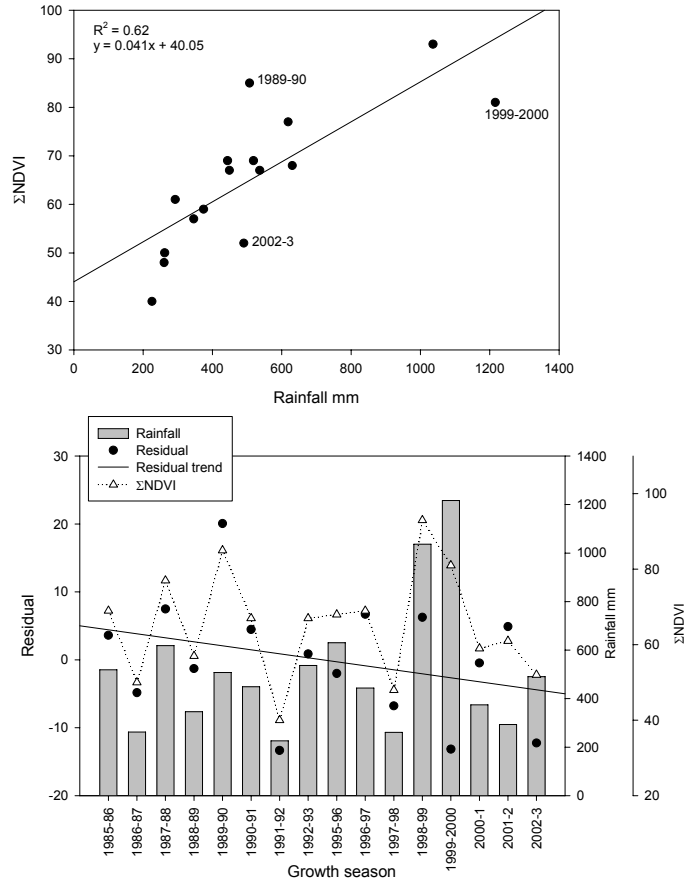


**Figure 4.14** Linear regression between  $\Sigma$ NDVI and rainfall (top panel). Trend of residuals plotted against  $\Sigma$ NDVI and rainfall per growth season for a typical pixel in area 6 in (Kruger National Park) of fig. 4.12 (bottom panel).

at the beginning of the time-series (1985-88) and very positive residuals in the late nineties (1996-99)(fig. 4.15). The negative residuals at the beginning of the time-series could have been caused by the extended El Niño conditions of the preceding early 1980's. Since human impacts are highly unlikely inside this national park, these are examples of where natural ecological processes may cause significant positive or negative residual trends.

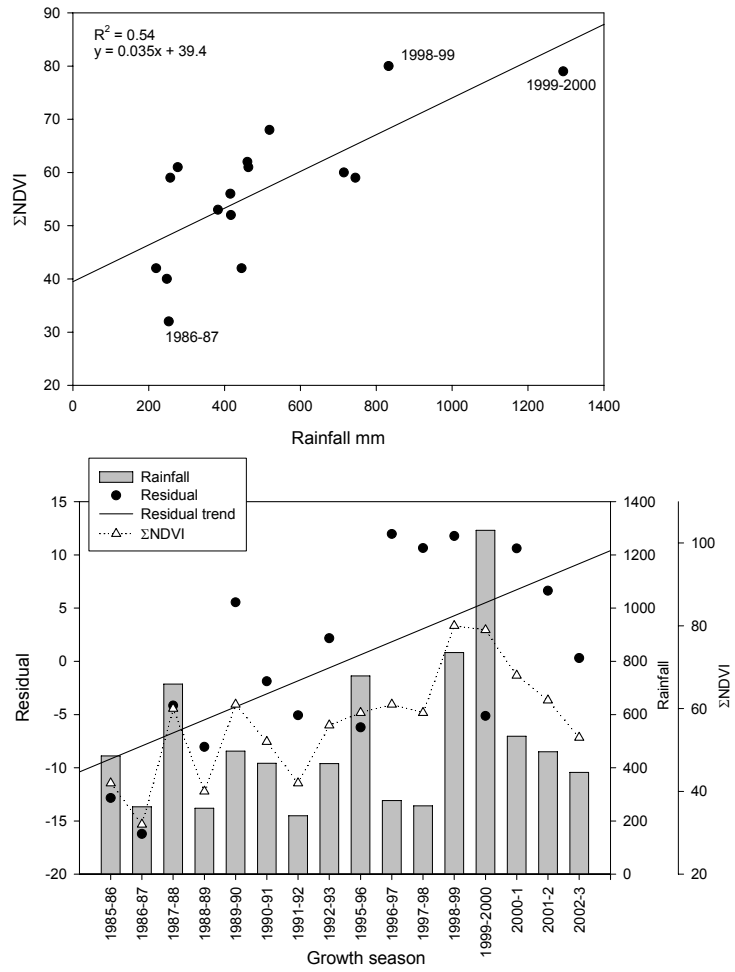


**Figure 4.15** Linear regression between ΣNDVI and rainfall (top panel). Trend of residuals plotted against ΣNDVI and rainfall per growth season for a typical pixel in Kruger National Park (fig. 4.12) (bottom panel).

A large area around the town of Upington in the Northern Cape had negative residual trends (fig. 4.10b). Large areas in the Karoo south of Hopetown also showed negative residual trends partly due to very low  $\Sigma$ NDVI values during the 2000-1 and 2002-3 growth seasons (fig. 4.16). The reasons for these negative trends have not yet been determined.

Since a non-degraded reference period does not exist,

both the underlying rainfall-production relationship and degradation impacts have to be extracted from the same time-series. Since the time-series include unknown degrees of degradation, the observed rainfall-production relationships (OR) may be quite different from an underlying, non-degraded relationship (NR). If there has been degradation, the OR will generally underestimate the production expected for a given amount of rainfall (fig. 4.17a) and, as a result, the residuals will underestimate the magnitude of degradation (fig. 4.17b). However, as long as the degradation causes a fixed reduction in production, independent of rainfall (fig. 4.17a), the calculated slope of the residuals with respect to time is not affected (fig. 4.17b)(Evans & Geerken, 2004).

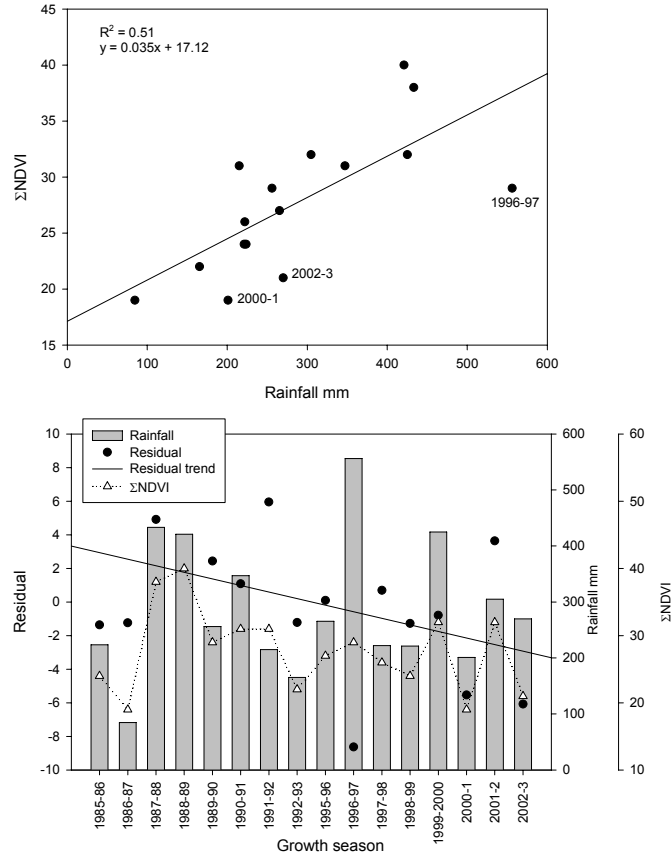


**Figure 4.16** Linear regression between  $\Sigma$ NDVI and rainfall (top panel). Trend of residuals plotted against  $\Sigma$ NDVI and rainfall per growth season for a typical pixel in large area with negative residual trends around Hopetown in fig. 4.10b (bottom panel).

If degradation reduces production more at lower rainfall, the OR will be biased towards underestimating negative residuals at lower rainfall (fig. 4.17c). If there was also a reduction in rainfall through the time-series, the trend in the residuals would be less negative than if calculated using a NR (fig. 4.17d).

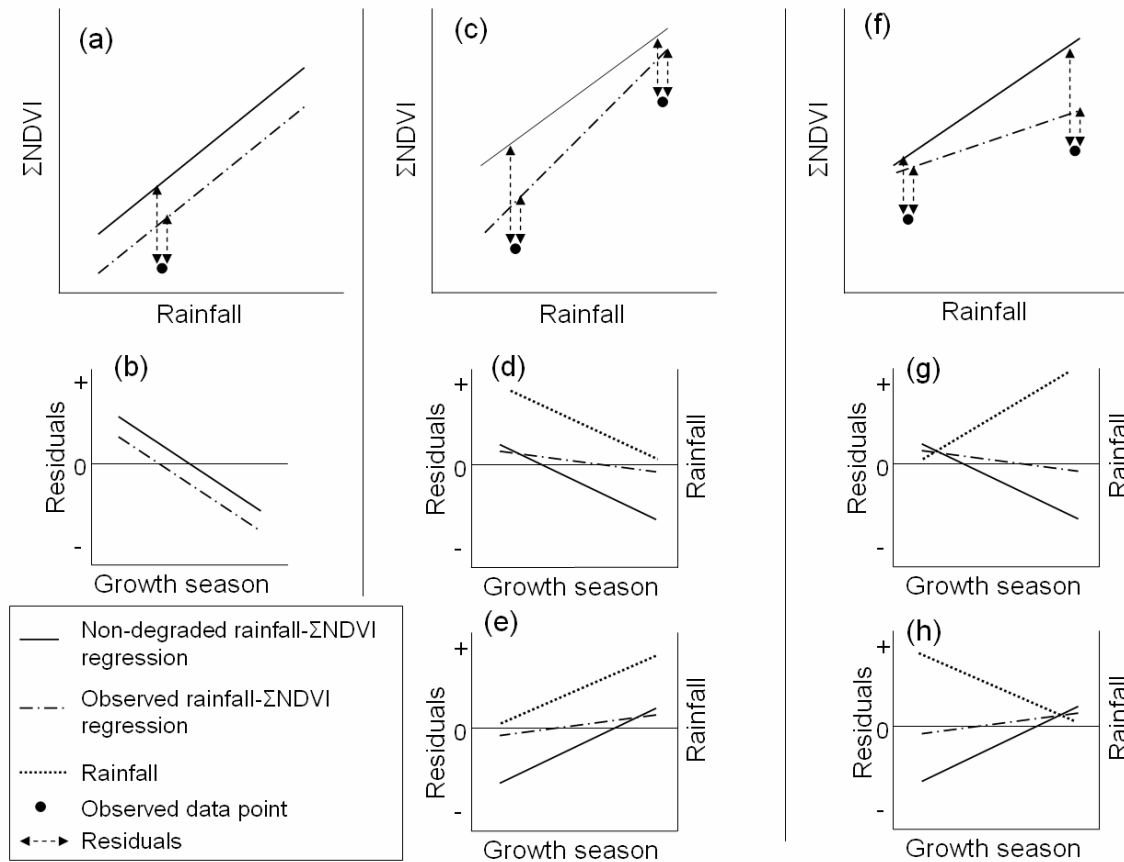


**Figure 4.17** Potential effects of degradation on the observed rainfall- $\Sigma$ NDVI relationships (OR) in comparison with the non-degraded rainfall- $\Sigma$ NDVI relationships (NR)(top panel), and trends in the residuals with respect to time (lower two panels). (a-b) Condition 1, degradation causes a fixed reduction in production, independent of rainfall. (c-e) Condition 2, degradation reduces production more at lower rainfall, showing the effect on trends in the residuals if rainfall decreases (d) or increases (e) during the time-series. (f-h) Condition 3, degradation reduces production more at higher rainfall, showing the effect on trends in the residuals if rainfall increases (g) or decreases (h) during the time-series.

Alternatively, if there was an increase in rainfall through the time-series, the trend in the residuals of both the OR and NR cases may be positive, despite the occurrence of degradation (fig. 4.17e). Conversely, if degradation were to reduce production more at higher rainfall, the OR will be biased towards underestimating negative residuals at higher rainfall (fig. 4.17f). Then, if there was an increase in rainfall, the trend in the residuals will be less negative than if calculated using a NR (fig. 4.17g) or, if there was a decrease in rainfall, the trend in the residuals of both the OR and NR cases may be positive, despite the occurrence of degradation (fig. 4.17h). It is therefore theoretically possible that certain circumstances may prevent degradation impacts from being detected by the RESTRENDS method. However, in the present study, there was no evidence for correlations between residuals and rainfall, indicating that the impact of degradation on production was not related to rainfall.

The trend in the residuals is also affected by the point in the time-series when the degradation takes place.

Simulations showed that a fixed 15% reduction in  $\Sigma$ NDVI starting in the middle of the time series will result in the most negative slope, while the same reduction applied near the beginning or end of the time series results in less negative trends in residuals (fig. 4.18).

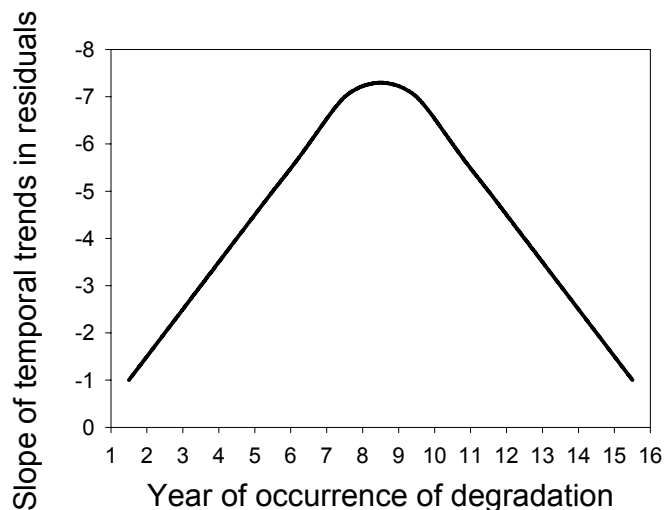


**Figure 4.18** Effect of timing of the occurrence of degradation on the slope of temporal trends of residuals. Simulations were based on a fixed 15% reduction in  $\Sigma$ NDVI starting in each of the 16 years in the time-series.

Degradation occurring within the first or last two years of the time-series would be very difficult to detect. The trend of the residuals through time is therefore influenced by both the timing and the magnitude of the degradation and the results should therefore be interpreted with the appropriate checks, such as the existence of any correlations between residuals and rainfall.

#### **4.4 Conclusions**

The large number of rainfall stations available in SA ( $N > 1800$ ) and the rainfall maps derived from them allowed a comprehensive spatial analysis of the relationship between rainfall and remotely sensed estimates of vegetation productivity. In the past similar studies have been based on point data for 25-200 weather stations (Nicholson & Farrar, 1994; Nicholson *et al.*, 1998; Prince *et al.*, 1998; Diouf & Lambin, 2001). In this study the rainfall-production relationship was derived for every pixel, which effectively accommodated any local variations in topography and soils, thus providing a more discriminating analysis. The drier areas of SA ( $< 700$ mm mean annual precipitation) had the strongest relationship between rainfall and both NPP and  $\Sigma$ NDVI (figs 4.3a,b). The relationships between rainfall and  $\Sigma$ NDVI were comparable to those reported elsewhere (Malo & Nicholson, 1990; Nicholson *et al.*, 1998; Prince *et al.*, 1998; Yang *et al.*, 1998; Diouf & Lambin, 2001). The strength of both relationships decreased towards the east (figs 4.3a,b), where rainfall was higher and less variable (fig. 4.4), and therefore had a lesser influence on NPP and  $\Sigma$ NDVI. The geographic pattern of the CV rainfall, CV NPP and CV  $\Sigma$ NDVI were very similar, decreasing eastward across SA with increasing mean annual rainfall (fig. 4.4), indicating a cause and effect relationship.

The growth season total rainfall, NPP and NDVI may represent an oversimplification of more complex relationship between water availability and primary production in areas with low  $R^2$  values, since the timing and effectiveness of precipitation have a large influence on vegetation production (Le Hou rou, 1984; Justice & Hiernaux, 1986; Tucker *et al.*, 1986; Du Plessis, 1999; Wang *et al.*, 2001; Evans & Geerken, 2004). It is possible that estimates of available soil moisture, that allow for variables such as soil water holding capacity, run-off, net radiation and actual evapotranspiration (Prentice, Sykes & Cramer, 1993), may give stronger relationships (Farrar, Nicholson & Lare, 1994). It may also be that, in some areas, non-linear functions could better describe the relationship between rainfall and production estimates (Rutherford, 1980; Snyman, 1998). The current results, however, indicate that rainfall has a major influence on the vegetation production of rangelands in SA and this factor must be controlled if the often lesser effects of human-induced land degradation are to be monitored.

The  $\Sigma$ NDVI-RUE of most of the degraded areas in north-eastern SA were consistently lower than paired non-degraded areas (fig. 4.5), illustrating that degraded areas produced less forage per unit rainfall in any given growth season (Wessels *et al.*, 2004). This also agrees with field experiments which compared degraded and non-degraded sites in SA (Snyman, 1998; Illius & O'Connor, 1999; O'Connor *et al.*, 2001). As in field observations (O'Connor *et al.*, 2001), the lowest  $\Sigma$ NDVI-RUE and NPP-RUE values occurred in the wettest growth seasons (e.g. 1999-2000) (figs 4.5, 4.6, 4.9). The RUE values varied considerably from year to year, associated with varying rainfall (fig. 4.5). In contrast, Nicholson *et al.* (1998) reported that the NDVI-RUE showed little inter-annual variability during a 13 year period in the Sahel. However, their calculation was

based on the average of all the weather stations (N=141), thus obscuring any inter-annual variation in RUE at specific sites and precluding the use of RUE for spatial monitoring.

RUE showed very large inter-annual variations as a result of a strong negative correlation with rainfall (country-wide average  $r = -0.82$ ) (figs 4.5, 4.6, 4.9). The RUE trend map showed negative trends over large areas (fig. 4.8) where very high rainfall towards the end of the time-series caused low RUE values despite exceptionally high NPP values (1998-99 and 1999-2000, fig. 4.9). It is clear that simply calculating the annual ratio of NPP or  $\Sigma$ NDVI and rainfall does not remove the effects of rainfall variability on vegetation production for individual years and that inter-annual comparisons of RUE maps can not be used to monitor land degradation as suggested elsewhere (Symeonakis & Drake, 2004).

The RESTREND method showed promising results in the Limpopo Province where negative trends were associated with degraded areas mapped by the NLC in and around communal areas (fig. 4.12). By accounting for rainfall the RESTREND method identified areas with negative residual trends (fig. 4.10b) which actually had positive  $\Sigma$ NDVI trends (fig 4.10a). These areas had lower  $\Sigma$ NDVI values than predicted by the rainfall- $\Sigma$ NDVI relationship and therefore may have experienced a reduction in production per unit rainfall. The examples from KNP showed that both negative and positive residual trends could result from natural ecological processes, such as the carry-over effect of successive dry or wet years (figs 4.14, 4.15) (Goward & Prince, 1995). The method can potentially be improved to address the effect of extreme rainfall conditions on subsequent years.

The RESTREND method can only be used as a regional indicator to highlight potential problem areas, while the cause of the negative trends should be determined by other means, such as ancillary data or field work. At a national scale it is very difficult to verify if areas showing negative residual trends were indeed being degraded during the time-series, since there has never been a country-wide rangeland monitoring program in SA. The National Report on Land Degradation (NRLD) (Hoffman *et al.*, 1999; Hoffman & Ashwell, 2001) does however, provide information on the perceived rate of change in rangeland condition of magisterial districts over a 10 year period (1989 to 1999), as judged by local experts. Although it was difficult to compare the rating of an entire district to trends in distinct locations, similar patterns are evident. Many of the former homeland districts in the Limpopo Province that were judged to have experienced increased rates of land degradation since 1989, showed negative trends in residuals (fig. 4.12). In agreement with the slowly increasing rate of degradation reported for some Northern Cape and Karoo districts (Hoffman *et al.*, 1999), the  $\Sigma$ NDVI trend and residuals trend maps also indicated reductions in vegetation productivity in these general areas (figs 4.10a, b). These results are relevant to the long-debated question of whether the semi-arid Karoo is expanding (Acocks, 1953; Dean *et al.*, 1995; Archer, 2004).

The communal homelands in SA were created as early as 1913 to 1936 (Christopher, 1994), so much of the land degradation in these areas most likely occurred before the satellite record started. The methods tested here can only detect changes that occurred within the satellite time-series, and therefore do not detect areas that suffered degradation before 1985. Although the requirement for a long time-series may be viewed as a limitation of the RESTREND method, it decreases the possibility of misinterpreting

transient, reversible vegetation changes as degradation, since degradation typically occurs over longer time periods, i.e. 10 to 20 years (Pickup & Chewings, 1994; Pickup, 1996; Prince, 2002).

The main disadvantage of the RESTRENDS method is the fact that the rainfall-production relationship is derived from a time-series which may include degradation impacts on production. The extent of the bias, caused by the mixture of degraded and non-degraded conditions in the time-series, depends on the relationship between rainfall and degree of degradation (fig. 4.17), and on the actual sequence of rainfall and degradation events in the time-series (figs 4.17, 4.18). It is possible, in certain circumstances, that degradation may remain undetected, even if a non-degraded rainfall-production relationship were used (figs 4.17e,h). In the current study, analyses showed that the residuals were not correlated with rainfall and Wessels *et al.* (2004) demonstrated that the degradation impacts, measured as the difference between degraded and non-degraded areas of the same LCU, were not related to rainfall. Consequently, the trends in the residuals calculated using the observed rainfall-production relationship should be very similar to those derived using a non-degraded reference period (Condition 1, fig. 4.17b)(Evans & Geerken, 2004). It is clearly essential to test if residuals are correlated with rainfall or if rainfall has a linear trend through the time-series before applying the RESTREND method.

The results suggest that the RESTREND method is a useful tool for controlling the effects of rainfall and local variations in soils and topography in order to detect human-induced land degradation. However, the resulting land condition trend maps have not yet been sufficiently validated for use in policy and management decisions.

Fortunately the SA National Department of Agriculture (DoA, Directorate: Land use and Soil Management) is actively evaluating the maps in the field.

## **Chapter 5. Synthesis, significance and global applications**

### **5.1 Synthesis of research**

There has long been a pressing need for quantitative information on the distribution and severity of regional land degradation (Dregne, 2002). The fundamental goal of this dissertation is therefore to develop improved land degradation monitoring approaches, based on remotely sensed estimates of vegetation production, which are capable of distinguishing human impacts from the effects of natural climatic and spatial variability. This chapter synthesizes the findings and discusses the significance of the research.

Kruger National Park (KNP) provides a valuable natural benchmark for studying ecological processes and testing remote sensing methods, because of the long absence of humans and its juxtaposition to similar occupied land. This study is the first effort to demonstrate the relationship between long-term biomass measurements and 1km AVHRR NDVI data in KNP and SA (Chapter 2). The study was, however, hampered by the fact that the biomass measurements were sampled from very small sites which were not fully representative of the local variations in the landscape and biomass. In response to these results KNP researchers are considering supplementing their surveys by sampling larger areas (1km<sup>2</sup>) around selected field sites. The results, nevertheless, showed that AVHRR  $\Sigma$ NDVI adequately estimated inter-annual changes in vegetation production and should therefore be useful for monitoring primary production as an indicator of land degradation. This study furthermore made a significant contribution

towards the incorporation of coarse resolution remotely sensing data into KNP's Strategic Adaptive Management system.

The existence of known degraded areas in communal lands and comparable, non-degraded areas in commercial rangelands provides a unique opportunity to characterize land degradation using the long-term AVHRR  $\Sigma$ NDVI data (Chapter 3). This analysis tested if known degraded areas could indeed be detected with the 1km AVHRR data and quantified the reductions in  $\Sigma$ NDVI that may be expected from future land degradation. The effect of natural landscape variability on  $\Sigma$ NDVI was controlled by stratifying according to land capability units which were based on detailed soil and climate data. According to the results, land degradation reduced the  $\Sigma$ NDVI an average of 10%, while the coefficient of variation of  $\Sigma$ NDVI amongst LCUs was 12.7%, indicating that landscape variability could have easily concealed human impacts if proper stratification had not been employed. Detailed stratification data are not necessarily available for all parts of the world and on a regional scale vegetation types (e.g. Low & Rebelo, 1996) or ecoregions (Olson *et al.*, 2001) are the only options. Investigations showed that these broad classes often contain significant precipitation gradients and diverse landscapes that can easily overshadow human impacts on vegetation production. Where sufficient stratification and land cover data are not available, it would be very difficult to map human-induced land degradation with direct remote sensing estimates of vegetation production (see Monitoring and Mapping Land Degradation below).

Compared to their paired non-degraded areas, the degraded areas showed a consistent reduction in  $\Sigma$ NDVI throughout the time-series, despite large variations in rainfall (Chapter 3). The degradation impact did not diminish in years of high rainfall,

thus suggesting that the degraded areas may have changed to a different, stable, ecological state, which produces less vegetation per unit rainfall (Noy-Meir, 1975; Holmgren & Scheffer, 2001). It was expected that degraded areas might also be less resilient (Abel & Behnke, 1996; Scheffer *et al.*, 2001; Folke *et al.*, 2002) and more vulnerable to dry episodes (Pickup, 1998). Surprisingly, the annual deviations from the long-term mean  $\Sigma$ NDVI revealed that the degraded areas were just as stable and resilient as the non-degraded areas.

For many years the fate of livestock production in the communal lands has been a highly controversial topic (Shackleton, 1993). For the past 60 years rangeland scientists have predicted a catastrophic collapse in the livestock numbers of communal areas, but in contrast, these areas have continuously supported very high animal numbers (Tapson, 1991; Shackleton, 1993). The current results are of great significance to this debate, since they demonstrated that degraded areas within the communal lands are functionally stable and resilient, albeit it at a lower level of productivity (production per unit rainfall). Despite years of interest and concern, this is the first study to use consistent, long-term estimates of vegetation production to quantitatively analyze the ecological function of the extensive, degraded communal areas in SA. These results clearly display the value of an extended time-series of remote sensing data and highlight the importance of multi-temporal analyses of ecosystem function to understanding land degradation.

Vegetation production in semi-arid areas is largely determined by rainfall and therefore it is essential to control for the effects of rainfall variability when attempting to tease out evidence for human-induced land degradation. The linear relationships between rainfall and NPP and  $\Sigma$ NDVI, were respectively determined on a per-pixel basis, which

effectively accommodated local variation in soils and terrain (Chapter 4). It has been proposed that Rain-Use Efficiency, the ratio of NPP or NDVI to rainfall, ( $RUE=NPP/Rainfall$ ), should normalize the inter-annual variability in NPP and consequently provide an index of degradation that is independent of the effects of rainfall variability (Tucker *et al.*, 1986; Justice *et al.*, 1991a; Nicholson & Farrar, 1994; Pickup, 1996; Nicholson *et al.*, 1998; Prince *et al.*, 1998; Diouf & Lambin, 2001). This is the first study to our knowledge, which has produced annual RUE maps and analyzed temporal trends in RUE using spatially-comprehensive data (Chapter 4). The results clearly showed that simply calculating RUE did not remove the effects of rainfall variability on vegetation production and that inter-annual comparisons of RUE maps can not be used to monitor land degradation.

An alternative approach, the Residual Trends method (RESTREND) was studied, which identified trends in the differences (residuals) between the observed  $\Sigma NDVI$  and the  $\Sigma NDVI$  predicted by the actual annual rainfall (Evans & Geerken, 2004)(Chapter 4). Negative trends in the residuals may indicate progressive reductions in the response of NPP to rainfall, that is degradation. This method identified areas in and around the degraded communal lands in north-eastern SA that showed negative trends and it appeared to be a useful tool for controlling the effects of rainfall. The trend of the residuals through time is however influenced by both the timing and the magnitude of the degradation and the results should therefore be interpreted with the appropriate checks, such as a test for existence of any correlations between residuals and rainfall. Negative trends can also potentially be caused by natural phenomena such as the cumulative effects of successive dry years in the same location (Goward & Prince, 1995). Equally,

positive trends can also be expected following a sequence of wet years. Major land use and land cover changes, such as the expansion of subsistence agriculture, can also result in negative trends. The RESTREND method can evidently only identify areas where there has been a reduction in production per unit rainfall, but the exact cause of the negative trend, e.g. overgrazing by livestock, can not be determined by this method alone. It is therefore envisaged that the RESTREND method would ultimately form an integral part of a multi-scale, monitoring system where it can serve as a regional indicator to identify potentially degraded areas which can then be closer investigated. Such a multi-scale, multi-sensor approach would rely on the regional coverage, high temporal frequency and synoptic quality of coarse resolution data (e.g. AVHRR, MODIS and Visible Infrared Scanner -VIRS) to effectively direct labor-intensive, high-resolution remote sensing efforts and costly field surveys to identified problem areas.

Currently the RESTREND results are the only country-wide maps of potential degradation which are based on systematic estimates of annual vegetation production. Compared to previous maps of land degradation in SA, that were mainly based on perceived susceptibility to soil degradation (figs 5.1b,c,d), or expert opinions on rangeland degradation (figs 5.1a,e,f), the RESTREND map provides a long overdue, quantitative alternative. The true value of the RESTREND method will however only become clear once it has been systematically evaluated in the field by natural resource managers and agricultural extension officers.

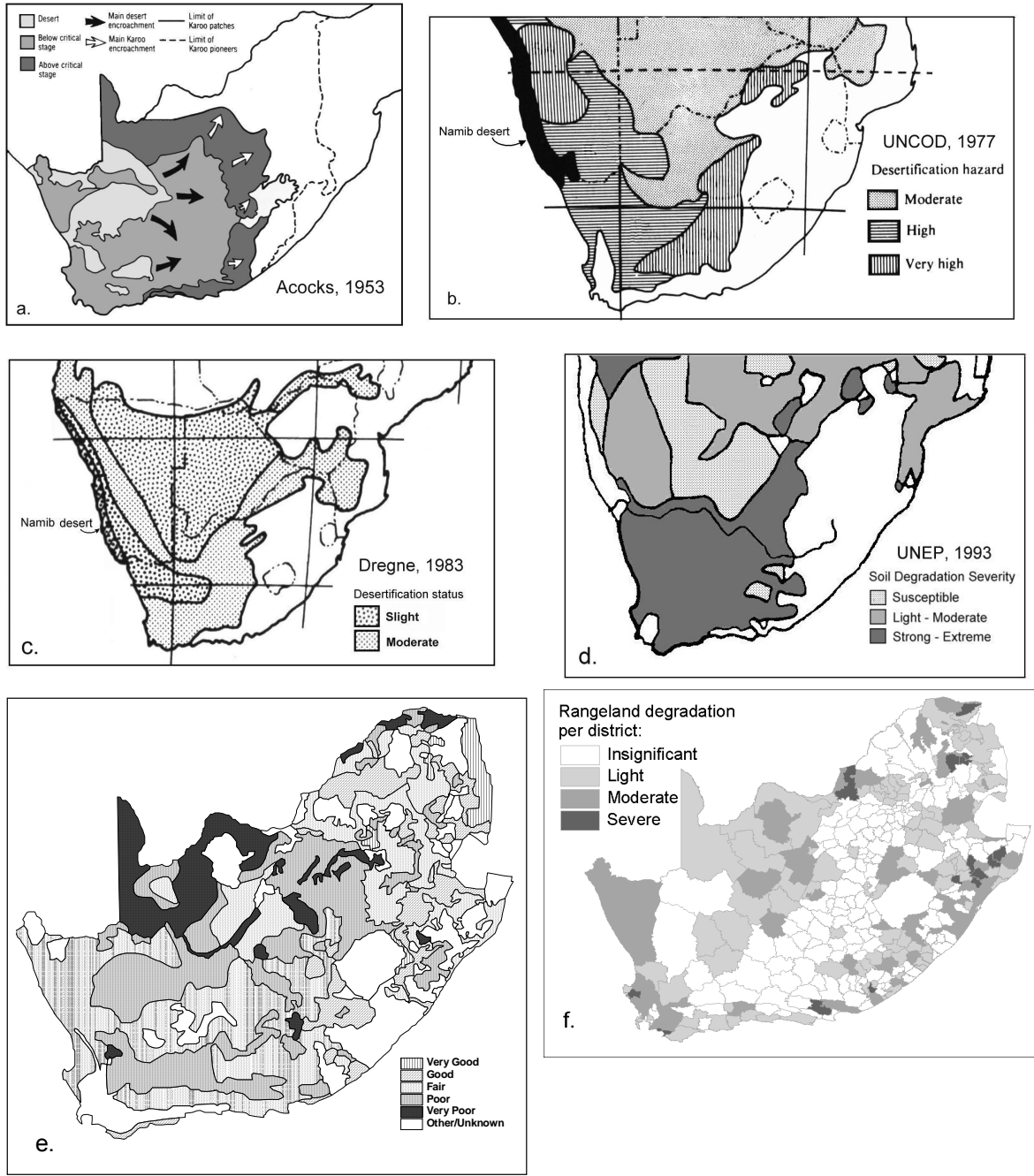


**Figure 5.1.** Previous maps of land degradation for South Africa: (a) Acocks, 1953, (b) UNCOD, 1977a, (c) Dregne, 1983, (d) UNEP, 1992, (e) Roux, 1990 and (f) Hoffman *et al.*, 1999.

## **5.2 Monitoring and Mapping land degradation.**

It is essential to make a distinction between monitoring ongoing degradation and mapping all past and present degradation. Most remote sensing based methods that have previously been employed to monitor land degradation, including the RESTREND method, are geared towards detecting changes that occurred during the AVHRR satellite record (1981 to present) (Hellden, 1991; Tucker *et al.*, 1991b; Lambin & Strahler, 1994). Consequently, areas that suffered degradation before the age of satellite remote sensing and are no longer changing, e.g. parts the communal homelands, will not be identified by these monitoring procedures. However, natural resource management agencies increasingly call for maps of all current and historically degraded lands in order to report to international forums, such as the UNCCD or the Millennium Ecosystem Assessment (MEA). Very few methods have been developed to address this demand (Prince & Wessels, 2005) and agencies often have no option but to revert to qualitative maps of degradation susceptibility (e.g. Dregne, 2002)

Since satellite imagery of a non-degraded reference period does not exist, the expected NDVI or NPP of a particular pixel have to be derived by other means. The Local NDVI Scaling method (LNS) derives the expected, non-degraded NDVI of a pixel from all the values observed within the same biophysical stratum or land unit (Prince, 2004). The NDVI of each pixel can then be scaled relative to the highest values observed in the same stratum. The resulting map represents the percentage of the potential NDVI of the stratum that is realized in each pixel. The stratification by land units allows spatial variations in climate, soils and terrain to be normalized. The method assumes that sufficient non-degraded pixels exist in every stratum. If such pixels are not present, the

estimates of the potential NDVI will be in error. It furthermore assumes that all pixels within the stratum have the same production potential and therefore the stratification should be based on very detailed spatial information on vegetation, soils and terrain. As discussed above, such detailed stratification data are not always available and more generalized regional or global strata may contain substantial variations in climate and soils that could conceal the more subtle human impacts. Where detailed stratification data are available, the number of strata increases rapidly as the study area expands, making the LNS method computationally demanding. For example, in SA there are more than 7600 land capability units, which would furthermore make a derived LNS map very hard to interpret at scales larger than 1: 100 000. In addition to the stratification data, detailed land cover data are required to separate natural vegetation from altered cover types, such as cultivation or human settlements, since the vegetation production of these transformed areas can be radically different (Stoms & Hardgrove, 2000; DeFries, 2002).

If the above-mentioned requirements and assumptions of the LNS method can be adequately accommodated, it promises to be a very useful tool for identifying potentially degraded areas at a local to regional scale. The LNS can be calculated annually to monitor the persistence of areas with low LNS values. This method is the subject of ongoing research. The LNS and RESTREND methods may be applied in tandem, to respectively tackle the spatial landscape variation and temporal rainfall variability in order to facilitate the detection of land degradation within the proposed, national, multi-scale monitoring system.

### 5.3 Global maps of land degradation

There have been several attempts to produce global maps of land degradation (table 5.1) (for SA portion of these maps see figs 5.1b,c,d). Maps were based on very limited quantitative data and mainly reflected expert opinions on the susceptibility or occurrence of soil degradation (figs 5.1b,c,d)(Dregne, 2002). Although these subjective, qualitative assessments were useful for directing attention to potential problem areas, they can not be used to monitor changes in land condition, because they do not involve repeatable measurements. One of the primary purposes of these global maps was to provide estimates of degradation that knowledgeable people could react to and improve upon in an iterative process that would ultimately lead to improved maps (Dregne, 2002). Unfortunately, this was not realized and the maps were severely criticized and dismissed as inaccurate and misleading by some scholars (Hellden, 1991; Thomas & Middleton, 1994; Stocking, 2001).

Most recently, the Millennium Ecosystem Assessment (MEA) synthesized diverse datasets to produce a global map of degraded drylands (Lepers *et al.*, 2005). Although the study managed to gather informative remotely sensed data to assess changes in forest cover and croplands, no such data were available for assessing degradation. The paucity of the quantitative data once again led to a qualitative aggregated map that can not be used for monitoring degradation (Lepers *et al.*, 2005). To date, none of the global maps have been based on assessments of biophysical measurements, such as remotely sensed estimates of vegetation production. The lingering question is whether the methods applied in SA at a regional scale can be applied at to the entire world's drylands?

**Table 5.1** Previous maps of global land degradation, methods used in assessments and references.

| <b>Name of map</b>   | <b>Method</b>  | <b>Reference</b>               |
|--|--|--------------------------------|
| World Map of Desertification (UNCOD)                           | Estimates of vulnerability to land degradation       | (UNCOD, 1977a)                 |
| Desertification of Arid lands                                  | Assessment of opinions, per country                  | (Dregne, 1983)                 |
| World map on status of human-induced soil degradation (GLASOD) | Informed opinions on soil degradation                | (Oldeman <i>et al.</i> , 1990) |
| World Atlas of Desertification                                 | Informed opinions on soil degradation = (GLASOD)     | (UNEP, 1992)                   |
| World Atlas of Desertification. 2 <sup>nd</sup> Edition        | Informed opinions on soil and vegetation degradation | (UNEP, 1997)                   |

Although it might seem hard to believe that any single indicator can capture the diverse and complex manifestations of land degradation around the world, it is reasonable to assume that all dryland degradation should be associated with reductions in vegetation production (Reynolds & Stafford Smith, 2002a). The LNS method could easily be applied to the world using readily available global NPP data (Running *et al.*, 1999; Cao *et al.*, 2004) and stratification maps, e.g. ecoregions (Olson *et al.*, 2001). Unfortunately, a global LNS map is likely to give inaccurate results, because the global stratification data are unlikely to provide strata that are sufficiently homogenous to elucidate human impacts on vegetation production. As more detailed global stratification data become available, the LNS method may become more feasible, but at the same time the total number of strata may become prohibitively large and the LNS map may simply be too

difficult to compute and interpret. Given the lack of alternatives, the global application of the LNS method is nevertheless worth investigating.

The RESTREND method was applied in a global test using annual NPP data (Prince & Goward, 1995; Cao *et al.*, 2004) and annual total Actual Evapotranspiration (AET) data (Willmott & Robeson, 1995) to control for variations in moisture availability (1981 to 1999)(fig. 5.2). Strong negative trends were evident in north-eastern Brazil, central Australia, Ethiopia, southern Madagascar and the Sahel regions of Mali and Senegal (fig. 5.2). It should be reiterated that the RESTREND map, does not represent the definitive map of degradation, but rather a map of potential degraded areas for closer investigation. The map should therefore be systematically interpreted on a regional basis using information from world-wide reviews (Le Hou  rou, 1996), meta-analyses of case studies (Geist & Lambin, 2004) and the recent Millennium Ecosystem Assessment maps (Lepers *et al.*, 2005). An organized, region-specific evaluation would avoid the anecdotal criticisms and misinterpretations that plagued previous global maps (Dregne, 2002). This is the subject of ongoing research.

In the absence of other biophysically-derived maps, the highly controversial debate on land degradation can only benefit from the quantitative RESTREND assessment. If this global assessment proves to be a useful, it may make a major contribution to international efforts to quantify, understand and combat land degradation.

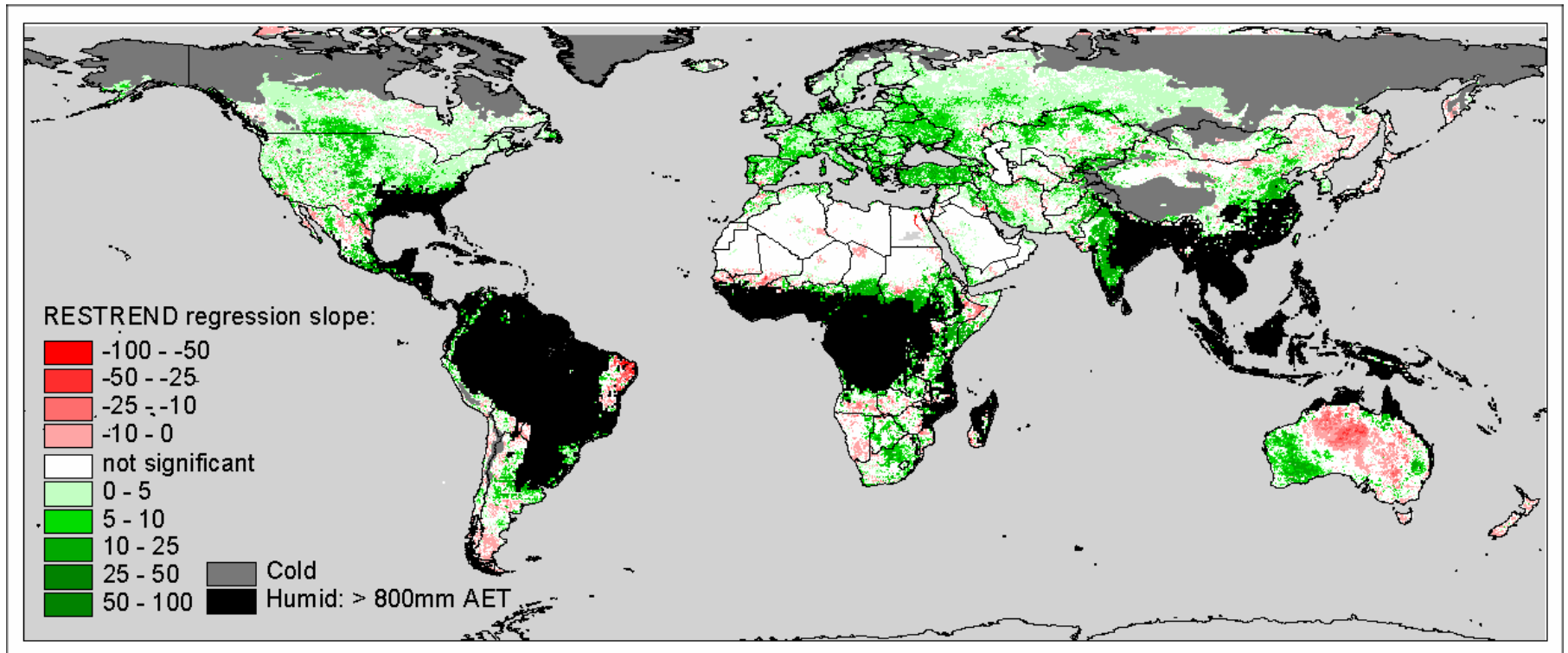


**Figure 5.2.** Global RESTREND map of the residual-time regression (1981-1999). The residuals were calculated as the difference between the observed annual NPP and NPP predicted using the linear NPP-AET relationships. Pixels without statistically significant slopes were omitted (white).

## Summary

Land degradation describes circumstances of reduced biological productivity and is believed to be one of the most serious global environmental problems of our time. There has long been a pressing need for quantitative information on the distribution and severity of land degradation. Vegetation production is greatly influenced by variations in the landscape and climate and as a result it is very difficult to detect human impacts on vegetation production against this background variability. The fundamental goal of this dissertation was therefore to develop improved land degradation monitoring approaches, based on remotely sensed estimates of vegetation production, which are capable of distinguishing human impacts from the effects of natural climatic and spatial variability. Communal homelands in South Africa (SA) are widely regarded to be severely degraded and the existence adjacent, non-degraded areas with the same soils and climate, provide a unique opportunity to test regional land degradation monitoring methods.

The relationship between 1km<sup>2</sup> Advanced Very High Resolution Radiometer (AVHRR), growth season-integrated Normalized Difference Vegetation Index (ΣNDVI) and multi-year biomass measurements (1989 to 2003) was tested in Kruger National Park (KNP), SA (Chapter 2). This was done to demonstrate the ability of the AVHRR, ΣNDVI to estimate vegetation production for the purpose of monitoring land degradation throughout the region. The objectives were: (1) to analyze the underlying relationship between ΣNDVI and herbaceous biomass of field sites (N=533) through time and (2) to investigate the possibility of producing reliable

herbaceous biomass maps for each growth season from the satellite  $\Sigma$ NDVI observations. Landsat ETM+ and TM data were used to identify highly heterogeneous field sites and exclude them from the analyses. The average  $R^2$  for the  $\Sigma$ NDVI-biomass relationship at individual sites was 0.42. Within landscape groups, both mean biomass and mean  $\Sigma$ NDVI were strongly correlated with rainfall and each other. Although measured tree cover and MODIS estimates of tree cover did not have a detectable effect on the  $\Sigma$ NDVI-biomass relationship, other observations suggest that tree cover should not be ignored.

The  $\Sigma$ NDVI was successful at estimating inter-annual variations in the biomass at single sites, but on an annual basis the relationship derived from all the sites was not strong enough (average  $R^2 = 0.36$ ) to produce reliable growth season biomass maps. This was mainly attributed to the fact that the biomass data were sampled from very small field sites that were not fully representative of the vegetation observed by a  $1\text{km}^2$  AVHRR pixel. Supplementary field surveys that sample a larger area for each field site (e.g.  $1\text{km}^2$  or larger) should account for the variability in biomass caused by local variations in the landscape and may improve the strength of biomass- $\Sigma$ NDVI relationships observed in a single growth season. The AVHRR  $\Sigma$ NDVI nevertheless adequately estimated inter-annual changes in vegetation production and should therefore be useful for monitoring land degradation.

Communal lands in northern SA have been reported to be severely degraded and the following analysis tested if degraded areas could indeed be detected with the  $1\text{km}^2$  AVHRR data (Chapter 3). A time-series of AVHRR  $\Sigma$ NDVI data was used to compare degraded rangelands to non-degraded rangelands within the same land

capability units (LCUs), which were mapped using detailed soil and climate data. Degraded areas were mapped by the National Land Cover (NLC) using Landsat Thematic Mapper (TM) imagery. Non-degraded and degraded areas in the same LCU (paired areas) were compared by: (i) testing for differences in spatial mean  $\Sigma$ NDVI values, (ii) calculating the relative degradation impact (RDI) as the difference between the spatial mean  $\Sigma$ NDVI values of paired areas expressed as a percentage of non-degraded mean value, (iii) investigating the relationship between RDI and rainfall, and (iv) comparing the resilience and stability of paired areas in response to natural variations in rainfall.

The  $\Sigma$ NDVI of degraded areas was significantly lower for most of the LCUs. Relative degradation impacts (RDI) across all LCUs ranged from 1% to 20% with an average of 9%. Although  $\Sigma$ NDVI was related to rainfall, RDI was not. Therefore, the degradation impacts did not diminish following high rainfall. Surprisingly, degraded areas were no less stable or resilient than non-degraded. However, the productivity of degraded areas, i.e. the forage production per unit rainfall, was consistently lower than non-degraded areas, even within years of above normal rainfall. The results indicate that there has not been a catastrophic reduction in ecosystem function within degraded areas. Instead, degradation impacts were reflected as reductions in productivity that varied along a continuum from slight to severe depending on the specific LCU. The effect of natural landscape variability on  $\Sigma$ NDVI was effectively controlled by stratifying according to the land capability units.

Vegetation production in semi-arid areas is largely determined by rainfall, which varies greatly, both spatially and temporally. AVHRR  $\Sigma$ NDVI (1km<sup>2</sup>, 1985-

2003) and modeled net primary production (NPP, 8km<sup>2</sup>, 1981-2000) data were used to estimate vegetation production in South Africa (SA) (Chapter 4). The linear relationships of rainfall with NPP and  $\Sigma$ NDVI were calculated for every pixel, thus accommodating the effects of local variations in slope, soil and vegetation. Maps of the parameters of the rainfall-production regressions showed significant spatial variation. Therefore, to monitor human-induced land degradation it is essential to allow for the effects of variation in rainfall on vegetation production. Two methods were tested (i) Rain-Use Efficiency (RUE = NPP/Rainfall or  $\Sigma$ NDVI/Rainfall) and (ii) negative trends in the differences between the observed  $\Sigma$ NDVI and the  $\Sigma$ NDVI predicted by the rainfall using regressions calculated for each pixel (residual trends method - RESTREND). Both methods were based on the notion that land degradation causes reductions in vegetation production per unit rainfall.

Known degraded areas in north-eastern SA had reduced RUE, however annual RUE had very large inter-annual variations associated with rainfall variability. Thus RUE did not normalize the variations in production to remove the effects of rainfall variability. The RESTREND method identified areas in and around the degraded communal lands in north-eastern SA that exhibit negative trends in residuals. Examples from KNP showed that natural processes, e.g. successive dry or wet years, can also respectively cause negative or positive residual trends. The main disadvantage of the RESTRENDS method is that mixture of degraded and non-degraded conditions in the time-series may cause a bias, the extent of which depends on the relationship between rainfall and degree of degradation, and on the actual sequence of rainfall and degradation events in the time-series. However, in the

present study there was no evidence that the impact of degradation on production was related to rainfall, and therefore the bias did not affect the trends in the residuals. The RESTREND method appears to be a useful quantitative tool for detecting potential human-induced land degradation in spite of inter-annual variation in rainfall.

It is envisaged that the RESTREND method would ultimately form an integral part of a multi-scale, monitoring system where it can serve as a regional indicator to identify potentially degraded areas which can then be closer investigated using higher resolution remote sensing data and field surveys. Currently the RESTREND results are the only country-wide maps of potential degradation which are based on systematic estimates of annual vegetation production. Compared to previous maps of land degradation in SA, that were mainly based on perceived susceptibility to soil degradation or expert opinions on rangeland degradation, the RESTREND should provide a long overdue, quantitative alternative. The true value of the RESTREND map will however only become clear once it has been systematically evaluated in field by natural resource managers and agricultural extension officers.

The RESTREND method was also tested globally and will have to be systematically evaluated using world-wide reviews and meta-analyses of case studies. If this global quantitative assessment proves to be a useful, it can potentially make a major contribution to international efforts to combat desertification.

## Bibliography

- Abel, N. (1997). Mis-measurement of the productivity and sustainability of African communal rangelands: A case study and some principles from Botswana. *Ecological Economics*, 23, 113-133.
- Abel, N. & Behnke, R. (1996). Revisited: The overstocking controversy in semi-arid Africa. *World Animal Review*, 87, 4-27.
- Acocks (1953). The veld types of South Africa. *Memoirs of the Botanical Survey of South Africa.*, 8, 1-128.
- Adger, W.N., Benjaminsen, T.A., Brown, K., & Svarstad, H., eds. (2000). *Advancing a Political Ecology of Global Environmental Discourse*. London Centre of Social and Economic research on the global Environment, University of East Anglia.
- Agbu, P.A. & James, M.E. (1994). *The NOAA/NASA Pathfinder AVHRR Land Data Set User's Manual*: Goddard Distributed Active Archive Center, NASA, Goddard Space Flight Center, Greenbelt
- Anyamba, A. & Eastman, J.R. (1996). Interannual variability of NDVI over Africa and its relation to El Niño/Southern Oscillation. *International Journal of Remote Sensing*, 17, 2533-2548.
- Anyamba, A., Justice, C.O., Tucker, C.J., & Mahoney, R. (2003). Seasonal to interannual variability of vegetation and fires at SAFARI 2000 sites inferred from advanced very high resolution radiometer time series data. *Journal of Geophysical Research*, 108(D13), 8507, doi:10.1029/2002JD002464.
- Anyamba, A., Tucker, C.J., & Eastman, J.R. (2001). NDVI anomaly patterns over Africa during the 1997/98 ENSO warm event. *International Journal of Remote Sensing*, 22, 1847-1859.
- Anyamba, A., Tucker, C.J., & Mahoney, R. (2002). From El Niño to La Niña: Vegetation response pattern over East and Southern Africa during the 1997-2000 Period. *Journal of Climate*, 15, 3096-3103.
- Archer, E.R.M. (2004). Beyond the “climate versus grazing” impasse: using remote sensing to investigate the effects of grazing system choice on vegetation cover in the eastern Karoo. *Journal of Arid Environments*, 57, 381-408.
- Asrar, G.M., Fuchs, M., Kanemasu, E.T., & Hatfield, J.L. (1984). Estimating absorbed photosynthetically active radiation and leaf area index from spectral reflectance in wheat. *Agronomy Journal*, 87, 300-306.
- Bastin, G.N., Pickup, G., & Pearce, G. (1995). Utility of AVHRR data for land degradation assessment: a case study. *International Journal of Remote Sensing*, 16, 651-672.
- Behrenfeld, M.J., Randerson, J., McClain, C.R., Feldman, G.C., Los, S.O., Tucker, C.J., Falkowski, P.G., Field, C.B., Frouin, R., Esaias, W.E., Kolber, D.D., & Pollack, N.H. (2001). Biospheric Primary Production during and ENSO transition. *Science*, 291, 2594-2597.
- Beinart, W. (1996). Environmental destruction in southern Africa: Soil erosion, animals, and pastures over the longer term. In *Time-scales and environmental*

- change* (Eds T.S. Driver & G.P. Chapman), (pp. 149-167). London and New York: Routledge.
- Biggs, H. (2002) Proposed Policy For The Ecosystem Management Of Fire In The Kruger National Park. SANParks Unpublished Internal Report. SANParks, Skukuza.
- Biggs, H.C. & Rogers, K.H. (2003). An adaptive system to link Science, monitoring and management in practice. In *The Kruger experience: Ecology and management of savanna heterogeneity*. (Eds J. Du Toit, H.C. Biggs & K.H. Rogers), (pp. 59-80). London: Island Press.
- Botha, J.H. & Fouche, P.S. (2000). An assessment of land degradation in the Northern Province from satellite remote sensing and community perception. *South African Geographical Society*, 82, 70-79.
- Cao, M., Prince, S., Small, J., & Goetz, S.J. (2004). Remote sensing interannual variations and trends in terrestrial net primary productivity 1981-2000. *Ecosystems*, 7, 233-242.
- Cao, M. & Prince, S.D. (2005). Climate-induced regional and interannual variations in terrestrial carbon uptake. *Tellus*, in press.
- Carpenter, S., Walker, B., Anderies, J.M., & Abel, N. (2001). From Metaphor to Measurement: Resilience of What to What? *Ecosystems*, 4, 765-781.
- Charney, J., Quirk, W.J., Chow, S.H., & Kornfield, J. (1977). A comparative study of the effects of albedo change on drought in semi-arid regions. *Journal Atmospheric Sciences*, 34, 1366-1385.
- Christopher, A. (1994) The Atlas of Apartheid. Witwatersrand University Press, Johannesburg.
- Cihlar, J., I. Tcherednichenko, R. Latifovic, Z. Li, & Chen, J. (2001). Impact of Variable Atmospheric Water Vapor Content on AVHRR Data Corrections over Land. *IEEE Transactions on GeoScience and Remote Sensing*, 39, 173-180.
- Cihlar, J., Ly, H., Chen, J., Pokrant, H., & Huang, F. (1997). Multi-temporal, multichannel AVHRR data set for land biosphere studies: artifacts and correction. *Remote Sensing of Environment*, 60, 35-57.
- Cihlar, J., R. Latifovic, J. Chen, A. Trishchenko, Y. Du, G. Fedosejevs, & Guindon, B. (2004). Systematic corrections of AVHRR image composites for temporal studies. *Remote Sensing of Environment*, 89, 217-233.
- Cramer, W., Kicklighter, D.W., Bondeau, A., Moore, B., Churkina, G., Nemry, B., Ruimy, A., & Schloss, A.L. (1999). Comparing global models of terrestrial net primary productivity (NPP): overview and key results. *Global Change Biology*, 5, 1-15.
- Cramer, W., Olson, R.J., & Prince, S.D. (2001). Global productivity: determining present and future. In *Terrestrial global productivity: past, present, and future* (Eds J. Roy, B. Saugier & H. Mooney), (pp. pp 429-448). San Diego: Academic Press.
- Dahlberg, A. (2000). Interpretations of environmental change and diversity: A critical approach to indications of degradation - The case of Kalakamate, northeast Botswana. *Land Degradation and Development*, 11, 549-562.

- Dean, W., Hoffman, M., Meadows, M., & Milton, S. (1995). Desertification in the semiarid Karoo, South-Africa - review and reassessment. *Journal of Arid Environments*, 30, 247-264.
- Dean, W.R.J., Hoffman, M.T., & Wills, C.K. (1996). The light and the way in South African desertification research. *South African Journal of Science*, 92, 170-172.
- Deering, D.W., Rouse, J.W., Hass, R.H., and Schell, J.A. (1975). Measuring forage production of grazing units from Landsat MSS data. In Proceedings of the 10th International Symposium on Remote Sensing of Environment, 1169-1178: Ann Arbor, MI. 6-10 October, 1975.
- DeFelicis, T.P., Lloyd, D., Meyer, D.J., Baltzer, T.T., & Piraino, P. (2003). Water vapour correction of the daily 1km AVHRR global land dataset: part I - validation and use of the water vapour input field. *International Journal of Remote Sensing*, 24, 2365-2375.
- DeFries, R. (2002). Past and future sensitivity of primary production to human modification of the landscape. *Geophysical Research Letters*, 29, 36-1-4.
- DeFries, R.S., Townshend, J.R.G., & Hansen, M.C. (1999). Continuous fields of vegetation characteristics at the global scale at 1km resolution. *Journal of Geophysical Research*, 104, 16911-16925.
- Diallo, O., Diouf, A., Hanan, N.P., Ndiaye, A., & Prévost, Y. (1991). AVHRR monitoring of savanna primary productivity in Senegal, West Africa: 1987-1988. *International Journal of Remote Sensing*, 12, 1259-1279.
- Diouf, A. & Lambin, E. (2001). Monitoring land-cover changes in semi-arid regions: remote sensing data and field observations in the Ferlo, Senegal. *Journal of Arid Environments*, 48, 129-148.
- Dregne, H.E. (1983). Desertification of arid lands. Hardwood Academic Publications, New York.
- Dregne, H.E. (2002). Land degradation in Drylands. *Arid Land Research and Management*, 16, 99-132.
- Dregne, H.E., Kassas, M., & Rozanov, B. (1991). A new assessment of the world status of desertification. *Desertification Control Bulletin*, 20, 6-19.
- Du Plessis, W.P. (1999). Linear regression relationships between NDVI, vegetation and rainfall in Etosha National Park, Namibia. *Journal of Arid Environments*, 42, 235-260.
- Dube, O. & Pickup, G. (2001). Effects of rainfall variability and communal and semi-commercial grazing on land cover in southern African rangelands. *Climate Research*, 17, 195-208.
- Eckhardt, H.C., Van Wilgen, B.W., & Biggs, H.C. (2000). Trends in woody vegetation cover in the Kruger National Park, South Africa, between 1940 and 1998. *African journal of Ecology*, 38, 108-115.
- El Saleous, N.Z., Vermotte, E.F., Justice, C.O., Townshend, J.R.G., Tucker, C.J., & Goward, S.N. (2000). Improvements in the global biospheric record from the Advanced Very High Resolution Radiometer (AVHRR). *International Journal of Remote Sensing*, 21, 1251-1277.
- Evans, J. & Geerken, R. (2004). Discriminating between climate and human-induced dryland degradation. *Journal of Arid Environments*, 57, 535-554.

- Fairbanks, D.H.K., Thompson, M.W., Vink, D.E., Newby, T.S., Van den Berg, H.M., & Everard, D.A. (2000). The South African Land-cover characteristics database: a synopsis of the landscape. *South African Journal of Science*, *96*, 69-82.
- Farrar, T.J., Nicholson, S.E., & Lare, A.R. (1994). The influence of soil type on the relationships between NDVI, rainfall and soil moisture in semi-arid Botswana. Part II. Response to soil moisture. *Remote Sensing of Environment*, *50*, 121-133.
- Fensholt, R., Sandholt, I., & Rasmussen, M.S. (2004). Evaluation of MODIS LAI, fAPAR and the relation between fAPAR and NDVI in a semi-arid environment using in situ measurements. *Remote Sensing of Environment*, *91*, 490-507.
- Field, C.B., Randerson, J.T., & Malmstrom, C.M. (1995). Global Net Primary Production: combining ecology and remote sensing. *Remote Sensing of Environment*, *51*, 74-88.
- Folke, C., Holling, C.S., Walker, B., Carpenter, S., Elmqvist, T., & Gunderson, L. (2002). Resilience and sustainable development: Building adaptive capacity in a world of transformations. *Ambio*, *31*, 437-440.
- Fox, R. & Rowntree, K. (2001). Redistribution, restitution and reform: prospects for the land in the Eastern Cape Province, South Africa. In *Land Degradation* (Ed., A. Conacher (pp. 167-186). London: Kluwer Academic Publishers.
- Fuller, D.O., Prince, S.D., & Astle, W.L. (1997). The influence of canopy strata on remotely sensed observations of savanna-woodlands. *International Journal of Remote Sensing*, *18*, 2985-3009.
- Geerken, R. & Ilaiwi, M. (2004). Assessment of rangeland degradation and development of a strategy for rehabilitation. *Remote Sensing of Environment*, *in press*.
- Geist, H.J. & Lambin, E.F. (2004). Dynamic causal patterns of desertification. *BioScience*, *54*, 817-829.
- Gertenbach, W.P.D. (1983). Landscapes of the Kruger National Park. *Koedoe*, *26*, 1-121.
- Goetz, S.J., Prince, S.D., Small, J., & Gleason, A. (2000). Interannual variability of global terrestrial primary production: results of a model driven with satellite observations. *Journal of Geophysical Research Atmospheres*, *105*, 20077-20091.
- Goward, S.N. & Dye, D.G. (1987). Evaluating North American Net Primary Productivity with satellite observations. *Advances in Space Research*, *7*, 165-174.
- Goward, S.N. & Prince, S.D. (1995). Transient effects of climate on vegetation dynamics: satellite observations. *Journal of Biogeography*, *22*, 549-563.
- Goward, S.N., Tucker, C.J., & Dye, D.G. (1985). North American vegetation patterns observed with the NOAA-7 advanced very high resolution radiometer. *Vegetatio*, *64*, 3-14.
- Gower, S.T., Kucharik, C.J., & Norman, J.M. (1999). Direct and indirect estimation of leaf area index, FAPAR, and Net Primary Production of terrestrial ecosystems. *Remote Sensing of Environment*, *70*, 29-51.

- Grimm, V. & Wissel, C. (1997). Babel, or the ecological stability discussions: an inventory and analysis of terminology and a guide for avoiding confusion. *Oecologia*, 109, 323-334.
- Hansen, M.C., DeFries, R.S., Townshend, J.G.R., Marufu, L., & Sohlberg, R. (2002). Development of a MODIS tree cover validation data set for Western Province, Zambia. *Remote Sensing of Environment*, 83, 320-335.
- Hellden, U. (1991). Desertification - time for an assessment. *Ambio*, 20, 372-383.
- Hoffman, M.T. & Ashwell, A., eds. (2001). *Nature Divided: Land degradation in South Africa.*, (pp 168). Cape Town Cape Town University Press.
- Hoffman, M.T. & Todd, S. (2000). National review of land degradation in South Africa: the influence of biophysical and socio-economic factors. *Journal of Southern African studies*, 26, 743-758.
- Hoffman, T., Todd, S., Ntoshona, Z., & Turner, S., eds. (1999). *Land Degradation in South Africa*, (pp 245). CapeTown National Botanical Institute.
- Holben, B.N. (1986). Characteristics of maximum-value composite images for temporal AVHRR data. *International Journal of Remote Sensing*, 7, 1435-1445.
- Holmgren, M. & Scheffer, M. (2001). El Niño as a window of opportunity for the restoration of degraded arid ecosystems. *Ecosystems*, 4, 151-159.
- Huete, A., Didan, K., Miura, T., Rodrigues, E.P., Gao, X., & Ferreira, L.G. (2002). Overview of the radiometric and biophysical performance of the MODIS vegetation indices. *Remote Sensing of Environment*, 83, 195-213.
- Huete, A.R. & Tucker, C.J. (1991). Investigation of soil influences in AVHRR vegetation imagery. *International Journal of Remote Sensing*, 12, 1223-1242.
- Illius, A.W. & O'Connor, T.G. (1999). On the relevance of nonequilibrium concepts to arid and semiarid grazing systems. *Ecological Applications*, 9, 798-813.
- Jury, M.R., Weeks, S., & Godwe, M.P. (1997). Satellite-observed vegetation as an indicator of climate variability over southern Africa. *South African Journal of Science*, 93, 34-38.
- Justice, C.O., Dugdale, G., Townshend, J.R.G., Narracott, A.S., & Kumar, M. (1991a). Synergism between NOAA-AVHRR and Meteosat data for studying vegetation development in semi-arid West Africa. *International Journal of Remote Sensing*, 12, 1349-1368.
- Justice, C.O., Eck, T., Tanre, D., & Holben, B.N. (1991b). The effect of water vapor on the normalized difference vegetation index derived for the Sahelian Region from NOAA AVHRR data. *International Journal of Remote Sensing*, 12, 1165-1188.
- Justice, C.O. & Hiernaux, P.H.Y. (1986). Monitoring the grasslands of the Sahel using NOAA/AVHRR data: Niger 1983. *International Journal of Remote Sensing*, 7, 1475-1497.
- Karfs, R., Applegate, R., & Wallace, J. (2000) Regional land condition and trend assessment in Tropical Savannas - Final report: Audit Rangeland Monitoring Implementation Project. NT Department of Lands Planning and Environment.
- Kelly, R.D. & Walker, B.H. (1977). The effects of different forms of land use on the ecology of the semi-arid region in south-eastern Rhodesia. *Journal of Ecology*, 62, 553-576.

- Kerr Watson, H. (2001). Soil sustainability and land reform in South Africa. In *Land Degradation* (Ed., A. Conacher) (pp. 153-166). London: Kluwer Academic Publishers.
- Kiguli, L.N., Palmer, A.R., & Avis, A.M. (1999). A description of rangeland on commercial and communal land, Peddie District, South Africa. *African Journal of Range & Forage Science*, 17, 89-95.
- Klingebiel, A.A. & Montgomery, P.H. (1961) Land Capability Classification. Agriculture Handbook No. 210, USDA, Washington DC.
- Kumar, M. & Monteith, J.L. (1982). Remote sensing of plant growth. In *Plants and the Daylight Spectrum* (Ed., H. Smith) (pp. 133-144). London: Academic Press.
- Land Type Staff (1977-200). Land types of South Africa on 1:250 000 scale. Memoirs of the Agricultural Natural Resource of South Africa. Vol1-13. Pretoria: ARC-ISCW.
- Lambin, E.F. & Strahler, A.H. (1994). Change vector analysis: a tool to detect and categorize land-cover change processes using high temporal-resolution satellite data. *Remote Sensing of Environment*, 48, 231-244.
- Lamprey, H.F. (1975). *Report on the desert encroachment reconnaissance in northern Sudan, 21 October to 10 November 1975*. Nairobi: UNESCO/UNEP
- Le Hou rou, H.N. (1996). Climate change, drought and desertification. *Journal of Arid Environments*, 34, 133-185.
- Le Hou rou, H.N. (1984). Rain -Use Efficiency: A Unifying Concept in Arid-Land Ecology. *Journal of Arid Lands*, 7, 213-247.
- Le Hou rou, H.N., Bingham, R.L., & Skerbek, W. (1988). Relationship between the variability of primary production and the variability of annual precipitation in world arid lands. *Journal of Arid Environments*, 15, 1-18.
- Lepers, E., Lambin, E.F., Janetos, A.C., DeFries, R., Achard, F., Ramankutty, N., & Scholes, R.J. (2005). A synthesis of information on rapid land-cover change for the period 1981-2000. *BioScience*, in press.
- Liniger, L. & Van Lyden, G. (1998) WOCAT : A framework for the evaluation of soil and water conservation: Questionnaire on the SWC Map (Revised edition) Lang Druck AG, Bern.
- Lo Seen Chong, D., Mouglin, E., & Gastellu-Etchegorry, J.P. (1993). Relating the Global Vegetation Index to net primary productivity and actual evapotranspiration over Africa. *International Journal of Remote Sensing*, 14, 1517-1546.
- Low, A.B. & Rebelo, A.G. (1996) Vegetation of South Africa, Lesotho and Swaziland. Department of Environmental Affairs and Tourism, Pretoria, South Africa.
- Lupo, F., Reginster, I., & Lambin, E.F. (2001). Monitoring land-cover changes in West Africa with SPOT Vegetation: impact of natural disasters in 1998-1999. *International Journal of Remote Sensing*, 2633-2639.
- Mabunda, D., Pienaar, D.J., & Verhoef, J. (2003). The Kruger National Park: A century of management and research. In *The Kruger experience: Ecology and management of savanna heterogeneity*. (Eds J. Du Toit, H. Biggs & K. Rogers), (pp. 3-21). London: Island Press.

- MacVicar, C.N., de Villiers, J.M., Loxton, R.F., Verster, E., Lambrechts J.J.N., Merryweather, F.R., Le Roux J., Van Rooyen, T.H., & Harmse, H.J. (1977) Soil classification. A binomial system for South Africa. Science Bull. 390 Agricultural Research Council - Institute for Soil, Climate and Water., Pretoria.
- Malherbe, J. (2001). Integration of Radar rainfall estimates, point station data and long-term interpolated rainfall surfaces to estimate rainfall for the Umlindi monitoring system. In South African Society for Atmospheric Sciences Conference.: Cape Town.
- Malo, A.R. & Nicholson, S.N. (1990). A study of rainfall and vegetation dynamics in the African Sahel using Normalized Difference Vegetation Index. *Journal of Arid Environments*, 19, 1-24.
- Meadows, M.E. & Hoffman, M.T. (2002). The nature, extent and causes of land degradation in South Africa: legacy of the past, lessons for the future. *Area*, 34, 428-437.
- Monnik, K. (2001). Agrometeorological database management strategies and tools in South Africa. In Software for Agroclimatic Data Management: Proceedings of an Expert Group Meeting. Report WAOB-2001-2 (eds R.P. Motha & M.V.K. Sivakumar), 194. USDA: Washington D.C.
- Monteith, J.L. (1977). Climate and the efficiency of crop production in Britain. *Philosophical Transactions of the Royal Society, London, B* 281, 277-294.
- Monteith, J.L. (1972). Solar radiation and productivity in tropical ecosystems. *Journal of Applied Ecology*, 9, 747-766.
- Myneni, R., Keeling, C.D., Tucker, C.J., Asrar, G., & Nemani, R.R. (1997). Increased plant growth in northern high latitudes from 1981-1991. *Nature*, 386, 698-702.
- Nicholson, S.E., Davenport, M.L., & Malo, A.R. (1990). A comparison of the vegetation response to rainfall in the Sahel and East Africa, using normalized difference vegetation index from NOAA AVHRR. *Climate Change*, 17, 209-241.
- Nicholson, S.E. & Farrar, T. (1994). The influence of soil type on the relationships between NDVI, rainfall and soil moisture in semi-arid Botswana. Part I. NDVI response to rainfall. *Remote Sensing of Environment*, 50, 107-120.
- Nicholson, S.E., Tucker, C.J., & Ba, M.B. (1998). Desertification, drought, and surface vegetation: an example from the West African Sahel. *Bulletin of the American Meteorological Society*, 79, 1-15.
- Noy-Meir, I. (1985). Desert ecosystem structure and function. In *Ecosystems of the world* (Eds M. Evenari, I. Noy-Meir & D.W. Goodall), Vol. 12A (pp. 92-103). Amsterdam: Elsevier.
- Noy-Meir, I. (1975). Stability in grazing systems: An application of predator-prey graphs. *Journal of Ecology*, 63, 495-481.
- Noy-Meir, I. & Walker, B.M. (1986). Stability and resilience in rangelands. In *Rangelands: a resource under siege* (Eds P.J. Joss, P.W. Lynch & O.B. Williams), (pp. 21-25). Canberra: Australian Academy of Sciences.
- O'Connor, T.G., Haines, L.M., & Snyman, H.A. (2001). Influence of precipitation and species composition on phytomass of a semi-arid African grassland. *Journal of Ecology*, 89, 850-860.

- Oldeman, L.R., Hakkeling, R.T.A., & Sombroek, W.G. (1990) World map on status of human-induced soil degradation (GLASOD) UNEP/ISRIC, Nairobi, Kenya.
- Olson, D. (2001). Terrestrial Ecoregions of the World: A New Map of Life on Earth. *BioScience*, 51, 933-938.
- Palmer, A.R., Ainslie, A., & Hoffman, M.T. (1999) Sustainability of commercial and communal rangeland systems in southern Africa?, Townsville, Australia.
- Parsons, D.A.B., Shackleton, C.M., & Scholes, R.J. (1997). Changes in herbaceous layer condition under contrasting land use systems in the semi-arid Lowveld, South Africa. *Journal of Arid Environments*, 37, 319-329.
- Pickup, G. (1998). Desertification and climate change - the Australian perspective. *Climate Research*, 11, 51-63.
- Pickup, G. (1996). Estimating the effects of land degradation and rainfall variation on productivity in rangelands: an approach using remote sensing and models of grazing and herbage dynamics. *Journal of Applied Ecology*, 33, 819-832.
- Pickup, G., Bastin, G.N., & Chewings, V.H. (1998). Identifying trends in land degradation in non-equilibrium rangelands. *Journal of Applied Ecology*, 35, 365-377.
- Pickup, G. & Chewings, V. (1994). A grazing gradient approach to land degradation assessment in arid areas from remotely-sensed data. *International Journal of Remote Sensing*, 15, 597-617.
- Pickup, G., Chewings, V.H., & Nelson, D.J. (1993). Estimating changes in vegetation cover over time in arid rangelands using Landsat MSS data. *Remote Sensing of Environment*, 43, 243-263.
- Pickup, G. & Smith, D. (1993). Problems, prospects, and procedures for assessing the sustainability of pastoral land management in arid Australia. *Journal of Biogeography*, 20, 471-487.
- Pollard, S., Shackleton, C.M., & Curruthers, J. (2003). Beyond the fences: People and the Lowveld landscape. In *The Kruger experience: Ecology and management of savanna heterogeneity*. (Eds J. Du Toit, H. Biggs & K.H. Rogers), (pp. 422-446). London: Island Press.
- Potter, C.S., Randerson, J.T., Field, C.B., Matson, P.A., Vitousek, P.M., Mooney, H.A., & Klooster, S.A. (1993). Terrestrial ecosystem production: a process model based on global satellite and surface data. *Global Biogeochemical Cycles*, 7, 811-841.
- Prentice, I.C., Sykes, M.T., & Cramer, W. (1993). A simulation model for the transient effects of climate change on forested landscapes. *Ecological Modelling*, 65, 51-70.
- Prince, S.D. (2004). Mapping desertification in Southern Africa. In *Land Change Science: Observing, Monitoring, and Understanding Trajectories of Change on the Earth's Surface* (Eds .G. Gutman, Anthony Janetos, Christopher O. Justice, Emilio F. Moran, John F. Mustard, Ronald R. Rindfuss, David Skole, and B.L. Turner II ), (pp. 163-184). Kluwer.
- Prince, S.D. (1987). Measurement of canopy interception of solar radiation by stands of trees in sparsely wooded savanna. *International Journal of Remote Sensing*, 8, 1747-1766.

- Prince, S.D. (1991a). A model of regional primary production for use with coarse-resolution satellite data. *International Journal of Remote Sensing*, 12, 1313-1330.
- Prince, S.D. (1991b). Satellite remote sensing of primary production: comparison of results for Sahelian grasslands 1981-1988. *International Journal of Remote Sensing*, 12, 1301-1311.
- Prince, S.D. (2002). Spatial and temporal scales of measurement of desertification. In *Global desertification: do humans create deserts?* (Eds M. Stafford-Smith & J.F. Reynolds), (pp. 23-40). Berlin: Dahlem University Press.
- Prince, S.D. & Astle, W.L. (1986). Satellite remote sensing of rangelands in Botswana. I. Landsat MSS and herbaceous vegetation. *International Journal of Remote Sensing*, 7, 1533-1553.
- Prince, S.D., Brown de Colstoun, E., & Kravitz, L. (1998). Evidence from rain use efficiencies does not support extensive Sahelian desertification. *Global Change Biology*, 4, 359-374.
- Prince, S.D. & Goward, S.N. (1995). Global primary production: a remote sensing approach. *Journal of Biogeography*, 22, 815-835.
- Prince, S.D. & Justice, C.O. (1991). Coarse resolution remote sensing in the Sahelian environment. *International Journal of Remote Sensing*, 12, 1133-1421.
- Prince, S.D. & Tucker, C.J. (1986). Satellite remote sensing of rangelands in Botswana II: NOAA AVHRR and herbaceous vegetation. *International Journal of Remote Sensing*, 7, 1555-1570.
- Prince, S.D. & Wessels, K.J. (2005). Satellite remote sensing and desertification. In *Millennium Ecosystem Assessment*. In Press.
- Rao, C.R.N. & Chen, J. (1995). Inter-satellite calibration linkages for the visible and near-infrared channels of the advanced very high resolution radiometer on NOAA-1, -9, and -11 spacecraft. *International Journal of Remote Sensing*, 16, 1931-1942.
- Rao, C.R.N. & Chen, J. (1996). Post-launch calibration of the visible and near-infrared channels of the Advanced Very High Resolution Radiometer on the NOAA-14 spacecraft. *International Journal of Remote Sensing*, 17, 2743-2747.
- Reich, P.B., Turner, D.P., & Bolstad, P. (1999). An approach to spatially distributed modeling of net primary production (NPP) at the landscape scale and its application in validation of EOS NPP products. *Remote Sensing of Environment*, 70, 69-81.
- Reynolds, J.F. (2001). Desertification. In *Encyclopedia of biodiversity* Vol. 2 (Ed. S. Levin), (pp. 61-78). San Diego: Academic Press.
- Reynolds, J.F. & Stafford Smith, M. (2002a). Do Humans Create Deserts? In *Global Desertification: Do humans cause deserts?* (pp. 1-22). Berlin: Dahlem University Press.
- Riggs, D.S., Guarnieri, J.A., & Addelman, S. (1978). Fitting straight lines when both variables are subject to error. *Life Sciences*, 22, 1305-1360.
- Rosenzweig, M.L. (1968). Net primary productivity of terrestrial communities: prediction from climatological data. *American Naturalist*, 102, 67-72.
- Ross, R. (1999) A concise history of South Africa. Cambridge University Press, Cape Town.

- Roux, P.W. (1990). The general condition of the veld in the RSA. In, *Save of Soil - Conference proceedings of the Veld Trust Conference on the conservation status of agricultural resources in RSA*. Pretoria: National Veld Trust.
- Ruimy, A., Dedieu, G., & Saugier, B. (1996). TURC: a diagnostic model of continental gross primary productivity and net primary productivity. *Global Biogeochemical Cycles*, 10, 269-285.
- Running, S.W., Baldocchi, D., Gower, S.T., Turner, D., Bakwin, P., & Hibbard, K. (1999). A global terrestrial monitoring network scaling tower fluxes with ecosystem modeling and EOS satellite data. *Remote Sensing of Environment*, 70, 108-127.
- Rutherford, M.C. (1980). Annual plant production-precipitation relations in arid and semi-arid regions. *South African Journal of Science*, 76, 53-56.
- SADC-ELMS (1999) SADC sub-regional report on the implementation of the United Nations Convention to Combat Desertification in Southern Africa. Southern African Development Community - Environment and Land Management Sector. Ministry of Environment, Gender and Youth Affairs, Government of the Kingdom of Lesotho., Maseru.
- Scheffer, M., Walker, B., Carpenter, S., Foley, J.A., & Folke, C. (2001). Catastrophic shifts in ecosystems. *Nature*, 413, 591-596.
- Schloss, A.L., Kicklighter, D.W., & Kaduk, J. (1999). Comparing global models of terrestrial net primary productivity (NPP): Comparison of NPP to climate drivers and the Normalized Difference Vegetation Index. *Global Change Biology*, 5, 25-34.
- Schoeman, J.L., M. van der Walt, K. A. Monnik, A. Thackrah, Malherbe, J., & Roux, R.E.L. (2002) Development and application of a land capability classification system for South Africa.- Unpublished ARC-ISCW report GW/A/2000/57. Agricultural Research Council - Institute for Soil, Climate and Water., Pretoria.
- Schulze, R.E. (1997). Climate. In *Vegetation of Southern Africa* (Eds R.M. Cowling, D.M. Richardson & S.M. Pierce), (pp. 21-42). New York: Cambridge University Press.
- Scurlock, J.M.O., Cramer, W., Olson, R.J., Parton, W.J., & Prince, S.D. (1999). Terrestrial NPP: Toward a consistent data set for global model evaluation. *Ecological Applications*, 9, 913-919.
- Sellers, P., Randall, D.A., Betts, A.H., Hall, F.G., Berry, J.A., Collatz, G.J., Denning, A.S., Mooney, H.A., Nobre, C.A., Sato, N., Field, C.B., & Henderson-Sellers, A. (1997). Modeling the exchanges of energy, water and carbon between continents and the atmosphere. *Science*, 275, 502-509.
- Sellers, P.J. (1987). Canopy reflectance, photosynthesis and transpiration. II. The role of biophysics in the linearity of their interdependence. *Remote Sensing of Environment*, 21, 143-183.
- Shackleton, C.M. (1993). Are the communal grazing lands in need of saving? *Development South Africa*, 10, 65-78.
- Shackleton, C.M., Shackleton, S.E., & Cousins, B. (2001). The role of land-based strategies in rural livelihoods: the contribution of arable production, animal husbandry and natural resource harvesting in communal areas in South Africa. *Development South Africa*, 18, 581-604.

- Snyman, H.A. (1998). Dynamics and sustainable utilization of rangeland ecosystems in arid and semi-arid climates of southern Africa. *Journal of Arid Environments*, 39, 645-666.
- Solomon, M., Zambatis, N., Biggs, H.C., & Maré, N. (1999). Comparison of classifications commonly used as templates for management, scientific and GIS work in the Kruger National Park. *Koedoe*, 42, 131-142.
- Stocking, M. (2001). Agriculture, land degradation and desertification: Concluding comments. In *Land Degradation: Sixth Meeting of the International Geographical Union's commission on Land Degradation and Desertification*. (Ed. A. Conacher ), (pp. 387-390). London: Kluwer.
- Stoms, D.M. & Hardgrove, W.W. (2000). Potential NDVI as a baseline for monitoring ecosystem functioning. *International Journal of Remote Sensing*, 21, 401-407.
- Swets, D.L., B. C. Reed, J. D. Rowland, & Marko, S.E. (1999). A Weighted Least-squares approach to temporal NDVI smoothing. In *Proceedings of the American Society of Photogrammetric Remote Sensing*, 526-536. American Society of Photogrammetric Remote Sensing (ASPRS): Portland, Oregon.
- Symeonakis, E. & Drake, N. (2004). Monitoring desertification and land degradation over sub-Saharan Africa. *International Journal of Remote Sensing*, 25, 573-592.
- Tanser, F.C. & Palmer, A.R. (1999). The application of a remotely-sensed diversity index to monitor degradation patterns in a semi-arid, heterogeneous, South African landscape. *Journal of Arid Environments*, 43, 477-484.
- Tapson, D.R. (1991) The overstocking and offtake controversy reexamined for the case of KwaZulu. Pastoral Development Network, Paper no. 31a. Overseas Development Institute, London.
- Thomas, D.S.G. & Middleton, N.J. (1994) Desertification: exploding the myth John Wiley, Chichester.
- Thompson, M. (1996). A standard land-cover classification scheme for remote sensing applications in South Africa. *South African Journal of Science*, 92, 34-42.
- Tongway, D. & Hindley, N. (2000). Assessing and monitoring desertification with soil indicators. In *Rangeland desertification*. (Eds O. Arnalds & S. Archer), Vol. 19 (pp. 89-98). Dordrecht: Kluwer.
- Trollope, W.S.W. (1990). Development of a technique for assessing veld condition in the Kruger National Park using key grass species. *Journal of the Grassland Society of southern Africa*, 7, 46-51.
- Trollope, W.S.W. & Potgieter, A.L.F. (1986). Estimating grass fuel loads with a disc pasture meter in the Kruger National Park. *Journal of the Grassland Society of southern Africa*, 3, 148-152.
- Tucker, C.J., Dregne, H.E., & Newcomb, W.W. (1991a). Expansion and contraction of the Sahara desert from 1980 to 1990. *Science*, 253, 299-301.
- Tucker, C.J., Justice, C.O., & Prince, S.D. (1986). Monitoring the grasslands of the Sahel 1984-1985. *International Journal of Remote Sensing*, 7, 1571-1582.

- Tucker, C.J., Newcomb, W.W., Los, S.O., & Prince, S.D. (1991b). Mean and inter-annual variation of growing-season normalized difference vegetation index for the Sahel 1981-1989. *International Journal of Remote Sensing*, 12, 1133-1135.
- Tucker, C.J. & Sellers, P.J. (1986). Satellite remote sensing of primary production. *International Journal of Remote Sensing*, 7, 1395-1416.
- UNCCD (1994) United Nations Convention to combat desertification in countries experiencing serious drought and/or desertification, particularly in Africa. A/AC.241/27, Paris.
- UNCED (1992) Managing Fragile Ecosystems: Combating Desertification and Drought United Nations Conference on Environment and Development.
- UNCOD (1977a) Desertification: Its Causes and Consequences Pergamon Press, Oxford.
- UNCOD (1977b) Plan of action to stop desertification UNEP, Nairobi.
- UNEP (1987). Sands of Change. UNEP Environmental Brief No. 2.
- UNEP (1992). *United Nations Conference on Environment and Development*. New York: United Nations
- UNEP (1994). *United Nations Convention to Combat Desertification in Countries Experiencing Serious Drought and/or Desertification, Particularly in Africa*. A/AC.241/27. Paris
- UNEP (1997) The World Atlas of Desertification, 2nd edn. Arnold, New York.
- USDA (1992) National Soil Survey Interpretations Handbook. USDA, Washington DC.
- Van Wilgen, B.W., Govender, N., Biggs, H.C., Ntsala, D., & Funda, X.N. (2004). Response of savanna fire regimes to changing fire-management policies in a large African national park. *Conservation Biology*, 18, 1535-1540.
- Venter, F.J., Scholes, R.J., & Eckhardt, H.C. (2003). The abiotic template and its associated vegetation pattern. In *The Kruger experience: Ecology and management of savanna heterogeneity*. (Eds J. Du Toit, H. Biggs & K.H. Rogers), (pp. 83-129). London: Island Press.
- Veroustraete, F., Sabbe, H., & Eerens, H. (2002). Estimation of carbon mass fluxes over Europe using the C-Fix model and Euroflux data. *Remote Sensing of Environment*, 83, 376-399.
- Vink, A.P.A., ed. (1975). *Land use in Advancing Agriculture.*, (pp 394). Berlin Springer-Verlag.
- Viovy, N. & Arino, O. (1992). The Best Index Slope Extraction (BISE): A method for reducing noise in NDVI time-series. *International Journal of Remote Sensing*, 13, 1585-1590.
- Walker, B.H., Abel, N., Stafford Smith, D.M., & Langridge, J.L. (2002). A Framework for the determinants of degradation in arid ecosystems. In *Global desertification: do humans create deserts?* (Eds J.F. Reynolds & D.M. Stafford Smith), (pp. 75-94). Berlin: Dahlem University Press.
- Wang, J., Price, K.P., & Rich, P.M. (2001). Spatial patterns of NDVI in response to precipitation and temperature in the central Great Plains. *International Journal of Remote Sensing*, 22, 3827-3844.

- Ward, D., Ngairorue, B., & Apollus, A. (2000). Perceptions and realities of land degradation in arid Otjimbingwe, Namibia. *Journal of Arid Environments*, 45, 337-356.
- Ward, D., Ngairorue, B.T., & Kathena, J. (1998). Land degradation is not a necessary outcome of communal pastoralism in arid Namibia. *Journal of Arid Environments*, 40, 357-371.
- Wessels, K.J., S.D. Prince, Frost, P.E., & van Zyl, D. (2004). Assessing the effects of human-induced land degradation in the former homelands of northern South Africa with a 1km AVHRR NDVI time-series. *Remote Sensing of Environment*, 91, 47-67.
- Wessels, K.J., van Den Berg, H.M., & Pretorius, D.J. (2000). Spatial Natural Resource Monitoring in the Mpumalanga Province of South Africa. In *Response to Land Degradation*. (Eds E.M. Bridges, I.D. Hannam, L.R. Oldeman, F.W.T. Penning de Vries, S.J. Scherr & S. Sombatpanit), (pp. 237-248). New Hampshire, USA.: Science Publishers Inc..
- Williams, M.A. & Balling, R.C. (1996) Interactions of Desertification and Climate. Arnold, London.
- Willmott, C.J. & Robeson, S.M. (1995). Climatologically Aided Interpolation (CAI) of Terrestrial Air Temperature. *International Journal of Climatology*, 15, 221-229.
- Wylie, B.K., Harrington, J.A., Prince, S.D., & Denda, I. (1991). Satellite and ground-based pasture production assessment in Niger:1986-1988. *International Journal of Remote Sensing*, 12, 1281-1300.
- Xue, Y. & Fennessy, M.D. (2002). Under what conditions does land cover change impact regional climate? In *Report of the 88th Dahlem Workshop on an Integrated Assessment of the Dimensions of Global Desertification*. (Eds J.F. Reynolds & D.M.S. Smith), Berlin: Dahlem University Press.
- Yang, L., B.K. Wylie, L.L. Tieszen, & Reed, B.C. (1998). An Analysis of Relationships among Climate Forcing and Time-Integrated NDVI of Grasslands over the U.S. Northern and Central Great Plains. *Remote Sensing of Environment*, 65, 25-37.
- Zambatis, N. (2002) Revised Procedures For Veld Condition Assessment In The Kruger National Park. Unpublished internal report. SANParks, Skukuza.
- Zheng, D., Prince, S., & Wright, R. (2003). Terrestrial net primary production estimates for 0.5 degree grid cells from field observations - a contribution to global biogeochemical modeling. *Global Change Biology*, 9, 46-64.